TECHNICAL REPORT BRL-TR-3277

BRL

CRACK PATH PREDICTION NEAR AN ELLIPTICAL INHOMOGENEITY

EDWARD M. PATTON

SEPTEMBER 1991

U.S. ARMY LABORATORY COMMAND

BALLISTIC RESEARCH LABORATORY
ABERDEEN PROVING GROUND, MARYLAND

NOTICES

Destroy this report when it is no longer needed. DO NOT return it to the originator.

Additional copies of this report may be obtained from the National Technical Information Service, U.S. Department of Commerce, 5285 Port Royal Road, Springfield, VA 22161.

The findings of this report are not to be construed as an official Department of the Army position, unless so designated by other authorized documents.

The use of trade names or manufacturers' names in this report does not constitute indorsement of any commercial product.

UNCLASSIFIED

REPORT DOCUMENTATION PAGE

Form Approved
OMB No. 0704-0188

1. AGENCY USE ONLY (Leave blank)	2. REPORT DATE	3. REPORT TYPE AND DATES COVERED
	September 1991	Final, June 1989 - April 1991

4. TITLE AND SUBTITLE

Crack Path Prediction Near an Elliptical Inhomogeneity

5. FUNDING NUMBERS

1L162618AH80

6. AUTHOR(S)

Edward M. Patton

7. PERFORMING ORGANIZATION NAME(S) AND ADDRESS(ES)

8. PERFORMING ORGANIZATION REPORT NUMBER

9. SPONSORING / MONITORING AGENCY NAME(S) AND ADDRESS(ES)

US Army Ballistic Research Laboratory
ATTN: SLCBR-DD-T
Aberdeen Proving Ground, MD 21005-5066

10. SPONSORING / MONITORING AGENCY REPORT NUMBER

BRL-TR-3277

11. SUPPLEMENTARY NOTES

12a. DISTRIBUTION / AVAILABILITY STATEMENT

Approved for public release; distribution is unlimited.

12b. DISTRIBUTION CODE

13. ABSTRACT *(Maximum 200 words)*

In this work, a new technique is presented which will predict the path of a naturally growing crack near a rigid elliptical inclusion, where the stress field can be modelled as two dimensional. The technique uses a boundary integral approach to the solution of the stress field at the tips of the crack which is in general not straight, and is interacting with a rigid elliptical inclusion. The crack is parameterized as a cubic spline, and the results of both a Green's Function solution to the interaction of a dislocation with an elliptical inclusion, and a first order perturbation solution to account for the generally curvilinear nature of the crack have been employed. The singular nature of the stresses is accounted for using a numerical technique which describes the distribution of dislocations along the crack as a piecewise quadratic polynomial to transform the problem's resulting integral equations into algebraic equations well suited to a matrix-type solution. Results of each step of the analysis have been verified with previously published results, and with experimental results of a crack propagating near an open circular hole. New and significant results are also presented as paths of cracks interacting with inclusions of differing ellipticity ratios, and at different orientations with respect to the initial crack.

14. SUBJECT TERMS	15. NUMBER OF PAGES
crack propagation; fracture mechanics; stress analysis; composite material; microcrack	129
	16. PRICE CODE

17. SECURITY CLASSIFICATION OF REPORT	18. SECURITY CLASSIFICATION OF THIS PAGE	19. SECURITY CLASSIFICATION OF ABSTRACT	20. LIMITATION OF ABSTRACT
UNCLASSIFIED	UNCLASSIFIED	UNCLASSIFIED	UL

INTENTIONALLY LEFT BLANK.

TABLE OF CONTENTS

LIST OF FIGURES

INTENTIONALLY LEFT BLANK.

LIST OF TABLES

INTENTIONALLY LEFT BLANK.

Chapter 1

INTRODUCTION

1.1 Background and Motivation

Two dimensional complex potential methods have been used for some time for the prediction of the stress field near the tips of a crack in an elastic medium. These methods have proven to be very accurate and generally lead to the solution of two dimensional boundary value problems with Cauchy type singularities. Using these methods, the study of the interaction between inclusions and cracks has been active for many years. Applications of the results of theoretical analyses of cracks interacting with inhomogeneities have had wide effect in the implementation of a broad range of new and emerging material systems. The understanding gained by the solution of appropriate elasticity problems provides researchers with insight into the mechanisms of strengthening and toughening, as well as material damage, because of the presence of material defects. The mechanisms of crack growth in composite materials and ceramics, and that of strain hardening in metal alloys, are primary examples of the direct application of the results of the study of crack inclusion interaction.

crack near an inclusion provides the ability to quantitatively assess the energy absorbed by crack path deflection. This provides a basis for a fundamental elasticity model for material toughening. Having such a method will provide researchers with a useful tool to investigate the sources of toughening in materials, or to guide material scientists in their efforts to improve the fracture toughness of present or new materials. It is just such a method which is described in this work, with appropriate examples, test cases, and verification of results in order to convince the reader that the proposed technique is a viable one, and a useful one.

Methods to predict the path of a crack have, in the past, been based upon the Finite Element Method using specialized crack tip elements which are intended to capture the singularity at the crack tip. These predictions, by their nature, have been computationally intensive. At each increment of crack growth, a new finite element mesh must be generated. The crack has propagated into the mesh during this increment of growth, and the crack tip element must stay at the crack tip. Therefore, at each increment of crack growth, significant computation has to be undertaken just to remesh the vicinity of the crack tip to model that increment of growth.

The proposed method for crack path prediction is based upon a Boundary Integral approach, similar to a reasonably elementary Boundary Element solution, where the boundary in question is the crack itself. This method has been used successfully with two dimensional potential theory to calculate the stress field around the tip of the crack, and therefore can be used to predict the direction of crack growth.

Once the direction of crack growth is known, the crack can be grown by an increment in the specified direction very simply by allowing the boundary (the crack) to grow by that increment in that direction. The re-meshing of the boundary, then, is simply the extension of a line by a known increment, in a predicted direction. If the crack is parameterized as a smooth set of cubic interpolating functions commonly referred to as a cubic spline, the extension can take on any orientation required to meet a specific crack growth criterion. This parameterization, using cubic splines, and a solution to account for the fact that the naturally growing crack is not straight, are developed in detail in this work.

One of the major side benefits of this type of prediction model is, therefore, that it is much less computationally intensive, and can be used as the basis for performing sensitivity studies, or for a stochastic model of material toughening. Of course, the major attraction of this method is that it uses an exact elasticity solution which can be used as a basis for a fundamental mechanics model of material toughening.

1.2 Survey of Past and Current Literature

The field of Linear Elastic Fracture Mechanics has had a long and venerable tradition. Early work by Griffith [1], and Irwin [2] laid the fundamentals for what has become an indispensable tool for the practicing Mechanical Engineer. As the technique has become established and accepted, many elasticians have solved

many problems of interest. Elasticity solutions have been mainly for two dimensional regions, both for their simplicity, and for the ability to apply two dimensional stress potentials to those regions. The potential methods of Muskhelishvili [3] have been used with tremendous success, to solve some very complicated and difficult elasticity problems in the field. Paris [4] and Erdogan [4,5], among others, have been instrumental in the application of these methods to solve problems of significant interest in the engineering community. These problems have involved interfaces, interactions, welded structures, open holes, and a multitude of stress problems where the stresses become singular at some point of interest in the field in question. This work deals with the solution of one of these problems in which the crack is interacting with an elliptical inclusion, and is growing along a path that is affected by the presence of that inclusion.

The problem of the interaction between a circular inclusion and a static crack has been solved by Atkinson [6] for a radial crack, and by Erdogan, Gupta, and Ratwani [7] for an arbitrarily oriented crack. Erdogan and Gupta [8] later solved the problem in which the crack crosses the interface. These solutions are based on the Green's Functions derived from one solution of a dislocation interacting with a circular inclusion (Dundurs and Mura [9] and Dundurs and Sendeckyj [10]). Grief and Sanders [11] used the same techniques to solve the problem of the effect of a stringer on a cracked sheet of material. Their solution with respect to this work represents the other extreme in ellipticity ratio from that done by Atkinson for the circular inclusion.

Santare and Keer [12], presented the two-dimensional solution for the dislocation outside a rigid elliptical inclusion, using the complex potential methods of Muskhelishvili [3]. Their Green's Function, when applied to a straight crack using the methods described in this work matches Atkinson's [6] results for a circular inclusion, and that of Grief and Sanders [11] for the line inclusion or stringer. Special attention was paid in [12] to the rotation of the elliptical inclusion and the effect that has on the stress field around the ellipse. Results were compared with a power series solution found by Stagni and Lizzio [13], which did not take into account the rotation of the ellipse. The comparison showed that the rotation has a significant effect on the stress field in many instances. In another paper, Santare, Keer, and Lewis [14] solved a related problem of an elliptical hole at a bone/implant interface, with symmetrical cracks radiating from the edges of the ellipse, along the x-axis. Solutions to the resulting singular integral equations were found using a numerical scheme proposed by Gerasoulis [15]. The technique described in this work uses the potentials calculated by Santare and Keer [12], and the numerical technique described by Gerasoulis [15] to calculate the stress intensity factors for the advancing crack. These static results were reported by Patton and Santare [16] in 1990.

Besides the interaction problem, the stress due to a non-straight crack path is also important, and must be taken into account. The kinked crack problem was attempted by several researchers in the early 1970's, with some success. Palinaswamy and Knauss [17] besides providing a very good review on the subject, solved the

problem of an infinitesimal branch or kink off the tip of a crack using a Fourier series approximation. Their results are in agreement with an earlier solution by Bilby and Cardew [18], and have been found by others to be correct. Other researchers (Dudukalenko and Romalis [19], and Hussain, Pu, and Underwood [20]) came up with analytical expressions for the complex potentials, but their results have been since found to be inconsistent with the results published by other authors. Chaterjee [21], Gupta [22], and Kitigawa, Yukki, and Ohira [23], all independently solved the problem of a finite extension to the crack, and their results agree with one another. K. K. Lo [24] finally, in a paper in 1978 presented a unified approach to solving the kinked crack problem that is most commonly regarded as correct and most commonly referenced at present. His results match those of [17] and [18] for the infinitesimal kink, and the results of [21], [22] and [23] for the finite length crack extension.

In the early 1970's, a group of Russian mathematicians solved the problem of a crack with a curved extension by the use of a first order perturbation method. Banichuk [25] found the first order perturbation solution and came up with complex potentials suitable to a solution using Muskhelishvili's [3] method. Goldstein and Salganik [26] then applied this set of potentials to the solution of a finite crack with a curved extension. The same authors reported this work in the western literature [27] in 1974. Since that time, Cotterell and Rice [28] used this technique to solve a similar problem, coming up with a somewhat different way of describing the problem. They explicitly calculate the stress intensity factors without the need to write integral

equations, as was done by Goldstein and Salganik in [26]. Their results compare favorably with that of Goldstein and Salganik [26]. Karihaloo et al. [29] included second order terms in the same solution to refine the prediction, and came up with an elaborate expression for the stress intensity factors. From these expressions, the authors derive approximate expressions for these stress intensity factors in terms of an infinite series. Their conclusions from this work were that the path of the propagating crack depends not only on the in-plane normal stress as concluded by Cottrell and Rice [28], but also on the derivatives of the stress intensity factors with respect to the original crack length. They go on to conclude that a crack without an initial kink in a non-homogeneous stress field can have a smooth curved path, as the Mode II stress intensity factor will be changing continuously along the path of crack growth, under the influence of the non-homogeneous stress field. That is exactly the situation that is examined in this work, that of a crack growing through the inhomogeneous stress field caused by the presence of a rigid elliptical inclusion.

Other solutions to the curved and/or kinked crack problem have been proposed in the literature in recent years. Sumi, Nemat-Nasser, and Keer [30] resolved the first order perturbation problem originally solved by Banichuk [25] and Goldstein and Salganik [26], with the additional complexity of taking into account the boundaries of the region. The original work by Banichuk [25], and Goldstein and Salganik [26] had been done for a finite crack in an infinite domain, with no geometry effects of the domain taken into account. Sumi, Nemat-Nasser, and Keer [31] went on to create a

combined analytical and finite element solution to the crack path prediction problem. Sumi [32] and Sumi, Ohashi, and Emura [33] have gone on to predict crack paths in welded structures [32] and near open holes in cracked sheets [33]. The second of these papers included an experimental investigation of cracks interacting with open circular holes. Their predictions come reasonably close to their experimental results, but more importantly for this work, it provides experimental results with which to verify the predictions made with the present technique. Another very interesting solution to the curved crack problem has been proposed by Sur and Altiero [34] in which they do not formulate the problem in terms of the derivative of displacement or Burger's vector, but rather in terms of the crack displacement itself. They claim that their technique avoids the singularities at the tips and kinks of the crack, and that their equations are not hypersingular, as other attempts to do this have been (see Ioakimidis [35]). They compare their results to those of Kitigawa et al. [23] for the kinked crack, with good agreement.

The criterion which is used to predict the direction in which a crack will kink has also been a rather controversial problem. There are basically two different schools of thought regarding the correct criterion to use for prediction of the path of an advancing crack, stress-based methods and energy-based methods. Erdogan and Sih [36] proposed a criterion which has come to be called the "Maximum Normal Stress Criterion," in which they state that a naturally growing crack in an isotropic material will grow in the direction in which the stress normal to the crack propagation direction

is greatest. This criterion implies that the stress parallel to that direction would be a minimum, or that the shear stress in that direction would vanish, as the crack would propagate in a direction normal to the maximum principal tensile stress. One can easily verify this by rotating a plane stress field into its principal directions. In the principal directions, there is no shear stress. The authors substantiate their claim with experimental data which seems to validate their analytical results. Other authors have applied their criterion to differing crack models. McClintock [37] and Cotterell [38] noticed a discrepancy when the elliptical edge crack model was used rather than the slit model used by Erdogan and Sih [36]. Other authors (Williams and Ewing [39], Finnie and Saith [40], and Ewing and Williams [41]) discussed the implication of including more terms in the near tip approximation using this criterion. Sih [42] proposed a new criterion which is supposed to be a combination of a stress method and an energy method, which he called the Strain Energy Density Criterion, or S-criterion. This criterion has come under some criticism, as it does not have as much fundamental basis as the energy and stress methods.

The name, Maximum Energy Release Rate Criterion, was initially proposed by C. H. Wu [43], in 1976 when he reviewed all of these works, and proposed a criterion for fracture which is consistent with Griffith's [1] energy release concept. This was the first real treatise on energy based methods that was published. This criterion was mentioned by Erdogan and Sih [36], and a solution was given by Palinaswamy and Knauss [17], even though none of these authors explicitly call it the

Maximum Energy Release Rate Criterion. In his work, Wu solved the problem of describing the energy released by an infinitesimal kink at the end of a straight crack with the use of the potential methods of Muskhelishvili [3], and then applied his criterion that the energy released by this infinitesimal propagation should be a maximum with respect to the direction at which the kink propagates. He compares his results to Erdogan and Sih [36], Sih [42], and the Fourier series solution found in Palaniswamy and Knauss [17]. The only discrepancies noted are for a crack loaded in pure shear, where the angle of the kink is on the order of 70 to 80 degrees. In the literature, there was much controversy about this particular problem, but in the work described in this document, the kink angles are very small, as the crack is growing in a stress field which is a tensile field normal to the original crack. The fact that these two major criteria produce identical results for small kink angles in a stress field which does not produce significant Mode II loading, leads to the conclusion that either is acceptable for the work described in the following pages, and the major reason to choose one over another is ease of implementation.

1.3 Dissertation Outline

The remainder of this chapter describes the content and organization of this dissertation, in enough detail that the reader should be able to understand the techniques presented, and follow the methodology presented.

Chapter 2 presents a brief summary of the fundamentals of the two

dimensional potential methods used in deriving the crack solution. The methods of Muskhelishvili [3] are presented along with the methods by which the singular integral equations used to calculate stress intensity factors are derived for crack solutions. Also included is a short description of the methods of solution that have been employed in the past by practitioners of Linear Elastic Fracture Mechanics. At the end of chapter 2, a brief discussion of toughening mechanisms in materials is presented in order to motivate the discussion of solutions for cracks near inhomogeneities.

Chapter 3 presents the solution to the point dislocation interacting with a rigid elliptical inclusion. The formulation of the problem, using complex potential methods, is presented, and the potentials that were calculated by Santare and Keer [12] are presented. The chapter closes with a summary of solution technique used to model a straight crack, using the point dislocation potentials. Results of that analysis, which are original, and a comparison with previous work are presented. This chapter concludes the review of work done by others, with the discussion of the solution for a dislocation interacting with an elliptical inclusion. The solution of the straight crack problem, and all subsequent work that is presented in chapters 4, 5, and 6 is original work.

The material presented in chapter 4 is intended as background for the technique used to predict the path of the crack. The most fundamentally difficult part of this is the ability to model a curvilinear crack in a complex stress field (created both by the applied load and by the inclusion itself). The chapter begins with a discussion

of crack kinking and curvature solutions, and their applicability and suitability to the chosen method of solution. Historically, these solutions have been used only to correctly calculate the stress intensity factors for a non-straight crack. They have been intended to model the reaction of a crack to a change in the direction of the applied load. There has been little done to extend these solutions to a path prediction model, or to include them in a model of interaction with inhomogeneities. The chapter continues with the description of a perturbation solution which was performed in the early 1970's by a group of Russian mathematicians which is particularly applicable to the problem at hand. As a result of the adoption of that solution, the crack must be parameterized in such a fashion as to yield the local spatial first and second derivatives along the crack. A cubic spline parameterization is particularly suitable for this parameterization, and that is also described. The chapter closes with a description of the crack extension algorithm, and a comparison of the solution with known kinked crack solutions.

Chapter 5 describes the method used to predict the crack path near the inclusion. It begins with a historical review of crack propagation laws, and a rationale for the choice of the Maximum Normal Stress as the criterion used to predict the local direction of incremental crack growth. The algorithm used to predict the local direction is described, and a verification of the prediction is described. The chapter continues with parametric studies of path deflection as a function of ellipticity ratio of the ellipse, and on the initial location and orientation of the crack. It concludes with

an estimate of energy absorbed by crack path deflection for several crack paths of interest.

The last chapter of this dissertation reviews significant results and presents conclusions obtained from the study of crack path deflection, along with a few ideas for future work that should come as a result of this study.

Chapter 2

FUNDAMENTALS

2.1 Two Dimensional Complex Potential Methods

It can be shown that the stress-strain relations for two dimensional plane problems can be written in indicial notation as follows (Muskhelishvili [3]):

$$\epsilon_{\alpha\beta}=\frac{1}{2\mu}(\sigma_{\alpha\beta}-\kappa\delta_{\alpha\beta}\sigma_{\gamma\gamma}) \tag{2.1}$$

where Muskheli ıvili's constant, $\kappa = (3-\nu)/(1+\nu)$ ıor plane stress, and $\kappa = 3-4\nu$ for plane strain, ν is the Poisson's ratio of the material, the strain is defined by $\epsilon_{\alpha\beta}$, the stress by $\sigma_{\alpha\beta}$, μ is the shear modulus of the material, and the kronecker delta (δ) has its usual indicial definition. Following the complex potential methods of Muskhelishvili, it is assumed that the complex variable **z** defines x and y coordinates as in $\mathbf{z} = x + iy$, where i is the imaginary number. Furthermore, displacements and forces can take on complex values as $\mathbf{D} = u + iv$ where u is displacement is the x-direction v is displacement in the y-direction, and the forces as $\mathbf{F} = F_x + iF_y$, where the subscripts refer to forces in those directions. From these quantities, the stresses

and displacements in the region can be written as a function of two holomorphic potential functions ϕ and ψ as follows:

$$\sigma_{xx}+\sigma_{yy}=2[\frac{d}{dz}\phi(z)+\overline{\frac{d}{dz}\phi(z)}] \tag{2.2}$$

$$\sigma_{yy}-\sigma_{xx}+2i\sigma_{xy}=2[\bar{z}\frac{d^2}{dz^2}\phi(z)+\frac{d}{dz}\psi(z)] \tag{2.3}$$

$$2\mu(u+iv)=\kappa\phi(z)-z\overline{\frac{d}{dz}\phi(z)}-\overline{\psi(z)} \tag{2.4}$$

In the stress analysis of a two dimensional region, therefore, what is required is the calculation of these two potential functions. In a great number of cases, these two potentials can be calculated by evaluating two Cauchy integrals, as given by Muskhelishvili. In the case of a single dislocation in an infinite homogeneous elastic medium, these integrals give the following potentials:

$$\phi_d(z)=\gamma\log(z-z_0) \tag{2.5}$$

$$\psi_d(z)=\bar{\gamma}\log(z-z_0)-\gamma\overline{\frac{z_0}{z-z_0}} \tag{2.6}$$

where the dislocation is included in the form $\gamma = \mu(b_x+ib_y)/i\pi(\kappa+1)$, z is some point in the complex plane and z_0 is the position of the dislocation. The dislocation, in the form described above (b_x and b_y), is called the Burger's vector, which is related to the derivative of the displacement at the point of the dislocation. Obviously, the stresses

become singular as one approaches the dislocation, as would be expected. Therefore, to study the stress field near a dislocation, or along the line of dislocations commonly used to model a crack, one must deal with the singularity in stress. In linear elastic fracture mechanics, the stresses along the crack are assessed by modelling the displacement of the two faces of the crack as a line of dislocations or crack opening displacements which is unknown. The stresses which are related to the strains, or derivatives of displacement, through the stress-strain relations (equation 2.1), therefore, can be written as a set of singular integral equations where the unknown distribution of dislocations is inside the integrals. The integrals are taken along the crack, and the value of the integrands are singular at the end points, namely the tips of the crack.

2.2 Solution Methods

Several techniques have been used in the past to solve the singular integral equations that result from the stress analysis of a crack, but the most commonly used is an approximation of the singular part of the integral with a suitable polynomial (Chebychev or LaGrange are common choices), and a direct numerical evaluation of the non-singular part of the integral. The technique developed by Gerasoulis [15] which is noted in the discussion of pertinent literature in the introduction is the one employed in this work.

Since the stress analysis is linear, the principle of superposition applies. Therefore, if the problem in question can be modeled as a superposition of several

stresses upon one another, the stresses due to each of them can be calculated, and then added up. In the analysis of cracks interacting with inclusions, much use of the principle of superposition is made. In practical use, the methods to evaluate the singular integral equations have a singular part which represents the crack tip singularity, and a non-singular part which represents the superposition of all of the other stresses which act on the crack at some distance from the crack tips. Therefore, to analyze the effect of an inclusion interacting with a crack, one needs to calculate potentials ϕ and ψ for the interaction between a dislocation and an inclusion. Using these potentials, the stresses are calculated, superposed and summed along the crack length, resulting in an integral equation valid along the length of the crack. Therefore, the integrals typically take the following form for a finite crack:

$$C_1 \int_{z_1}^{z_2} \frac{b(z_0)}{z - z_0} dz_0 + C_2 \int_{z_1}^{z_2} K(z, z_0) b(z_0) dz_0 = F(z) \tag{2.7}$$

where the two constants (C_1 and C_2) are based upon material and geometric properties, the integrals are taken between the two crack tips z_1 and z_2, and the dislocation density, $b(z_0)$, is an unknown function along the crack which is evaluated at the points z_0. This form explicitly separates the singular part of the integral equation as the first integral, and the non-singular part, or kernel ($K(z,z_0)$), as the second integral. The forcing function, or the load applied to the crack, is given as F(z) on the right hand side of the integral equation.

2.3 Toughening Mechanisms in Materials

One of the most common methods of strengthening and toughening engineering materials has been the incorporation of inhomogeneities into the base structure of the material. Composite materials are probably the most well known example of the purposeful use of this method for strengthening. In an organic composite material, the relatively weak and brittle organic matrix material is both strengthened and toughened by the incorporation of fiber reinforcement. In a typical discontinuously reinforced metal matrix composite material, the hard, tough reinforcing phase is interspersed within the metallic grain structure. The same is true of ceramic matrix composites, where a harder ceramic reinforcement is dispersed into the softer ceramic matrix surrounding it. A more mundane example of this toughening is that of high strength steels and aircraft grade aluminum alloys. In both of these materials, hard intermetallic compounds are precipitated out into the boundaries around the grains of the metal, and strength is increased. In many cases, if the bonding between the matrix material and the reinforcement is good, and if the reinforcement takes on certain geometric and physical properties, the toughness of the material is increased.

One of the more compelling theories that has been proposed to explain this phenomenon is that the deflection of the path of a crack through the material absorbs a significant amount of energy, thereby toughening the material. Rubinstein [45] discusses this mechanism at length, giving solutions to the problem of calculating toughness increase due to crack path and crack shielding effects. This work is used

in a later section of this document to estimate the energy absorbed by cracks which are effected by elliptical inclusions. It would seem that, from this work and that of Rubinstein, a fundamental model of this crack path deflection that would allow the estimation of energy absorbed by crack path deflection would be useful in investigations into material toughening. It is precisely this mechanism that provided the motivation for the work that is described in this document.

Chapter 3

ELLIPTICAL INHOMOGENEITY

3.1 Problem Formulation

The problem of calculating the interaction between a dislocation and an elliptical inhomogeneity can be solved by determining suitable potential functions ϕ and ψ such that the classical methods described in this work can be used. These potential functions can be calculated by solving an appropriate boundary value problem that can be cast as two integrals in the complex plane. This problem was solved by Santare and Keer [12], and the salient points are described in the following.

The geometry of the problem is simplified by using a conformal mapping of the region outside an ellipse onto the region outside the unit circle, as shown in Figure (3.1). The function that does this mapping can be written as,

$$z=\omega(\zeta)=R(\zeta+\frac{m}{\zeta}) \tag{3.1}$$

where

$$R=\frac{a+b}{2} \tag{3.2}$$

and the parameter which can be thought of as the ellipticity of the ellipse is given by

$$m=\frac{a-b}{a+b} \tag{3.3}$$

where a and b are the semi-axes of the ellipse shown in Figure (3.2). This figure

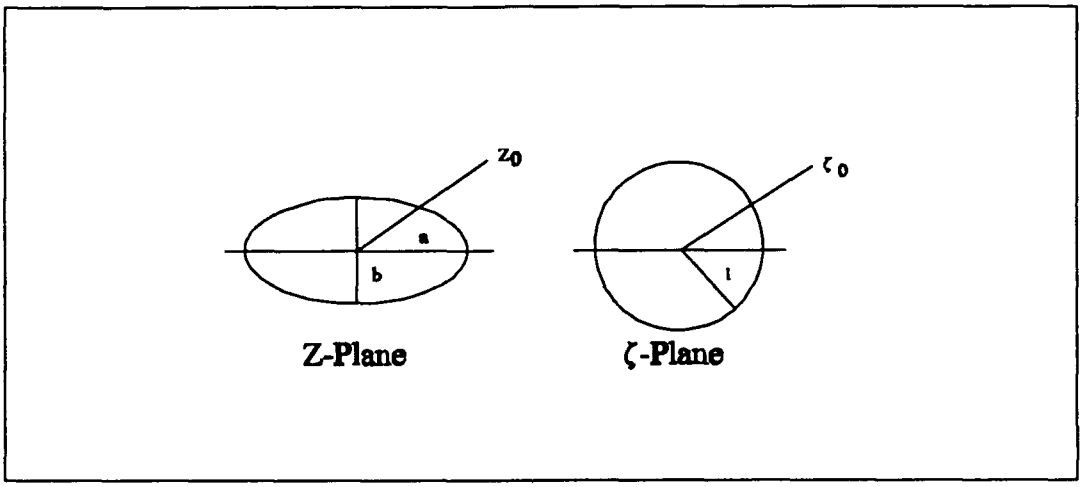

Figure 3.1. Mapping function for the dislocation-inclusion interaction problem.

displays the geometry of the problem of a crack interacting with an elliptical inclusion. In Figure (3.2), the two crack tips are shown as Z_1 and Z_2, the distance from the ellipse to the close crack tip is defined as d, the angle that the crack makes with respect to the x-axis is θ, and the angle that the close tip of the crack makes with respect to the major axis of the inclusion is α. The parameter that defines ellipticity, m, takes on a value of zero for a circle, and a value of one for a line along the x-axis. A value of m of -1 describes a line along the y-axis.

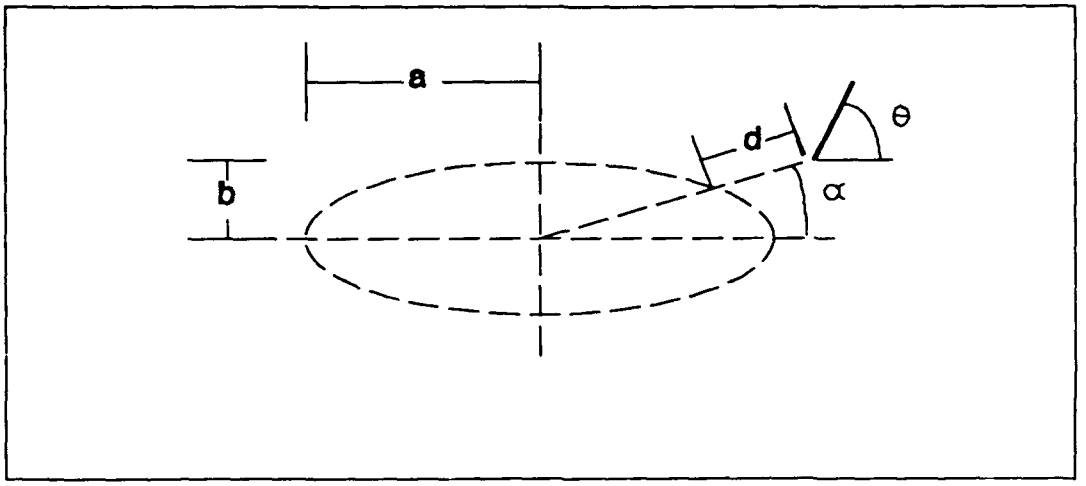

Figure 3.2. Geometry of crack-inclusion interaction problem.

The solution for a dislocation interacting with a rigid elliptical inclusion is used to formulate the Green's functions for the crack problem. The potentials were calculated by Santare and Keer [12], and are restated here for completeness. They include the dislocation in the form, described previously, of $\gamma = \mu\,(b_x + ib_y)/i\pi\,(\kappa + 1)$, the mapped coordinates ζ and ζ_o, which are the transformed z and z_o, and the rotation of the ellipse ε_o.

$$\phi(\zeta) = \frac{\gamma}{\kappa}\log[R(\zeta-\zeta_0+m/\zeta-m/\zeta_0)]$$

$$+\log[\frac{(\zeta-1/\overline{\zeta_0})}{\zeta}] - \gamma\log[\frac{(\zeta-m/\zeta_0)}{\zeta}] \qquad (3.4)$$

$$-\frac{\gamma}{\kappa m}\,\frac{(1/\overline{\zeta_0}-m/\zeta_0)\,(1/\overline{\zeta_0}-\zeta_0)}{(1/\overline{\zeta_0}-\overline{\zeta_0}/m)\,(1/\overline{\zeta_0}-\zeta)} + 2\mu i\epsilon_0 R\frac{m}{\kappa\zeta}$$

$$\psi(\zeta) = \gamma\log[R(\zeta-\zeta_0+m/\zeta-m/\zeta_0)] - \gamma\frac{\overline{\zeta_0}+m/\overline{\zeta_0}}{\zeta-\zeta_0+m/\zeta-m/\zeta_0}$$

$$+ \kappa\bar{\gamma}\log[\frac{(\zeta-1/\zeta_0)}{\zeta}] - \bar{\gamma}\log[\frac{(\zeta-m/\zeta_0)}{\zeta}]$$

$$+ \gamma m\frac{(m/\zeta_0-1/\overline{\zeta_0})\ (m/\zeta_0-\overline{\zeta_0}/m)}{(m/\zeta_0-\zeta_0)\ (m/\zeta_0-\zeta)} + 2\mu i e_0\frac{R}{\zeta} \qquad (3.5)$$

$$- \zeta\frac{1+m\zeta^2}{\zeta^2-m}\left[\frac{\gamma}{\kappa}\frac{1/\overline{\zeta_0}}{\zeta(\zeta-1/\zeta_0)} - \gamma\frac{m/\zeta_0}{\zeta(1/\zeta-m/\overline{\zeta_0})}\right.$$

$$\left. + \frac{\gamma}{\kappa m}\frac{(1/\overline{\zeta_0}-\frac{}{\zeta_0})\ (1/\overline{\zeta_0}-\zeta_0)}{(1/\overline{\zeta_0}-\overline{\zeta_0}/m)\ (\zeta-1/\overline{\zeta_0})^2} - \mu e_0\frac{m}{\kappa\zeta^2}\right]$$

where

$$e_0 = Re\ i[-\frac{\kappa\bar{\gamma}}{\overline{\zeta_0}}+\bar{\gamma}\frac{m}{\zeta_0}+\gamma\frac{m^2}{\zeta_0}$$

$$-\gamma\frac{m}{\kappa\overline{\zeta_0}} - \gamma m\frac{(m/\zeta_0-1/\overline{\zeta_0})\ (m/\zeta_0-\overline{\zeta_0}/m)}{(m/\overline{\zeta_0}-\zeta_0)} \qquad (3.6)$$

$$+ \frac{\overline{\gamma}}{\kappa}\frac{(1/\overline{\zeta_0}-m/\overline{\zeta_0})\ (1/\zeta_0-\zeta_0)}{(1/\overline{\zeta_0}-\overline{\zeta_0}/m)}]/2\mu R(1+\frac{m^2}{\kappa})$$

The first term in ϕ (equation 3.4) and the first two terms in ψ (equation 3.5) represent the potentials for dislocation in an unbounded medium, and are the restatement of equations 2.5 and 2.6 in the mapped plane. These terms, when applied to equations 2.2 and 2.3 to calculate the stresses, become singular, and constitute the first integral in equation 2.7. The remainder of the terms in both potentials account

for the interaction between the ellipse and the dislocation. These terms, when used in equations 2.2 and 2.3, constitute the nonsingular stresses due to the interaction between the dislocation and the inclusion. Note also that the rotation of the ellipse is taken into account through these nonsingular terms and is called ε_o. The last term in the expression for ψ (the bracketed terms) contains the first derivative of the interaction portion of the first potential ϕ. This is a natural consequence of the method of Muskhelishvili [3].

3.2 Solution Method for a Straight Crack

Summing these stresses along the crack length (Figure (3.2)) and setting them equal to the stresses due to the external load, two singular integral equations result. The solution of these equations will give the unknown distribution of dislocations along the crack, from which the stress intensity factors at the crack tips can be directly calculated. If the stresses are resolved into components normal to the crack (Mode I), and along the crack (Mode II), the two equations can be stated as follows:

$$\int_{z_1}^{z_2} \frac{b_n(z_0)}{z-z_0} dz_0 + \int_{z_1}^{z_2} \sigma_n(z,z_0) b_n(z_0) dz_0 = f_n(z) \tag{3.7}$$

$$\int_{z_1}^{z_2} \frac{b_t(z_0)}{z-z_0} dz_0 + \int_{z_1}^{z_2} \sigma_t(z,z_0) b_t(z_0) dz_0 = f_t(z_0) \tag{3.8}$$

where the n and t subscripts refer to the normal and tangential components with respect to the crack, f_n and f_t are the stresses due to the external load, and the non-singular parts of the potentials are denoted as σ_n and σ_t. The first term in each of these equations represents the Cauchy singular portion of the stresses (as noted above), and the second term contains the nonsingular parts. The normal and tangential cartesian stress components can be determined using a standard trigonometric transformation. The solution to this problem is non-unique, however, until one more

condition is met, that of crack closure. Simply stated, the crack must close, or the crack opening displacements must be identically zero at the two endpoints or crack tips. This condition can be stated in the formulation of this problem as follows:

$$\int_{z_1}^{z_2} b(z_0)dz_0 = 0 \quad (3.9)$$

If this condition is met, there will be a single, unique solution to the unknown distribution of dislocations.

Furthermore, if equations 3.7 and 3.8 are rewritten in terms of the polar form of a vector from z to z_0 as follows:

$$\hat{z} = \sqrt{z-z_0}e^{i\theta} = \rho e^{i\theta} \quad (3.10)$$

where the singularity is explicitly shown as ρ goes to zero, the stress due to the Cauchy singular portion of the above integral equation can be determined, in terms of the angle θ (the angle of the crack, as shown in figure 3.2), as follows:

$$\sigma_{yy} = \frac{1}{\rho}[b_y(\cos\theta + \cos 3\theta) - b_x(3\sin\theta + \sin 3\theta)] \quad (3.11)$$

$$\sigma_{xx} = \frac{1}{\rho}[b_y(3\cos\theta - \cos\theta) - b_x(\sin 3\theta - \sin\theta)] \quad (3.12)$$

$$\sigma_{xy} = \frac{1}{\rho}[b_y(\sin 3\theta - \sin\theta) + b_x(\cos 3\theta + \cos\theta)] \tag{3.13}$$

This permits calculation of the x and y components of the dislocation vector (Burger's vector) for a straight crack in any orientation.

Once these integral equations have been written, a numerical treatment must be used to solve for the unknown distributions of dislocations in the x and y directions, b_x and b_y. There are several treatments to this problem that have been published in the literature, all of which use a polynomial approximation of the unknown function. The numerical technique used in this work was proposed by Gerasoulis [15] in 1980. This technique uses a piecewise quadratic polynomial representation of the singular and non-singular parts of the integral equation, and reduces the integrals to a discretized set of algebraic equations well suited to a matrix type solution. However, in order to use the technique, first some assumptions about the nature of the singularities at the tips of the crack must be made. Following the method of fracture mechanics, it can be shown that the stresses at the crack tips become singular as $1/\rho^{1/2}$. The dislocation density will therefore also exhibit this square root singularity at both ends, and can be written in the following form:

$$b(s) = \frac{g(s)}{\sqrt{1-s^2}} \tag{3.14}$$

where $s = 2(z - z_1)/(z_2 - z_1) - 1$. The functions g(s) are therefore continuous and bounded along the interval $s \in [-1,1]$. Also, in general, the solution to the singular part of the integral equation is not unique, and an additional condition is required. In the present work, that condition is that the crack must close at the crack tips. Mathematically, this means that the value of the integral along the interval from -1 to 1 of the unknown distribution of dislocations (g(s)) must be zero.

For a given crack discretization parameter n, the numerical technique provides 2n+1 integration points and 2n collocation points, as follows:

$$\sum_{i=1}^{2N+1} [w_i(\xi_j) + v_i K(\xi_j, s_i)] g(s_i) = f(\zeta_j) \qquad (3.15)$$

$$j=1,2, \ldots ,2N$$

where the w's are the weighting functions that are applied to the singular part of the integral, the v's are the coefficients of the non-singular kernel (K), the i's are the integration points, and the j's are the collocation points. The weight functions $w_i(s)$ and v_i are calculated by using the LaGrange interpolation formula for three points to approximate the unknown bounded function in the case of the w's, or the unknown function multiplied by the kernel (K(s,t)) in the case of the v's, with the singularity explicitly removed, and integrating (summing) along the interval. The final expressions for the coefficients that make up the weight functions are rather complicated, and are found in the paper by Gerasoulis, and therefore will not be restated here.

The calculation of the unknown g(s), then, amounts to the creation of a matrix of the weighting functions, w(s), added to the non-singular kernel multiplied by the weighting functions v, in the form [A]{x} = {b}. As stated previously, the matrix [A] is not a square matrix, or there are 2n+1 equations with 2n+2 unknowns until the condition of crack closure is added by multiplying the non-singular weight function by the cosine or sine of the local angle and placing that value in the last row of the matrix, as follows:

$$A(2N+2\ ,\ j)=V_i(j)\ C_n \quad (3.16)$$

where C_n denotes the sine or cosine of the local angle of the crack. The solution then requires inversion of the matrix [A], and multiplying by {b}, the forcing function, to determine the unknown {x} or in this case, {g(t)}. Gerasoulis states that the method works equally well for unequal meshes, but in this work, the spacing was kept equal for simplicity in coding of the algorithm. A value of n above 6 was found to be unnecessary for crack lengths on the order of the size of the inclusion.

3.3 Results and Comparison to Previous Work

Figures (3.3) through (3.9) are shown to compare and contrast the results of the solution of a straight crack interacting with an elliptical inhomogeneity with those previously published. These results are original, and are reported in Patton and Santare [16]. In all of these figures, the results are presented in terms of the

normalized Mode I stress intensity factor. This stress intensity factor is normalized as follows:

$$normalized\ k_I = \frac{K_I}{\sigma_\infty \sqrt{L}} \tag{3.17}$$

where the stress, σ_∞ is the applied load on the infinite medium, the crack length is L, and the Mode I stress intensity factor is in the numerator. The normalization in this equation means that without the presence of an inclusion, the normalized stress intensity factor will have a value of one, or the stress intensity factor will be the same as that for a crack in an infinite medium without an inclusion.

Since the greatest interest in this work is with the crack tip closest to the inclusion, all results reported are for the stress intensity factor for the tip closest to the inclusion. Also, to make comparisons between different results meaningful, some of the specific geometry parameters are held fixed for the reported results. Specifically, the value of R (the size of the inclusion) was held fixed at unity, as was the length of the crack. For results reported for a rigid inclusion, Muskhelishvili's constant, κ, is held at a value of 1.67. Also, the shear modulus, μ, does not require formal specification as a result of the normalization procedure. Therefore, as m (the ellipticity ratio) is varied, the values of a and b from Figure 3.2 can be calculated using equations 3.2 and 3.3 for all of the results presented in this work. It was discovered during the course of this investigation that a crack length of approximately the size of the inclusion provided results both to compare with previous results, and also to make

the effect of the other crack tip on the results nearly negligible. By this it is meant that the results for a unit length crack interacting with a unit circular inclusion gave results that varied very little from a crack of length 10 or 100, when normalized according to equation 3.17, interacting with the same inclusion. Since the intention is finally to create a path prediction model, with the crack tip closest to the inclusion exhibiting growth, this result is meaningful in that the effect of the far crack tip is minimized in that prediction model.

The problem of a circular inclusion was treated by Atkinson [6] and by Erdogan and Gupta [8], and that for the elastic line inclusion by Grief and Sanders [11]. These are, of course, both extremes of the solution for the elliptical inclusion, and provide a good comparison. In the paper by Grief and Sanders, the integral equation is formulated somewhat differently, in that only the interaction terms are taken into account. The present solution takes into account not only the interaction terms, but also the stress singularities at the tips of the crack. The results of that paper therefore have to be added onto the stress due to the singularities to provide a comparison. That has been done, and the results for a rigid inclusion with a range of ellipticities (m) are shown in Figure (3.3). In this figure, the crack is oriented horizontally, aligned along the real axis (x-axis), and is at varying distances (d) from the edge of the inclusion. The curve in the figure labeled as m=0 (a circular inclusion) reproduces the results of Atkinson. A comparison of the two sets of results is given in Table 3.1. In the work by Grief and Sanders, rather than presenting stress intensity

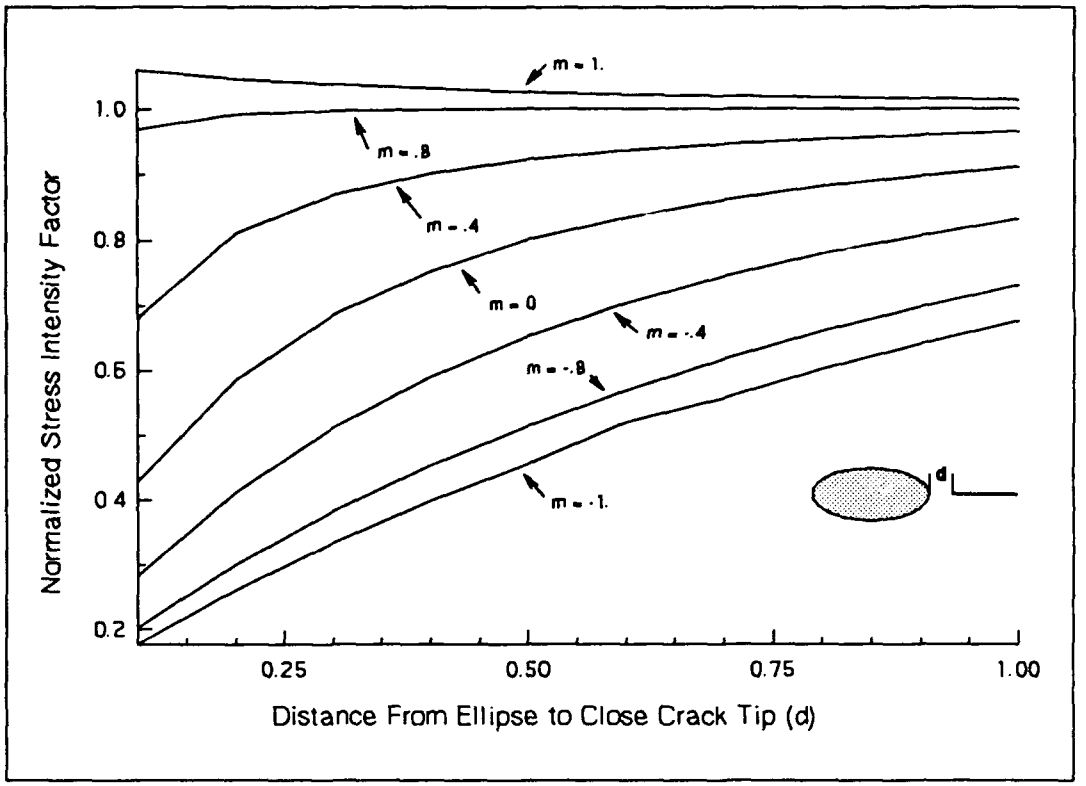

Figure 3.3. Stress intensity factor versus distance from ellipse for a radially oriented crack and varying ellipticity ratios (load normal to crack, R=1., L/R=1., κ=1.67).

factors, they present a ratio of the stress if the interaction between the crack and the line inclusion (stringer) is taken into account versus the stress if that interaction is not present. They also present results for an elastic stringer, rather than a rigid one. Therefore, if in the present analysis, such a ratio is calculated, it would represent the limit as their analysis approached a rigid stringer. Those results are shown in Table 3.2, where their flexibility parameter, Λ is varied from a value of 10 (flexible stringer) to 0.1 (stiff stringer), and compared to the rigid or limiting case presented in this work in which it would have the value zero. These results are reasonable and follow the

Table 3.1. Comparison of present results with those of Atkinson

Distance From Inclusion	Atkinson	Present Solution
.1	.43	.4276
.2	.58	.5867
.3	.68	.6857
.4	.76	.7527
.5	.80	.8002
.6	.84	.8353
.7	.86	.8619
.8	.88	.8825
.9	.90	.8988
1.0	.91	.9119

trend reported in the Grief and Sanders paper.

Figure (3.3) clearly shows the effect on the stress intensity factor due to the presence of the inclusion, and the effect of both the shape and orientation of the inclusion. For those inclusions that are long and slender, aligned normal to the crack (negative m's), the effect called crack shielding is predominant. This phenomenon, the lessening of the Mode I stress intensity factor due to the presence of an inclusion, called crack shielding, is exactly the phenomenon postulated to be the toughening mechanism attributed to inclusions. It is also interesting to note that there is slight anti-shielding, or a slight increase on K_I when a line inclusion is oriented in the same

Table 3.2. Comparison of present results with those of Grief and Sanders

Distance From Inclusion	Grief and Sanders (Λ = 10.)	Grief and Sanders (Λ = .1)	Present Work (Λ = 0)
.05	.92	.67	.5279
.1	.96	.78	.6619
.15	.975	.85	.7517
.2	.98	.88	.8159
.25	.985	.92	.8627
.3	.99	.94	.8974
.35	.99	.955	.9232
4.	.99	.96	.9428

direction as the crack. In a path prediction, one would expect that the rounder inclusions or inclusions oriented normal to the path of the crack would deflect the crack, whereas a line inclusion, or a long, thin inclusion oriented in the same direction as the crack would tend to attract the crack, because of this shielding or anti-shielding effect.

Figure (3.4) shows similar results to Figure (3.3) except that in this figure, the inclusion is an open hole. Muskhelishvili [3] noted, in his work, that if the material parameter, κ, was set to a value of -1, which is physically unrealistic, the solution to the rigid inclusion problem becomes that for an open hole. In Figure (3.4),

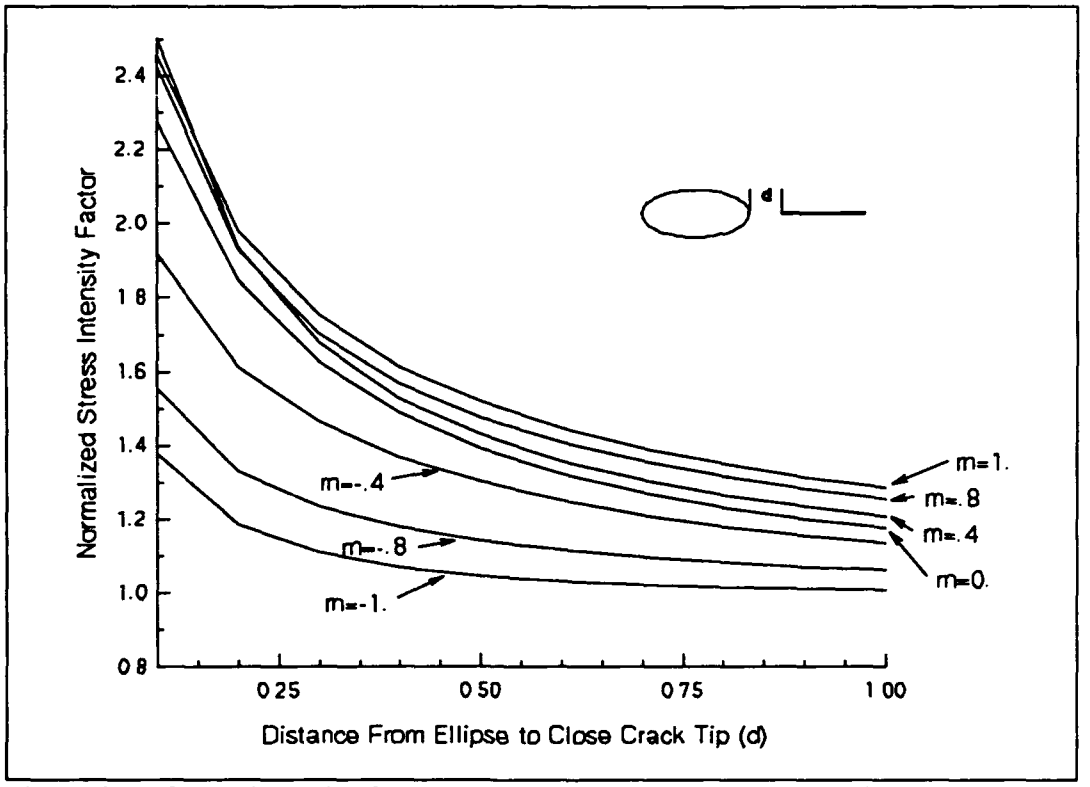

Figure 3.4. Stress intensity factor versus distance from open hole for a radial crack and varying ellipticity ratios (load normal to crack, R=1., L/R=1., κ=-1.)

then, the parameter, κ, is set to a value of -1, and the results are for open holes with varying ellipticity ratios. Note that the character of this figure is opposite that of the previous figure, in which the inclusion is rigid, in that as the close crack tip approaches the open hole, the stress intensity factor increases. If, therefore, an inclusion would be expected to deflect a crack because of shielding, a hole would be expected to attract a crack because of anti-shielding. This is physically reasonable, and has been seen in practice.

Figures (3.5) through (3.9) show interesting results of the solution for

differing cracks at differing orientations interacting with differing inclusions. Figure (3.5) shows results for a radial crack ($\theta = \alpha$ in Figure 3.2) at several different orientations interacting with an inclusion with varying ellipticity ratios. The distance from crack to inclusion is held constant in this figure at a value of 0.1R where R = (a+b)/2, and again, R and the crack length are held at a value of one. For a circular inclusion, this distance, d, is 0.1 times the radius of the circle. Note that for a relatively flat ellipse, or for a value of m greater than 0.5, the location of the close tip of the crack varies rapidly with small changes in the orientation angle α. This effect is shown schematically on the figure. In effect, once the crack is rotated slightly from the x-axis, it is shielded by the flat side of the ellipse. This phenomenon is most striking at the higher ellipticity ratios (m=.9).

Figure (3.6) presents an interesting result of the shielding effect of a flat ellipse. In this figure, the ellipticity ratio is held constant at a value of 0.9, and the distance of the close tip of the crack from the inclusion is varied for three different angles. The angles shown are very small, not exceeding 4 degrees, showing that very small changes in orientation of the crack can have very drastic changes in the stress field at the close tip of the crack. There is a 30 percent reduction in the stress intensity factor for an angular rotation of only 2 degrees, if the crack is shielded by the ellipse. As the close tip of the crack is moved away from the inclusion, it becomes unshielded, and asymptotically approaches the stress intensity factor for a crack at an orientation angle of 0 degrees with respect to the inclusion (see figure 3.2). This

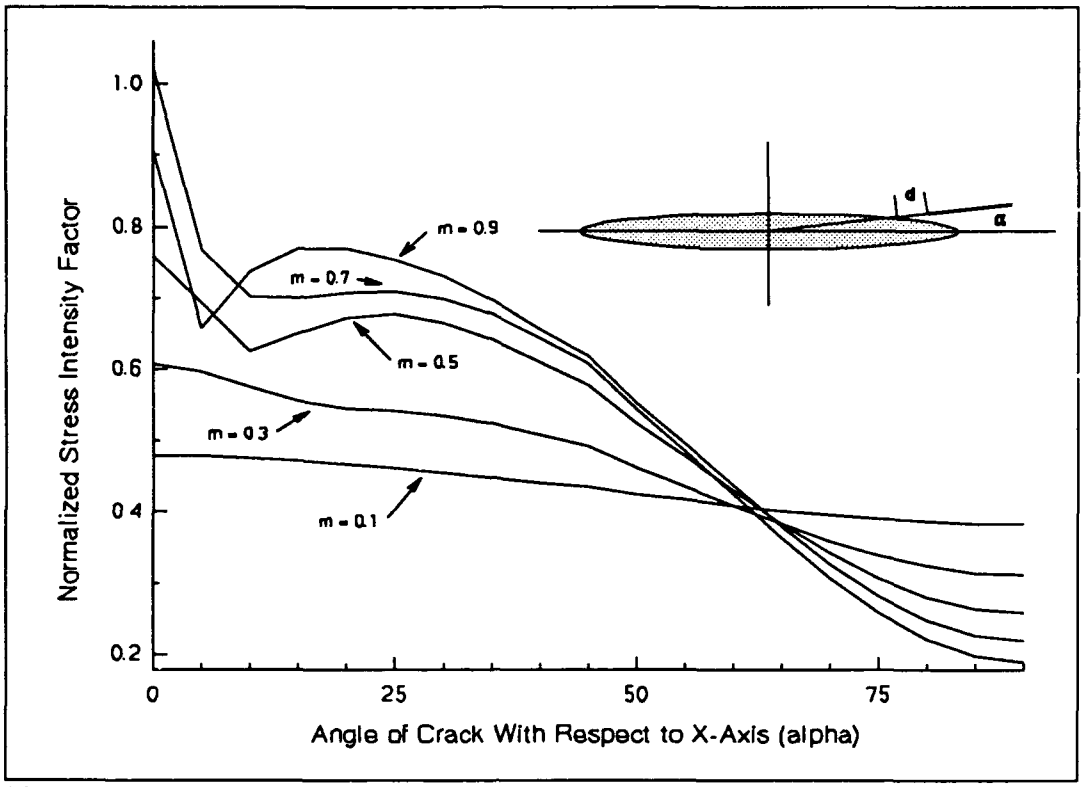

Figure 3.5. Stress intensity factor versus alpha for a radial crack and various ellipticical inclusions (load normal to crack, R=1., L/R=1., κ=1.67).

shielding is an expected result, and should provide the impetus for deflection of the path of a naturally growing crack. That is, of course, the final result of this research, and it will be discussed in that section of this document.

In Figure (3.7), a different approach was taken with regard to the location of the tip of the crack which is closest to the inclusion. In this figure, the distance held fixed is that from the close tip of the crack to the origin rather than to the elliptical inclusion. Again, the crack is oriented radially with respect to the origin, and normalized stress intensity factors are plotted for three different ellipticity ratios versus

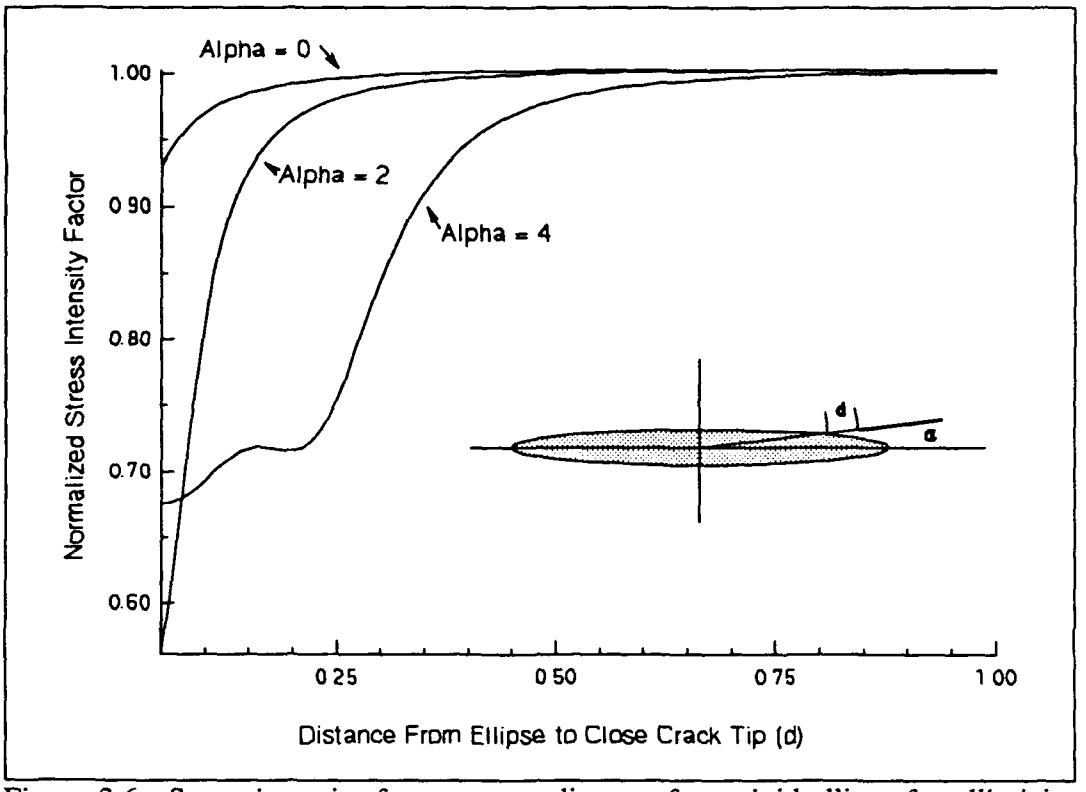

Figure 3.6. Stress intensity factor versus distance from rigid ellipse for ellipticity ratio of 0.9 and small alpha (load normal to crack, R=1., L/R=1., κ=1.67).

the angle that the crack makes with the x-axis. The distance from the close tip of the crack to the origin is held at a value of 2.1R, so that the elliptical inclusion with an m of 1.0 (line inclusion), with the crack at an angle of 0 degrees will give a distance from the crack to the inclusion of 0.1R. Note that there is still shielding of the crack, but since the close tip of the crack is at a much greater distance from the ellipse than in the previous figures, the shielding effect is much less pronounced.

Figure (3.8) is the only one in which the crack is not oriented radially with respect to the origin. In this figure the crack is either horizontal (Theta = 0.) or

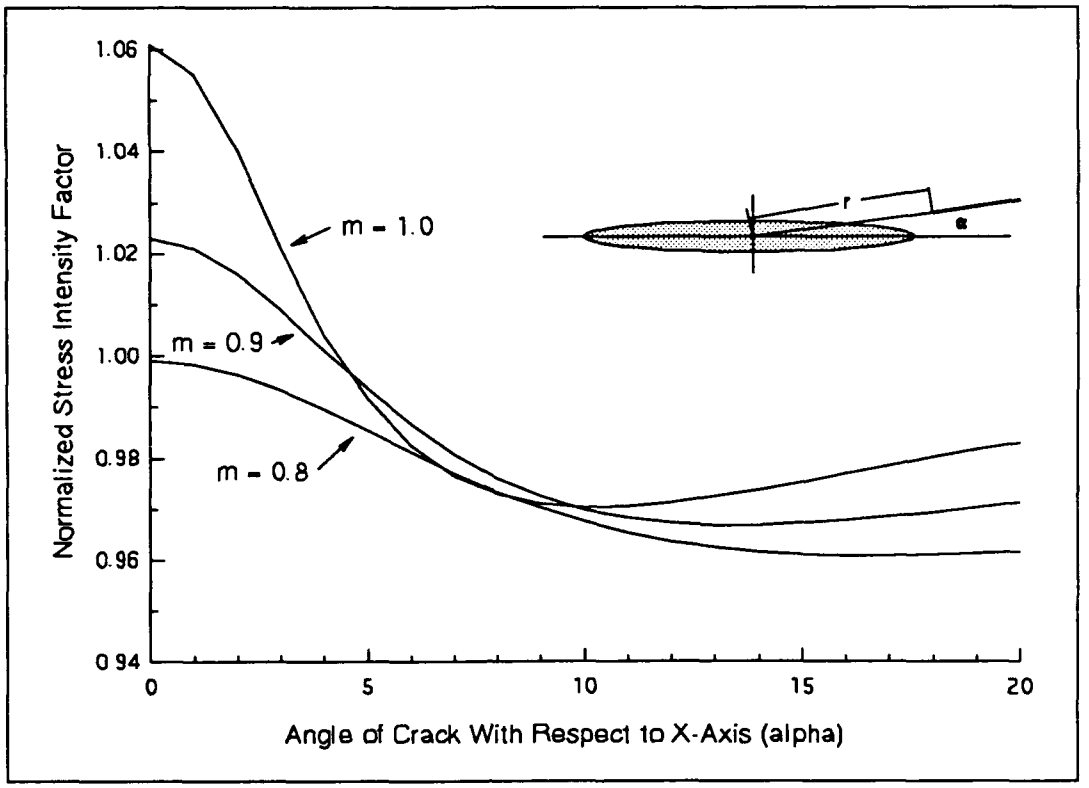

Figure 3.7. Stress intensity factor versus alpha for varying ellipticical inclusions with crack constant distance from origin (load normal to crack, R=1., L/R=1., κ=1.67).

vertical (Theta = 90.), and the normalized stress intensity factor is plotted against the x-coordinate of the close tip of the crack. The y-coordinate of the close tip is held at a value of 0.5R, and the ellipse has an ellipticity ratio of 0.8. A similar result was presented for the circular inclusion by Erdogan, Gupta, and Ratwani [7] for a circular inclusion, and if the ellipticity ratio is held at a value of 0.0, the present technique matches their results. Note in this figure that the crack becomes unshielded at an x-coordinate of approximately 1.8R, as one would expect, as that location is the right edge of the elliptical inclusion.

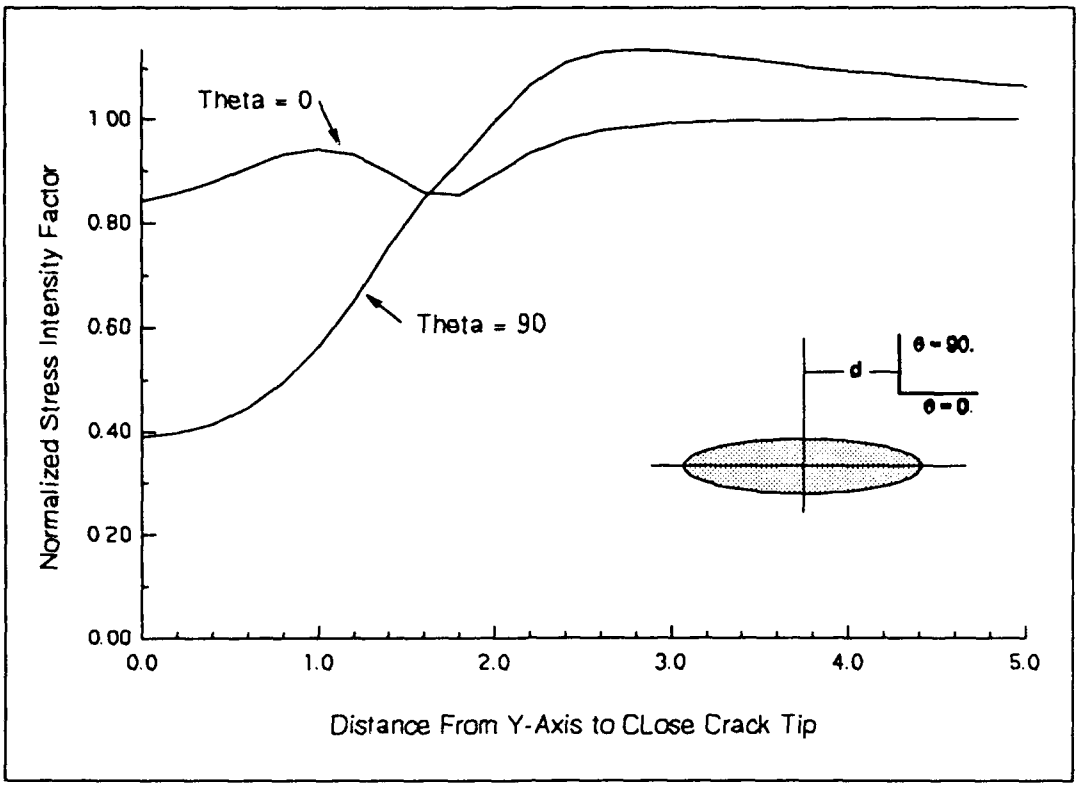

Figure 3.8. Stress intensity factor versus distance from y-axis for vertical and horizontal cracks (theta = 0 or 90, load normal to crack, R=1., L/R=1., κ=1.67).

The last figure of the series, Figure (3.9) shows the effect of varying the direction of the applied load with respect to the crack. In this figure, the distance between the inclusion and the crack was held fixed at d=.1R. The orientation and elevation of the crack was also held fixed, at θ=0, and the crack aligned along the x-axis. The direction of the applied load on the crack was varied from a value of 0 degrees to 90 degrees, for two ellipticity ratios, m=.4 and .7, and for two different inclusions, a rigid inclusion, where κ is greater than 1, and an open hole, where κ=-1. Note that the results for interaction with an open hole are significantly different than

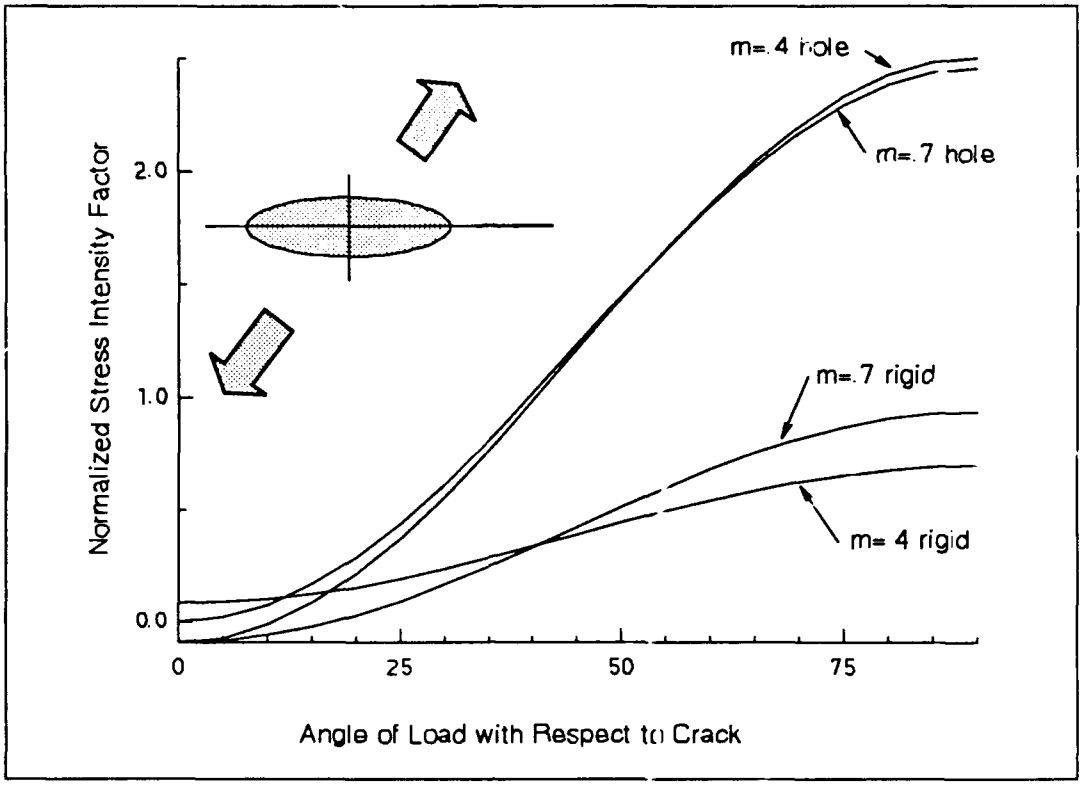

Figure 3.9. Stress intensity factor versus angle of applied load for rigid inclusions and open holes (R=1., L/R=1., d/R=.1, κ=1.67 or -1.)

those for a rigid inclusion, but that the trend with changing load angle is the same for all curves. The Mode I stress intensity factor increases to a maximum when the applied load is normal to the crack, as would be expected. This figure also portrays another interesting phenomenon, and a limitation to the numerical treatment of the problem. As the angle between the load and the crack approaches zero, note that the Mode I stress intensity factor does not identically approach zero for three of the four cases shown in the figure. In fact, for two of the cases, the stress intensity factor becomes less than zero. A negative Mode I stress intensity factor denotes

compression, and physically represents crack face overlap. Mathematically, what is presented is correct, but physically, the two crack faces cannot overlap. To exclude overlap in the numerical procedure would necessitate an iterative solution procedure which would look for the possibility of the two crack faces touching, and elimination of that portion of the crack from the solution. That procedure has not been implemented in the present solution. Also note that there is one case in which the Mode I stress intensity factor is greater than zero for a load parallel to the crack. This is both physically and mathematically correct, as the presence of the inclusion can cause a tensile stress to act on the crack even when the load is in the same direction as the crack.

The results presented in this section, which are original, both verify the solution for a straight crack interacting with a rigid elliptical inclusion, and also provide some interesting motivation for the prediction of the path of the crack near the inclusion. These results are valid, however, only for a crack which is straight. They cannot be applied to a crack with curvature, because as the crack curves, that curvature provides another component of stress which is not accounted for in the present method. In essence, the problem is a non-linear one in that the crack path is not straight. The method presented so far in this work is linear, and is to be used to solve a non-linear problem. The next chapters in this work will describe the means that were created to allow the incorporation of this non-linearity into the present solution, and therefore to incrementally predict the path of the quasi-statically growing crack. The discussion and the results that are presented are original.

Chapter 4

CRACK CURVATURE AND EXTENSION

4.1 Crack Kinking Solutions

As described in the survey of pertinent literature, there are several solutions to the kinked crack problem. Probably the one most referenced recently, and most commonly regarded as correct is the one published by K. K. Lo [24] in 1978. His solution unified the kinked crack problem by providing correct results for both the finite crack extension, and an infinitesimal crack extension. At the time, there was a good deal of discussion in the literature about this problem, as described in the literature review portion of this work, and there was also a good deal of controversy. Since that time, Lo's solution has been accepted as being correct, and has been referenced by many authors. His results match those of previous authors such as Kitigawa et al. [23] for the finite crack extension, and Bilby and Cardew [18] for the infinitesimal crack extension.

The solution proposed by Lo is one which maps the kinked crack onto a circle using a conformal mapping technique. He then calculates potentials for the

crack in the mapped space, solves the problem in the mapped space, and remaps the solution onto the kinked crack. His mapping is conformal, but is not the same mapping as that used in the present solution that maps an elliptical inhomogeneity onto a circular region. The solution proposed by Lo, therefore, cannot be used directly in the present work. Lo's results, however, can be used to verification the results of the present solution once that solution is found.

Another interesting solution to the kinked and curved crack problem is that proposed by Sur and Altiero [34]. In their solution, as described in the review of pertinent literature in the introduction, the unknown function is the crack displacement itself rather than the derivative of that displacement, or Burger's vector. In this way, the singularities at the tips of the crack and at the kink are avoided. Results are presented for this method which are in excellent agreement with other published results.

4.2 First Order Perturbation Solution

In the early 1970's, a group of Russian mathematicians [25, 26, and 27] solved the problem of a crack with a slightly curved extension, as shown in Figure 4.1. The straight portion of their crack extended to the right of the origin, and the curved extension extended to the left, as shown in the figure. In a sense, this solution avoids the problems of the weak singularity at the kink by assuming that the crack is smoothly curved, and therefore is not singular at the kink. They used the complex

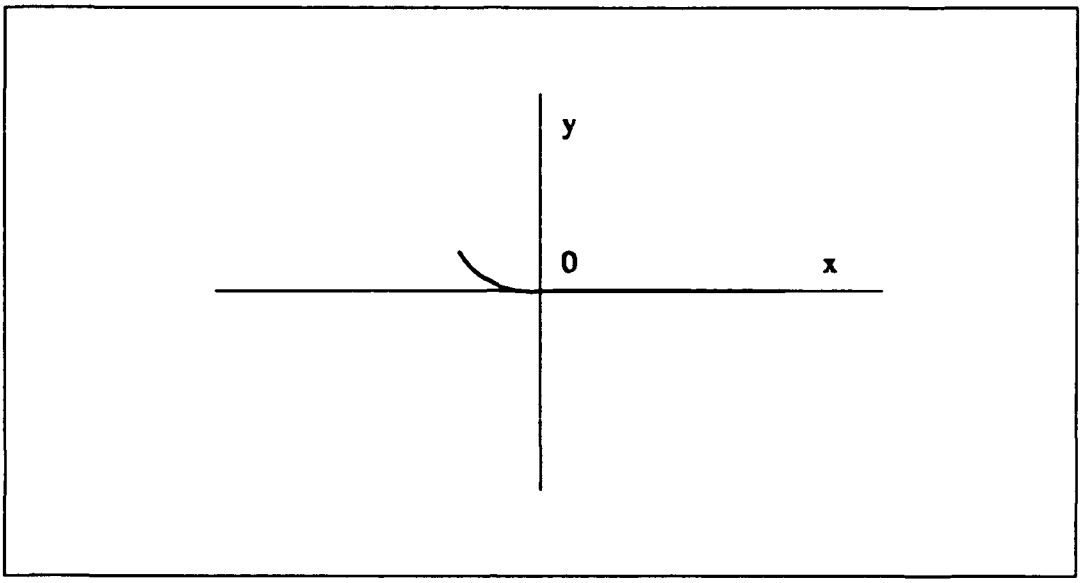

Figure 4.1 Schematic of crack problem solved by First Order Perturbation.

potential methods of Muskhelishvili, and wrote an integral equation that describes the singular and non-singular parts of their solution. Their solution requires knowledge of the local spatial derivatives of the crack, as a result of using perturbation methods. What results is an integral equation in exactly the same form as that used in the present method, with the singular and non-singular parts separated from each other, and with a forcing function applied along the crack on the right hand side of the equation. Their integral equation can be restated as follows:

$$\int_{-1}^{1} \frac{b(\tau)}{s-\tau} d\tau + \int_{-1}^{1} R(s,\tau) b(\tau) d\tau = \sigma^*(s) \tag{4.1}$$

where the integral is given on the interval from -1 to 1 as is done in most numerical crack solution methods, including Gerasoulis' method, and the star on the forcing

function denotes that the stress is normalized and also given on the interval from -1 to 1. The elements of their kernel, denoted as R(s,τ) are given as follows:

$$R_{nx} = \frac{Y[y^{*2} - 1 - y'(x)y^{*}(3+y^{*2})]}{(1 + y^{*2})^2} - y^{*'}$$

$$R_{ny} = \frac{Y(y^{*2}-1)(y^{*}-y'(x))}{(1 + y^{*2})^2}$$

$$R_{tx} = \frac{Y[y^{*}(3+y^{*2}) + y'(x)(y^{*2}-1)]}{(1 + y^{*2})^2} \qquad (4.2)$$

$$R_{ty} = \frac{Y(y^{*2}-1)(1+y'(x)y^{*})}{(1 + y^{*2})^2} + y^{*'}$$

where the capital letters and stars have significance as follows:

$$y^{*}(s,\tau) = \frac{y(s)-y(\tau)}{s-\tau}$$

$$Y(s,\tau) = \frac{y'(s)-y^{*}(s,\tau)}{s-\tau} \qquad (4.3)$$

in that they are approximations to the first and second derivatives of the y-coordinate along the crack. The prime notation is understood to be differentiation with respect to the crack. The n and t subscripts refer to the local normal and tangential directions along the crack, and the x and y subscripts refer to the x and y components of the Burger's vector. Close inspection of the four elements of this kernel reveal that the quantities in the numerator of each term are functions of the spatial derivatives and approximations of the spatial derivatives taken along the length of the crack, and the denominator is the square of the length of the curved crack. What this set of equations

contains, therefore, is an additional set of terms which take into account the curvature of the crack, and can be directly superposed upon any straight crack solution that has a similar form, to mimic the effect of the weak singularities inherent in crack kinking and curving. In the present work, the stresses that can be calculated with this set of equations are merely superposed upon the straight crack solution for a curved crack.

However, before the method can be applied to the current solution with an elliptical inhomogeneity, local spatial first and second derivatives along the crack must be calculated for use in Equation 4.2.

4.3 Parameterization of Crack - Cubic Spline

The simplest method of providing these derivatives is to borrow a technique from the design of curves and surfaces, the notion of a spline. A spline is merely a set of smoothed polynomial interpolation functions which are used to evaluate a function at any point along an interval, if the function is only known at discrete points on that interval. The functions used are smooth in the sense that the first derivative is continuous along the interval, and are independent of where the function is known or is to be evaluated. Splines have been used intensively in Computer Aided Design for the description of space curves and surfaces. A quadratic spline uses a second order polynomial to describe a curved line segment, a cubic spline uses a third order polynomial, and other splines use other orders and types of polynomials. By far the simplest splines are quadratic and cubic splines. Since a spatial second derivative

along the crack is needed, the cubic spline is the simplest choice, as the cubic polynomial which describes the line segment has four independent constants which can be varied. This is the correct number for the boundary conditions that are imposed on the endpoints of the spline. These conditions are that each endpoint of an interval must be connected to the endpoint of the next interval, and the first derivative must be continuous from one interval to the next, or there must be a smooth transition from one interval to the next with no kinks in the graph of the function. This lack of kinks in the graph of the function makes the spline a good match for the first order perturbation solution which also avoids kinks. Therefore there are two conditions at each end of each interval, producing a total of four conditions which must be satisfied. There are other types of splines which are relatively difficult to program, but that can describe extremely complex shapes. These spline functions are not necessary for this work, as the crack path will be reasonably smooth. Fortunately, there are subroutines that are widely available for fitting a cubic spline to a set of x and y points. The spline routine in [44] is a very good example. The algorithm which parameterizes the crack for the solution provides a set of x and y coordinates at the integration and collocation points along the crack. These locations are input directly into the spline routine, which calculates the second derivative at each location where there is a point. The distribution of first derivatives is calculated by assessing the local tangent to the crack at each of the integration and collocation points. These values are then sent to a subroutine which uses them to calculate the terms in equations 4.2.

4.4 Crack Extension

Once these results have been generated, the algorithm for extending the crack is relatively simple. At each integration point and collocation point, there is a local value of **z**, or a local position along the crack, which has x and y components. There is also a local value of the angle of the crack ϕ, which is initially, when the crack is straight, equal to θ, the initial crack angle. There is also a set of first and second derivatives along the crack which are calculated using the spline routine as described above. There is also a parameter n which describes the size of the matrix, and the number of integration and collocation points. There are 2n integration points and 2n+1 collocation points which describe the crack. Since the computer will not allow integers to be incremented by a value of 0.5, at some increment of crack extension, n must increase by 1, as this is the basis for describing the size of the problem. This really is a consequence of using the method of Gerasoulis, as his equations are based upon this parameter, n. Incrementing n by 1 will add two integration points and two collocation points to the crack parameterization. What is needed, then, is to decide how to add these points to the crack parameterization. The locations of the integration and collocation points are stored in complex arithmetic arrays in the computer, in order of where they are located along the crack. The values at the beginning of the arrays are at the close tip of the crack, and the values at the ends of the arrays are at the far tip of the crack. Since it is growth at the close tip of

the crack that is of interest, all of the values of the crack parameterization (integration and collocation points) need to be shifted down two locations in their respective arrays on the computer. This is done by starting at the end of the arrays, adding 2 to the maximum extent of the array, and copying the value from two locations before that location into the current location. In this way, all of the old values are shifted down 2 spots in the arrays. Two new values can then be added at the beginning of the arrays for the **z** location of the new close crack tip, for the local angle ϕ, and for the local first and second derivatives. This increment of crack extension will therefore be of length 1/n, and can be at any reasonable angle chosen. This technique is similar to incrementing pointers in the Pascal and C computer languages. Fortran, unfortunately, does not share this data type with these two other languages, and slightly more coding is required to implement this array shifting.

4.5 Results and Comparison to Previous Work

The results of the implementation of the solution described above are given in Figures 4.2 and 4.3. These figures give results respectively for the Mode I and Mode II stress intensity factors, in an infinite medium with no inclusion, for an asymmetrically kinked crack for three different angles. The crack is asymmetrically kinked in that it has a kink at only one end, as shown on the figures. These results compare favorably to Kitigawa et al. [23] and to the more recent results of Sur and Altiero [34]. The results given by Kitigawa et al. were verified by Lo [24], and were

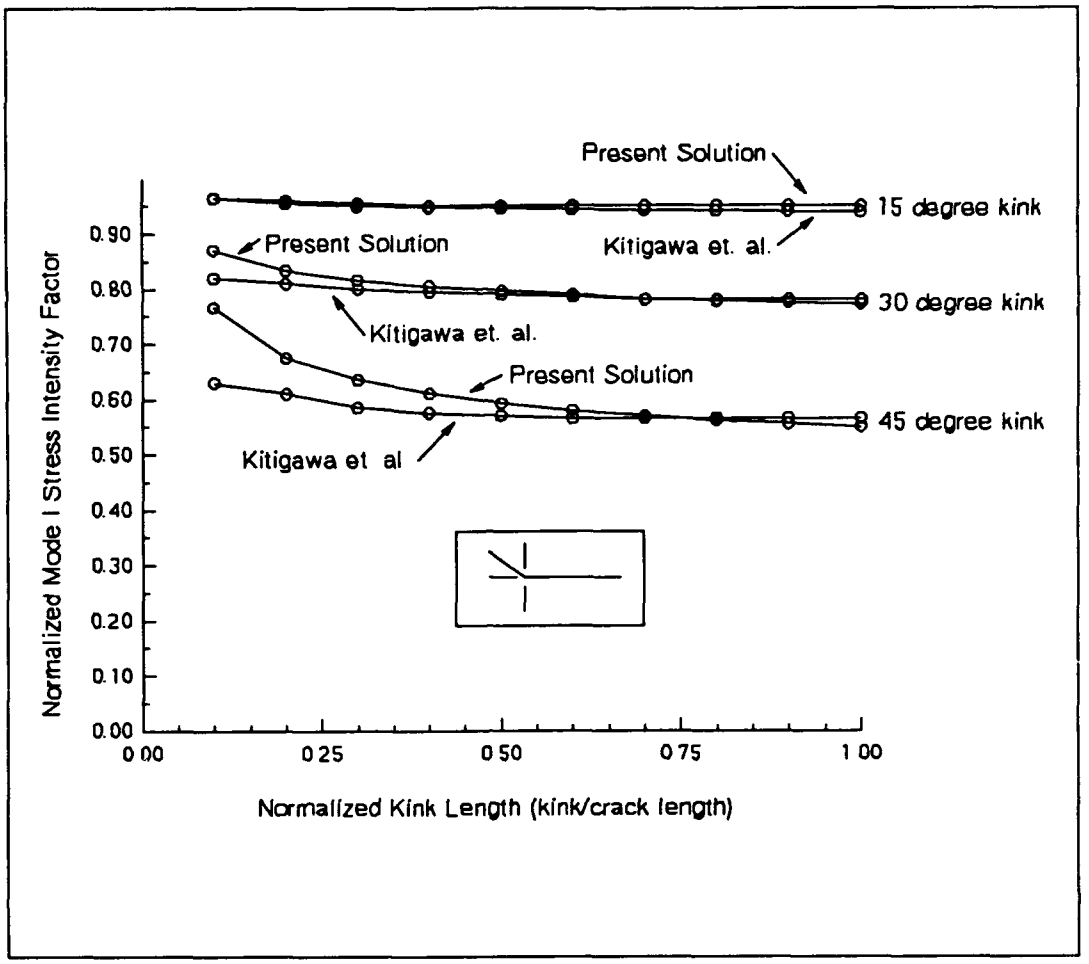

Figure 4.2. Normalized Mode I stress intensity factor versus normalized kink length for three different kink angles, with no inclusion.

used as a verification of Sur and Altiero's work. Note that the results of the present study are in good agreement with those previously published results, especially for small kink angles. This is a very encouraging result, as the formulation using the first order perturbation solution and the cubic spline crack description does not explicitly handle the singularity at the kink. In fact, the present solution is really for a curved crack rather than for a kinked crack. One can see, however, that the results of the

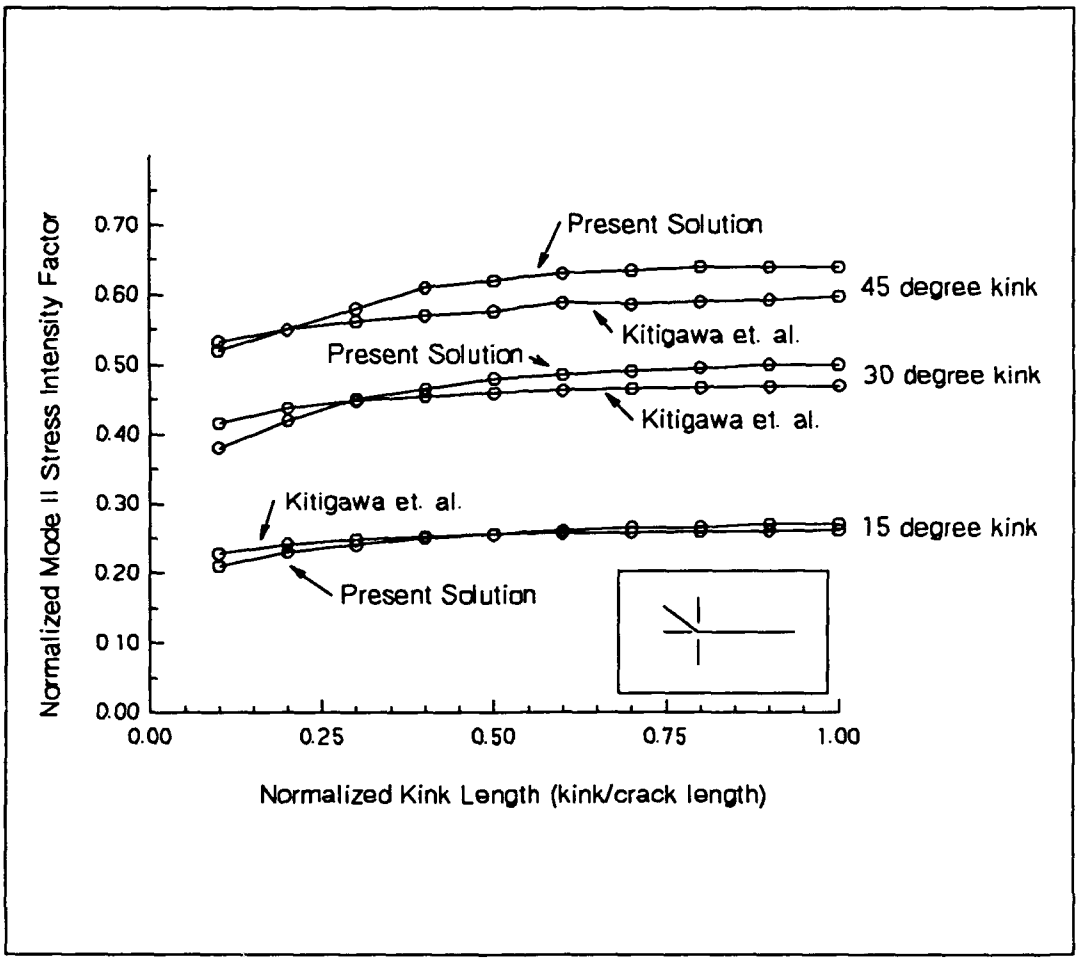

Figure 4.3. Normalized Mode II stress intensity factors versus normalized kink length for three different kink angles, with no inclusion.

present solution match the published kinked crack solutions quite well for kink angles less than about 30 degrees. The results for a kink angle of 45 degrees are not in as good agreement, and in fact fail to capture the singularity as the kink length becomes small with respect to the crack length. Fortunately, it is expected that the curvature of a naturally growing crack will be smooth, and therefore that any kink angles will be small. The first order perturbation solution, therefore, seems to give good results,

and allows the approximation of the weak singularities due to crack kinking without explicitly describing that weak singularity.

Chapter 5

CRACK PATH PREDICTION

5.1 Review of Crack Propagation Laws and Selection of Proper Criterion

There are several means which have been proposed to predict the direction of the onset of crack propagation. Most of these fall into two categories, stress methods and energy methods. Several authors [36, 37, 38, and 17] have proposed a criterion for growth which is called the Maximum Normal Stress Criterion, in which one looks for the direction where the Mode I stress intensity factor is greatest, and concludes that the crack propagates in that direction. Other authors [39, 40, 41, and 43] have proposed what has come to be called the Maximum Strain Energy Release Rate Criterion, in which one calculates the direction at which the maximum energy is released, and then concludes that the crack propagates in that direction. A very good review of those two major classes of crack propagation criteria, and some less well known ideas, is given by Palinaswamy and Knauss [17]. These authors correctly state that, for isotropic materials, and for cracks whose kink angle is fairly small (less than about 30 degrees), the two criteria produce identical results. Actually, there has been

a significant amount of controversy over which criterion is correct. The two criteria begin to diverge when the angle between the load and the crack is greater than 30 degrees. There have been several experiments performed in attempts to settle this controversy, with limited results. The divergence between the two criteria is a maximum when the load is parallel to the crack, a condition where the Maximum Stress theory predicts a kink angle of 70.5 degrees, whereas the Maximum Strain Energy Release Rate criterion predicts an angle of 77.4 degrees. Several authors have produced figures which portray this divergence, and also show the scatter of experimental data (Williams and Ewing [39], Finnie and Saith [40], Ewing and Williams [41], and Wu [42]). The controversy has not yet been settled. For this work, however, the fact that it is expected that the curvature of a naturally growing crack will not exhibit even a 30 degree kink leads to the conclusion that either criterion will be acceptable for the present discussion.

What results then, is the selection of which criterion best suits the crack path prediction algorithm. The strain energy released by an increment of crack growth can be calculated as follows:

$$\frac{G}{G_\infty} = \frac{K_I^2 + K_{II}^2}{(\sigma\sqrt{\pi a})^2} \tag{5.1}$$

where both the energy and the stress intensity factors are normalized to the value corresponding to the stress intensity of a finite crack in an infinite medium that is not under the influence of an inclusion. Since, in the direction of crack growth, the value

of the Mode II stress intensity factor is nearly zero, and the value of the Mode I stress intensity factor changes very little, there will be very small changes in the strain energy calculated as the square of a number close to one added to the square of a number close to zero. In fact, for a change in direction of as much as 5 degrees, the strain energy changes less than 1 percent. On the computer, looking for a local maximum of a number that is changing by about 0.1 percent per iteration is a very difficult task.

The application of the Maximum Normal Stress Criterion, requires that the Mode II stress intensity factor be made to come as close to zero as possible. This stress intensity factor may, in some situations, not identically equal zero, as there may be a Mode II component that is present in any case. That, in fact, is the situation that arises in this problem, there is a small amount of Mode II loading present just because of the presence of the inclusion. The application of that criterion, therefore, is implemented as a search for the direction in which the Mode II stress intensity factor is an absolute minimum in magnitude. It is reasonably simple to find an absolute minimum on the computer, rather than a relative maximum. For this reason, really one of simplicity, the algorithm which predicts the path of the crack searches for the angle at which the Mode II stress intensity factor is a minimum in magnitude.

5.2 Path Prediction Algorithm

It would appear, using the Maximum Normal Stress Criterion, that the path prediction would be a reasonably simple task, if one is merely to find the direction at which the shear stress vanishes. Erdogan and Sih [36] in fact, provide a formula which can be used to predict this initial tip-off angle given the stress intensity factors at the original crack tip. They use this equation to predict the initial tip-off angle of a crack which is loaded in pure shear, with very good results. This procedure was attempted in some initial tries at obtaining a path prediction, with no success. In the present solution, the effect of the elliptical inclusion is to alter the stress field significantly with advance of the crack. Therefore, the angle that would be predicted from the initial crack stress intensity factors is not the angle at which the natural crack will grow. With each infinitesimal crack extension that occurs with the naturally growing crack, the stress field changes significantly due to the interaction with the inclusion. This phenomenon is illustrated in Figures 5.1 through 5.7. Each of these figures displays contours of the maximum shear stress near the tip of a growing crack as it is interacting with an inclusion. These are the same stress contours that would appear as isoclines in a photoelastic stress analysis of this problem. The ellipticity ratio of the inclusion is 0.7, and the initial close crack tip is located at a **z** value of (2.5,.3), or 2.5 in the x-direction, and 0.3 in the y-direction. The initial value of n is 5, so the increments of crack growth are 0.2 in length. The ellipse has a unit R, and the crack is initially 1.0 units in length. Note that the crack grows until it reaches the

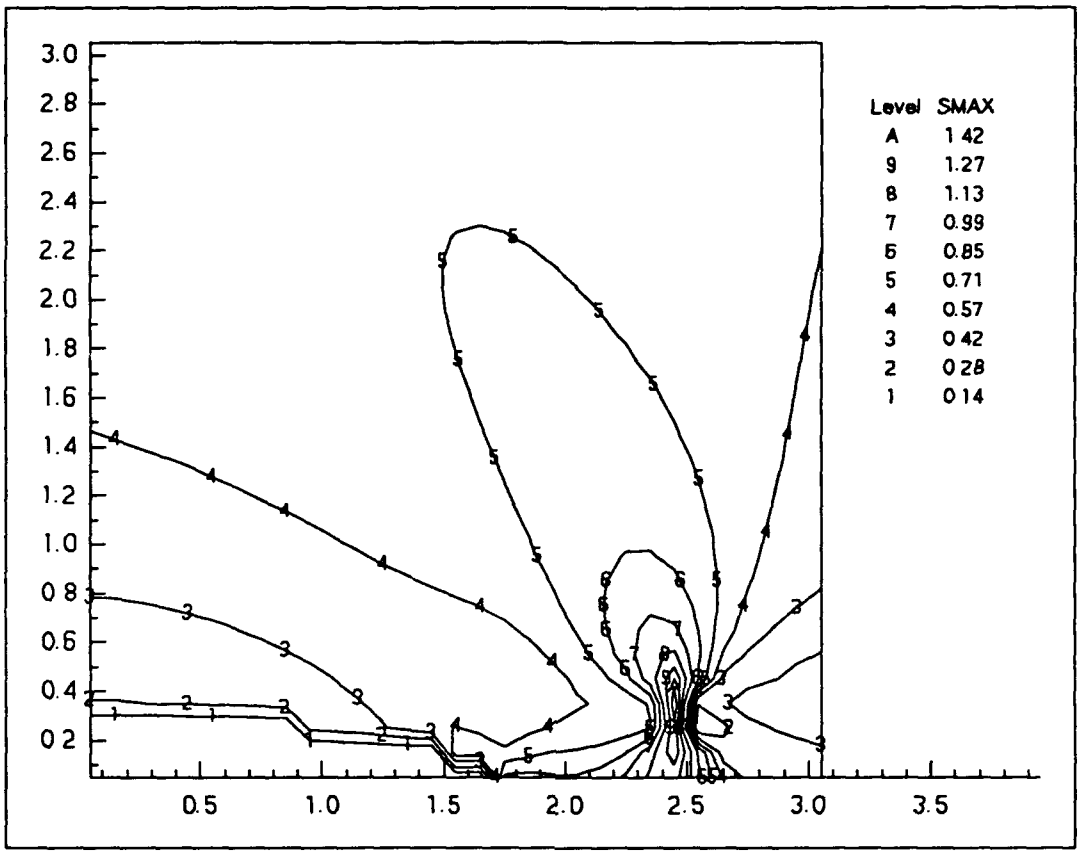

Figure 5.1. Contours of maximum shear stress near tip of original crack, before growth (load normal to crack, θ=0., R=1., L/R=1., κ=1.67).

ellipse, and then is stopped. This is an actual prediction of crack path, and will be one that is presented in a figure later in this work. Carcful investigation of these seven figures shows that the contours of stress tilt significantly with the advance of the crack. Also, they are not even similar in form on either side of the crack. In the solution presented by Erdogan and Sih [36], these contours of stress were identically reflected on opposite sides of the crack. Therefore, instead of a linear crack advance problem, the present situation is in fact non-linear. The significance of this and of these figures is that the prediction algorithm that is developed can at most be incrementally linear,

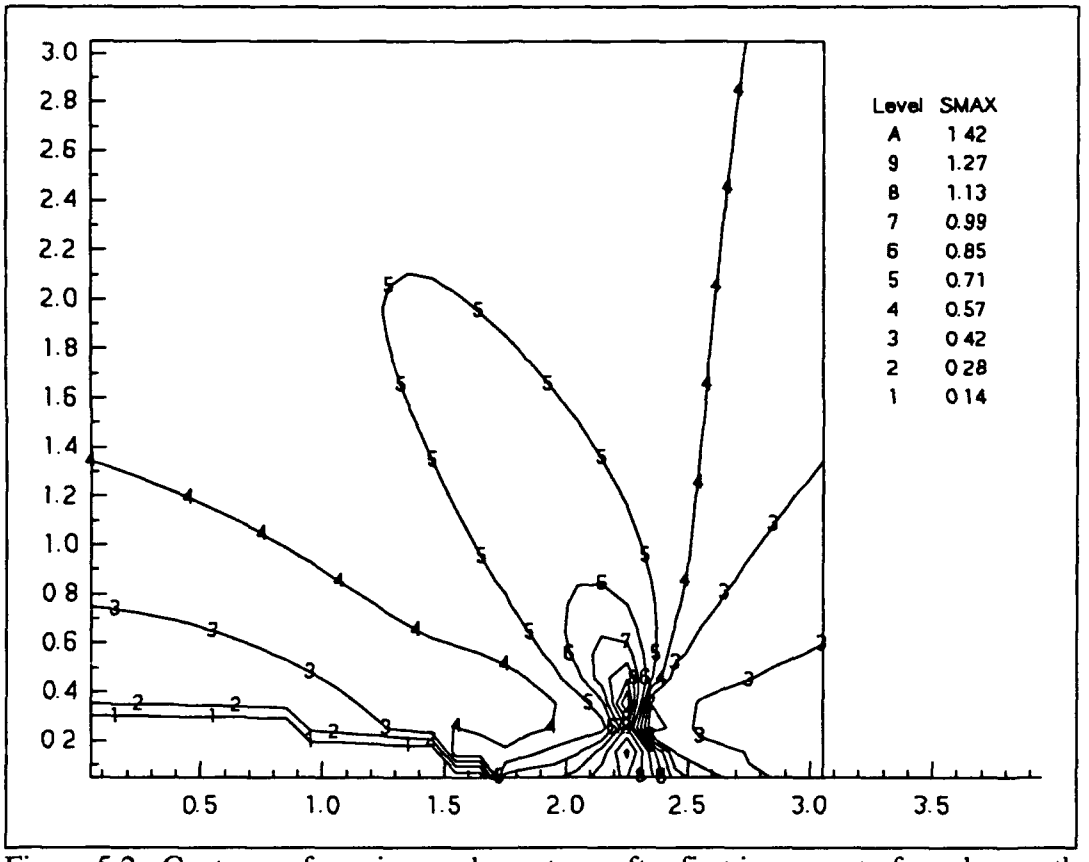

Figure 5.2. Contours of maximum shear stress after first increment of crack growth (load normal to crack, θ=0., R=1., original L/R=1., κ=1.67).

and the correct crack propagation direction cannot be determined with information available before the crack actually propagates.

The prediction algorithm for this problem therefore must be iterative in nature. An initial guess is made at the angle at which the crack is going to grow, and then is checked to see if that guess is correct. Actually, the prediction algorithm that is used to predict the direction of crack growth is reasonably straight-forward. It begins by initially solving the problem of a straight crack with unit length, as described previously. Then an increment of crack length is added to the crack by

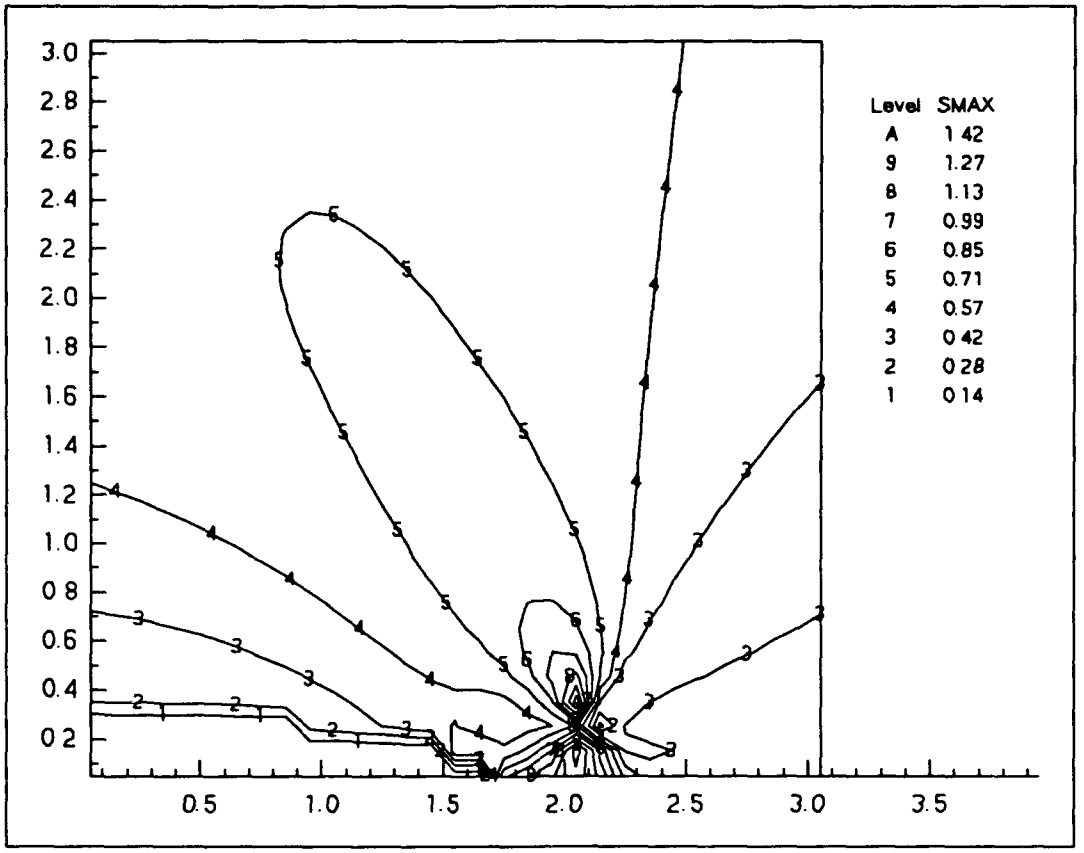

Figure 5.3. Contours of maximum shear stress after second increment of crack growth (load normal to crack, θ=0., R=1., original L/R=1., κ=1.67).

incrementing the problem size parameter n, then the arrays are incremented by 2, and the values are moved down 2 locations. Next, a choice for the angle at which the crack will deflect from its present path is made. A very efficient choice is for the angle to grow in the same direction that the crack is already growing, or for each increment, for there to be no more deflection. For a naturally growing crack, we expect that the path will be relatively smooth, or that there will be very little deflection observed during each increment of growth. Therefore, the angle that is implemented is no deflection from the current path, or algorithmically, the angle calculated during

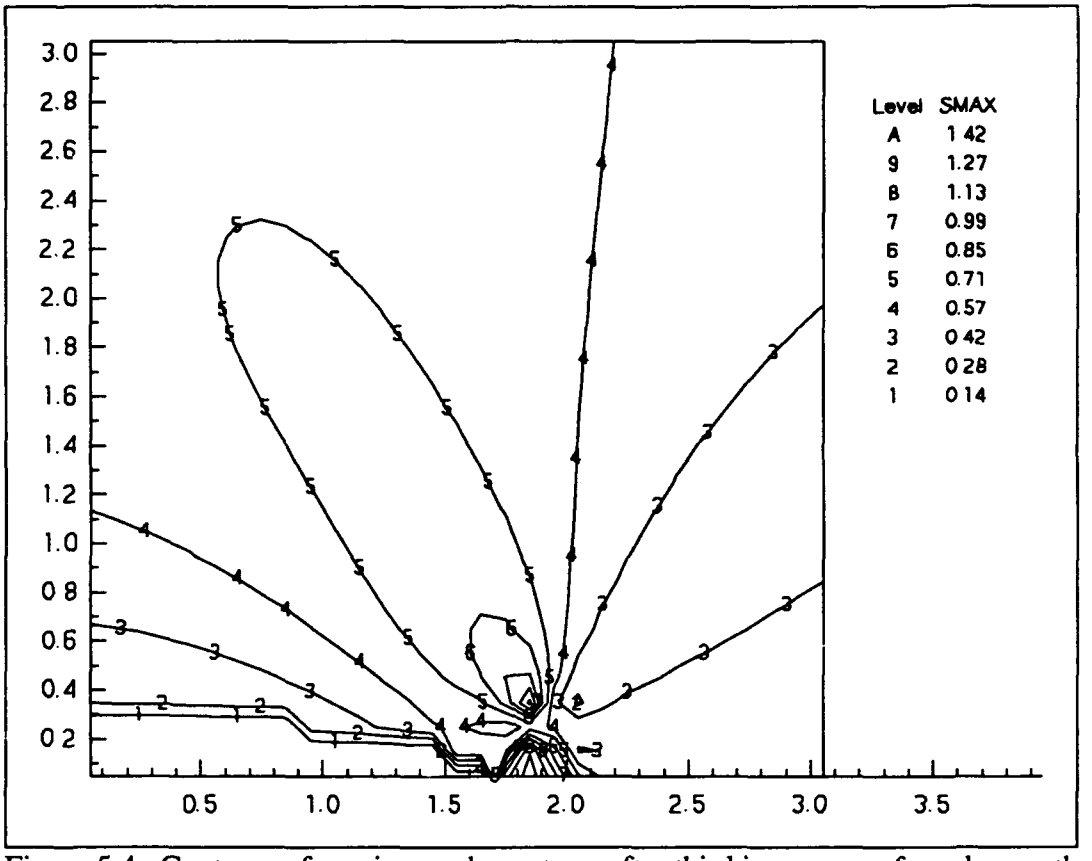

Figure 5.4. Contours of maximum shear stress after third increment of crack growth (load normal to crack, θ=0., R=1., original L/R=1., κ=1.67).

the last increment of growth. The problem is then solved again, and stress intensity factors are calculated. Once these values are known, the program proceeds to the next iteration. At this iteration, a known angle is added to the initial guess, and the problem is solved again. At this and subsequent iterations, however, there is no need to extend the crack, nor to increment the arrays nor move the values in the arrays. The first iteration, at zero angle and one increment of crack growth has done the extension of the crack, and the rearranging of the values in the arrays. To perform the second and subsequent iterations for this increment of crack growth, therefore, the first

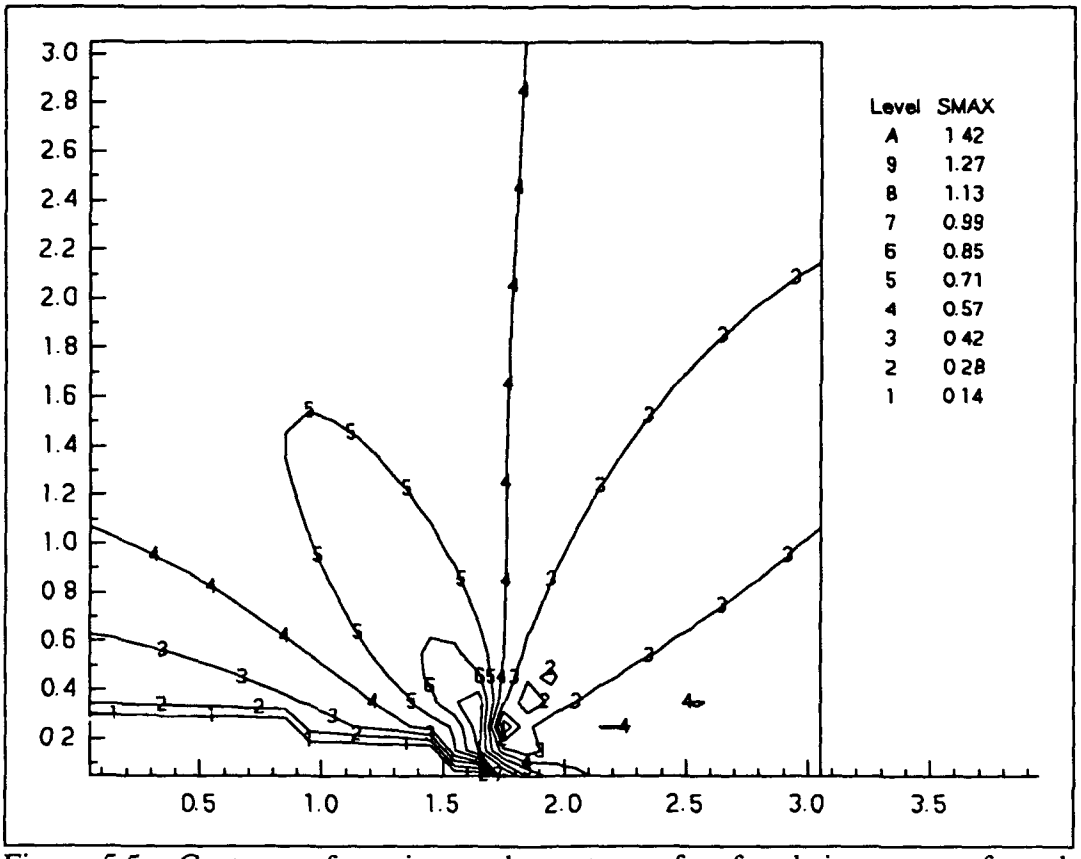

Figure 5.5. Contours of maximum shear stress after fourth increment of crack growth (load normal to crack, θ=0., R=1., original L/R=1., κ=1.67).

two values in each array need to be replaced with new values, as the new crack tip is at a new value of **z**, with a new angle, and new first and second derivatives. The problem then continues to be solved again and again with new kinked tips. The angle chosen for the initial tip-off after the first iteration with no deflection is an angle of 4 degrees. This angle was chosen after quite a bit of experimentation in reducing the number of iterations required to converge on the answer.

The next step is to determine whether the new increment of crack growth is in the correct direction. To do this, the new Mode II stress intensity factor that is

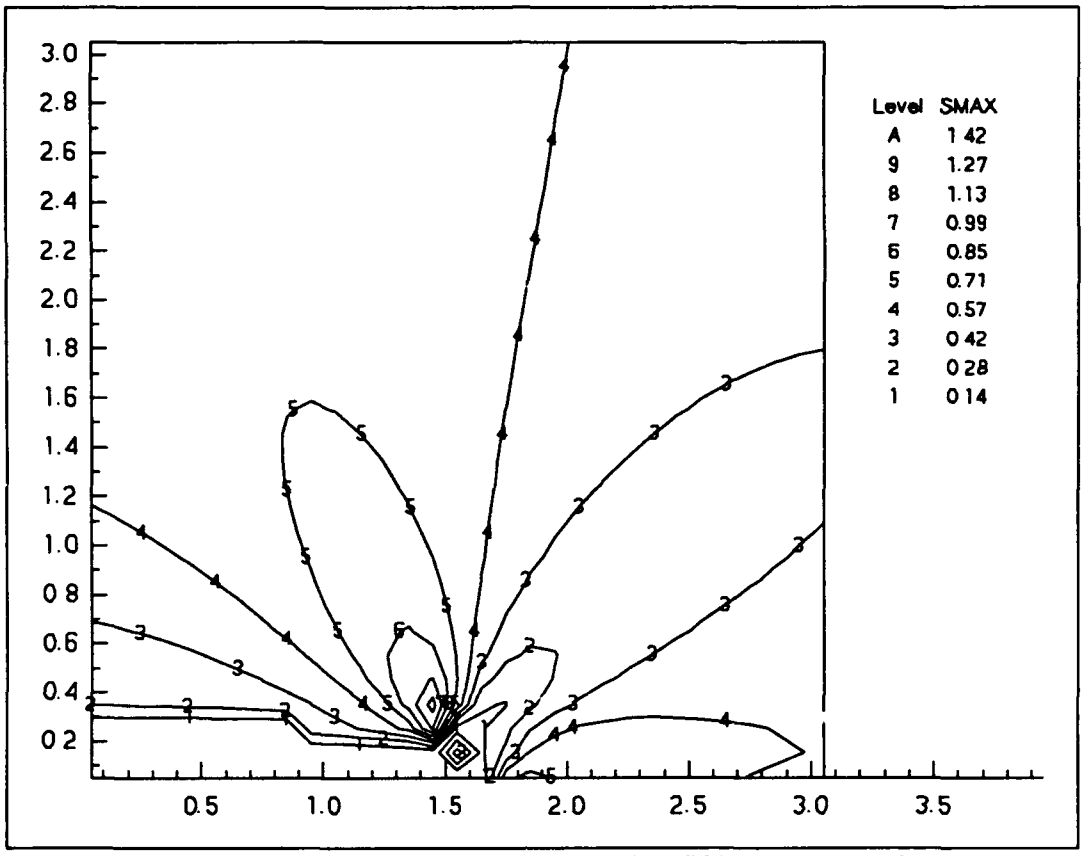

Figure 5.6. Contours of maximum shear stress after fifth increment of crack growth (load normal to crack, θ=0., R=1., original L/R=1., κ=1.67).

calculated in the current iteration is compared to the result from the previous calculation. If the new K_{II} is less than the old value, the crack tip-off angle is incremented by another 4 degrees and the problem is solved again. If the new Mode II stress intensity factor is, however, greater than the old value, the algorithm must have overshot the correct angle, or gone the wrong direction. Since it is not known for certain whether there has been an overshot or the prediction has gone the wrong direction, the best thing that can be done is to cut the increment in half and go back the other direction. If there were human interaction within this algorithm, the human

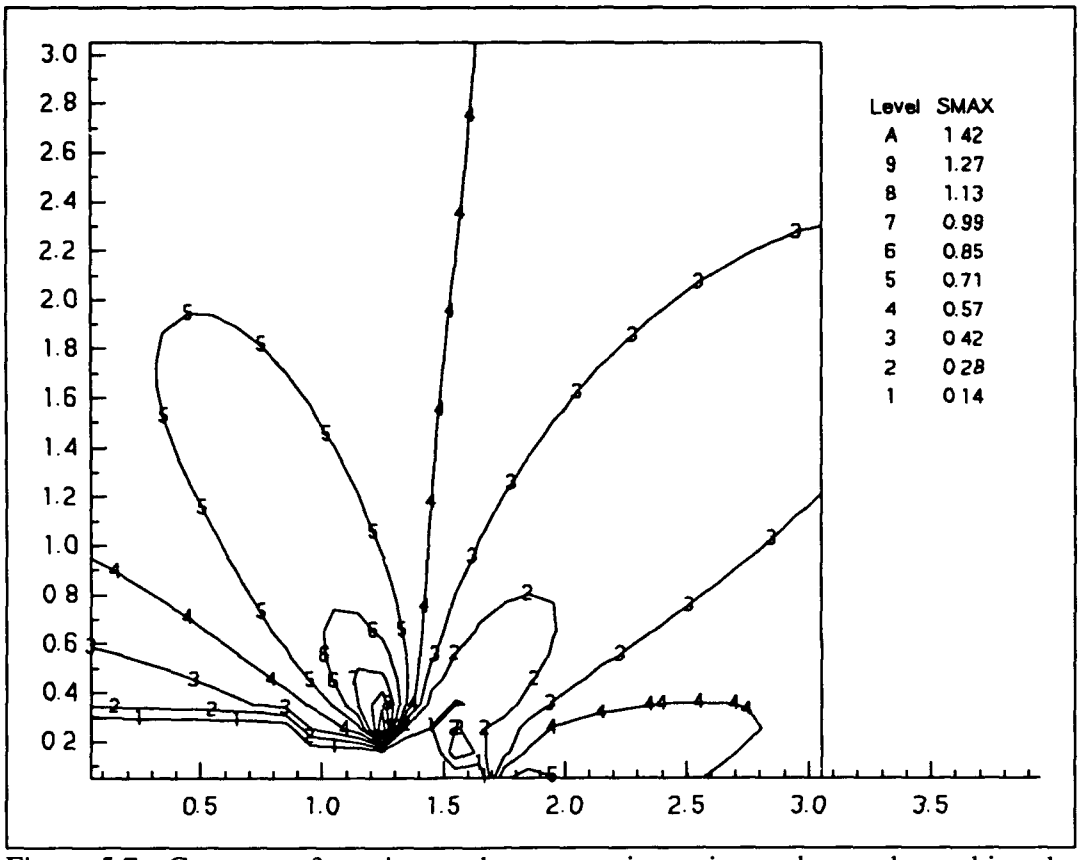

Figure 5.7. Contours of maximum shear stress just prior to the crack touching the inclusion (load normal to crack, θ=0., R=1., original L/R=1., κ=1.67).

could guess at the new value of the kink angle, and tell the computer to try that value. The intent of this algorithm, however, was to make the prediction automatic, and not require human intervention. It needs, therfore, to converge on the correct angle with a minimum of iterations, and no human intervention. The new guess at θ will therefore be 2 degrees less than the old value of the crack kink angle. Again, once the problem is solved, there is a new value for K_{II} with which to compare the old value. The guessing and going backwards with half the increment continues for one more reversal in direction, until the increment in angle is 1 degree. Once the increment is

reduced to 1 degree, and a minimum has been found again, the kink angle is defined as converged. This provides a solution that is incorrect by at most half that amount. That is, the correct answer will be off by at most 1/2 of a degree if the increment of change to the guess is 1 degree.

Once the algorithm has converged on an acceptable answer, the computer program goes back with its final answer for the crack kink angle, θ, and solves the new problem with the new angle. The prediction continues with the new crack and the procedure begins again for the next increment. There is only one thing that must be checked at each increment of growth, whether or not the crack has grown into the inclusion. This is also reasonably simple. The distance of the new crack tip from the origin can be easily calculated, as can the angle that a vector from the origin to that location would make with respect to the x-axis. The distance to the edge of the ellipse at that angle can then be calculated, and a comparison made of the two values. If the edge of the ellipse is closer than the crack tip, the crack is still outside the inclusion, and the algorithm can proceed. If not, the crack has grown to the edge of the ellipse, and the program ends the prediction. Actually, the crack will grow into the inclusion, or along the edge of the inclusion, but due to the limitations of rigidity of the inclusion, these problems cannot be solved presently.

5.3 Verification of Prediction

Sumi et al. [33] performed finite element crack path predictions near an open hole, and also performed experiments to verify their predictions. Figure 5.8 shows Sumi's predictions and experiments, and predictions done with the present algorithm. The inclusion in the present solution is a rigid one, but the value of κ (Muskhelishvili's constant) can be set to any value required. As stated previously, Muskhelishvili noted, in his work, at a value of $\kappa = -1$ the solution for a rigid inclusion reduces to the solution for a hole. This is helpful in that it allows the calculation of the interaction of a crack with an open hole to be done using the results for a rigid inclusion. This, in fact, is what was done to produce the predictions shown in the figure. Note that the predictions done with the current algorithm match the experimental results reasonably well, especially when the crack passes the open hole.

Figure 5.9 depicts the path of a crack which is growing naturally near either an open hole, a rigid inclusion, or no inclusion at all. Note that the hole attracts the crack, as has been observed by experiments (Sumi [33]), the rigid inclusion deflects the path of the crack as would be expected, and the case with no inclusion has no effect on the crack at all, as would be expected. All three of these cases are actual predictions using the method that is described in this work.

It appears that the predictions of a crack path are reasonable. The results using the present method compare well to predictions and experiments done by others. What remains, then, is to exercise the solution in order to learn about the paths of

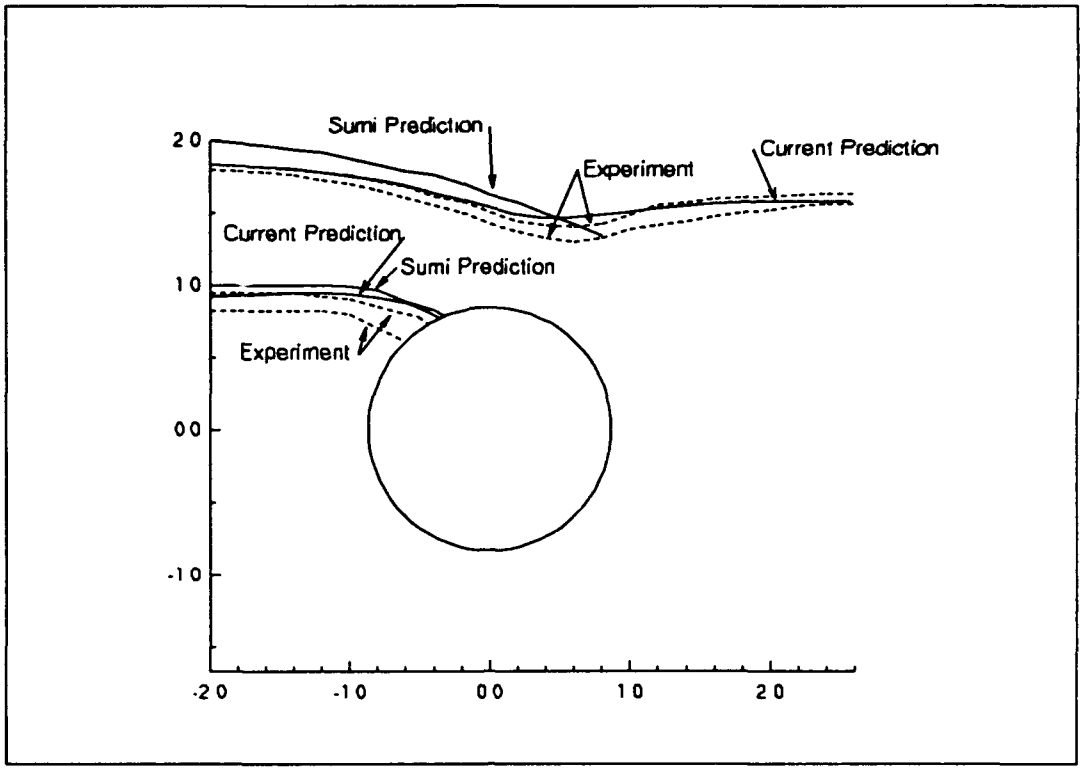

Figure 5.8. Verification of prediction by comparison to experimental results (load normal to crack, R=1., original L/R=1., κ=-1.).

cracks near inclusions.

5.4 Results

Figures 5.10 through 5.14 depict results of the crack path prediction. All of these figures represent the actual path of the cracks. In each figure, the initial crack is not shown, but is of length 1.0/R, extending in the positive x direction from the right-most end of the path shown in the figure. The x and y coordinates shown in each of the figures represent distances from the origin normalized by the average

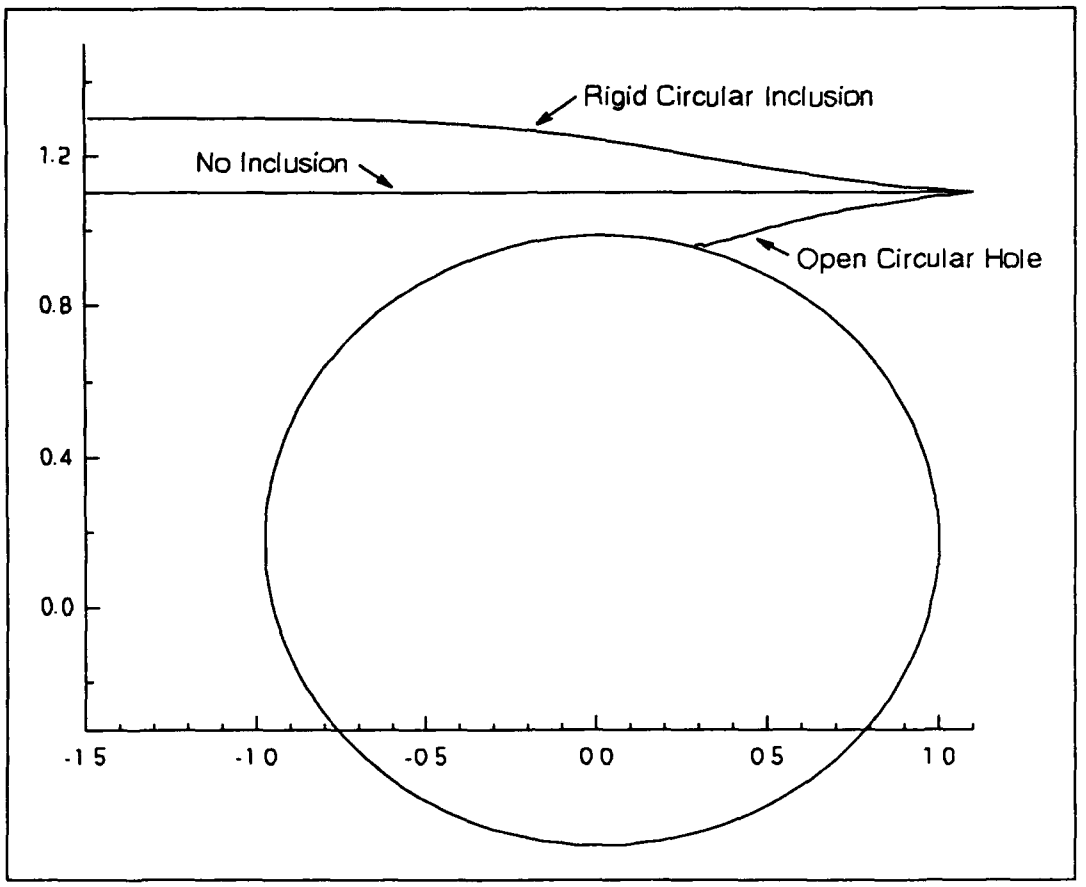

Figure 5.9. Paths of cracks given an open hole, no inclusion, and a rigid circular inclusion.

radius of the ellipse, R. There is therefore no labelling in any of these figures of the axes, as they are intended to portray x and y physical space. Figure 5.10 is the result of a parametric study on the ellipticity ratio of the inclusion. In this figure the initial location of the close tip of the crack is at an x-coordinate of 2.5, and a y coordinate equal to the uppermost extent of the edge of the inclusion. For instance, for an inclusion with an ellipticity ratio of 0.6, the initial close tip of the crack is at x = 2.5, and y = .4. Note that the inclusions with ellipticity ratios greater than 0.4 tend to

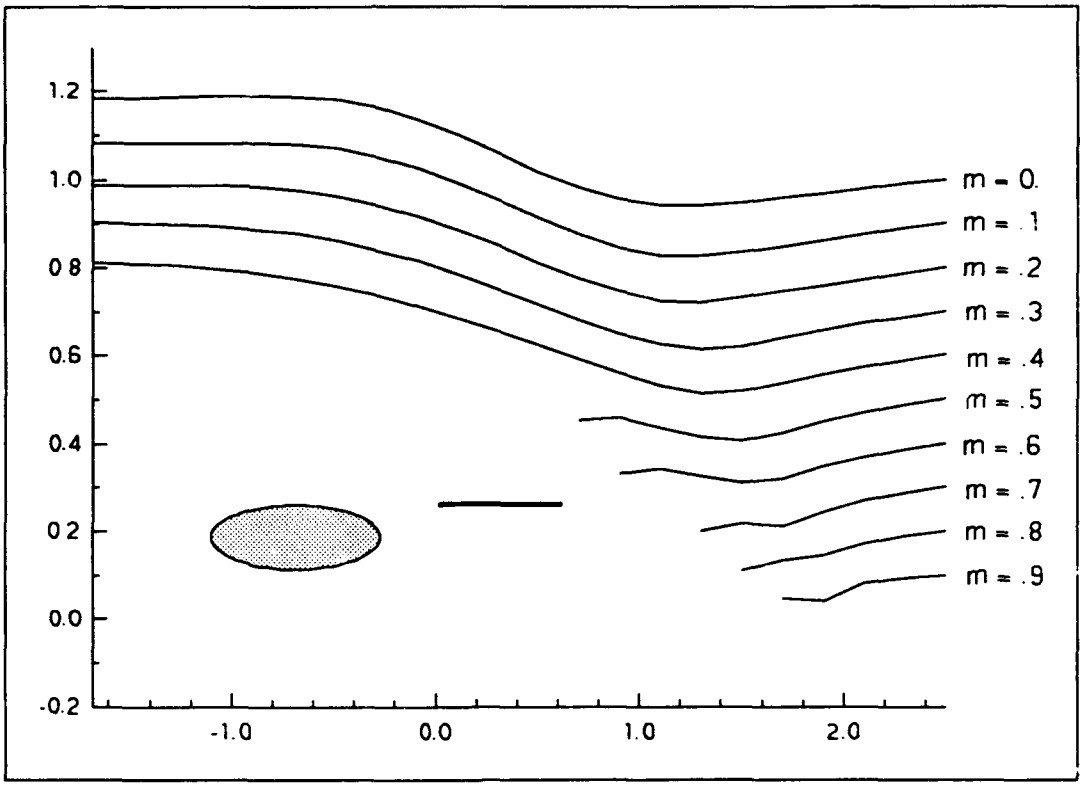

Figure 5.10. Paths of cracks initially aligned with the top edge of inclusions with varying ellipticity ratios (load normal to crack, R=1., original L/R=1., κ=1.67).

attract the crack, and the crack does not escape the inclusion. For an ellipticity ratio of 0.4 and less, the crack is deflected, and escapes the inclusion. In this figure, the ellipse is rigid. Figure 5.11 portrays exactly the same parametric study, only in this case, the value of κ is set to -1, modelling the interaction of the cracks with open elliptical holes with varying ellipticity ratios. Note in this figure that the crack never escapes the hole.

Figure 5.12 portrays a slightly different parametric study in which the initial location of the crack is held fixed, at x = 2.5 and y = .6, as is the ellipticity

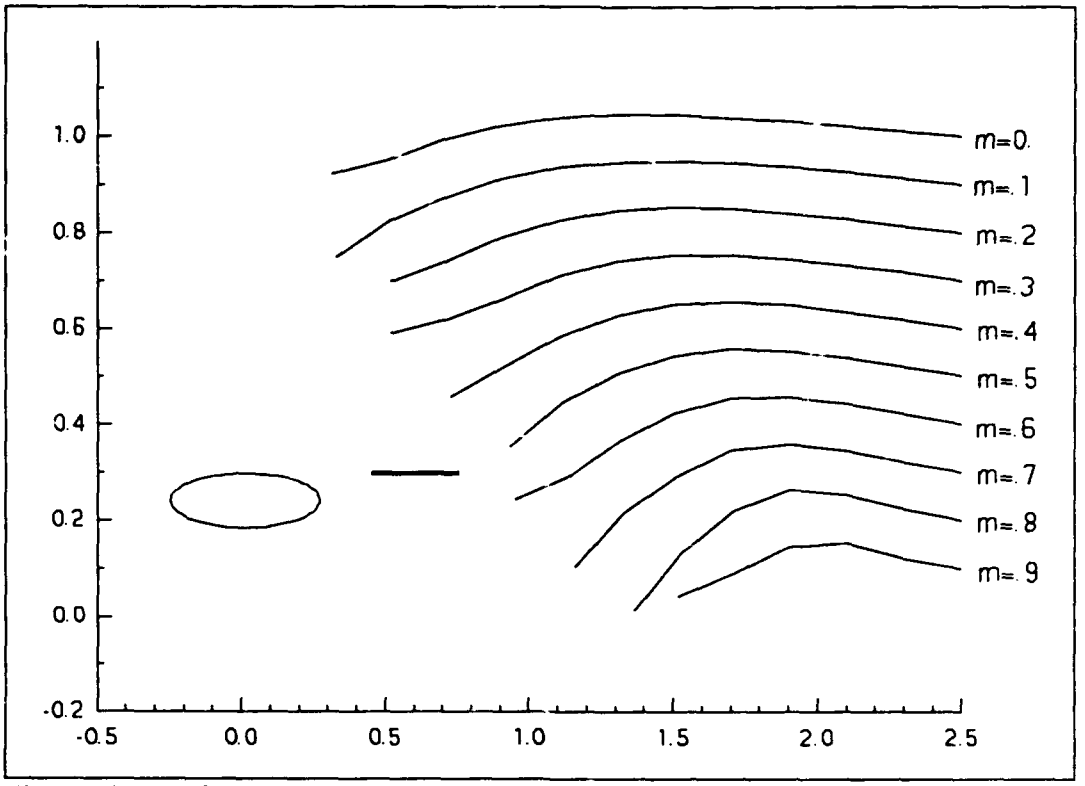

Figure 5.11. Cracks initially aligned with the top edge of elliptical holes (load normal to crack, R=1., original L/R=1., κ=-1.)

ratio, at a value of 0.4, and the initial angle that the crack makes with the x-axis is varied from 0 to 30 degrees in increments of 5 degrees. Note that the crack only escapes being attracted into the side of the inclusion for the case of a 0 degree (horizontal) crack. This is the only case in which a line drawn from the tip of the crack, aligned parallel to the initial crack would also not interfere with the inclusion.

In Figures 5.13 and 5.14, the ellipticity ratio is again held fixed for each figure, as is the initial angle of the crack. In these figures, the initial y-coordinate of the close tip of the crack is varied, to study the extent to which an inclusion will

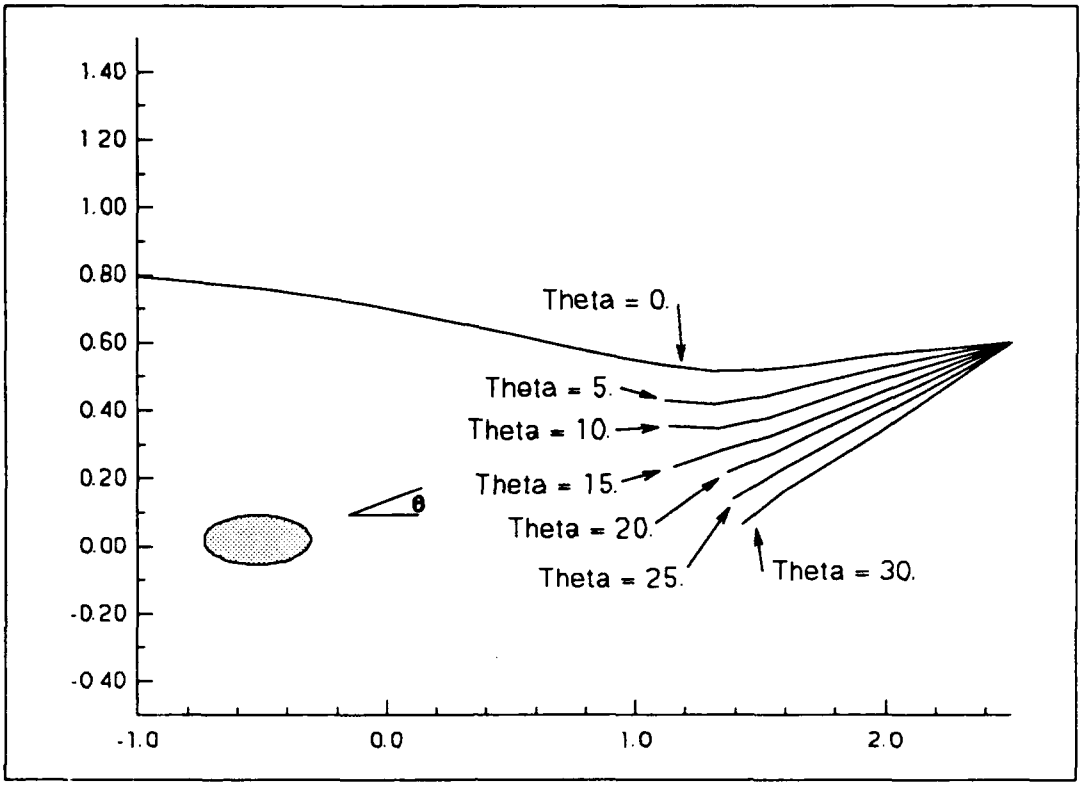

Figure 5.12. Paths of cracks with varying initial angles with respect to the x-axis (load normal to crack, R=1., original L/R=1., κ=1.67).

attract or repel a crack. Figure 5.13 depicts crack paths for a rigid inclusion with an ellipticity ratio of 0.9 (a long, flat inclusion). Note that cracks with a y-coordinate of 0.4 escape the side of the inclusion, whereas cracks with original y-coordinate of 0.3 and below are attracted into the side of the inclusion.

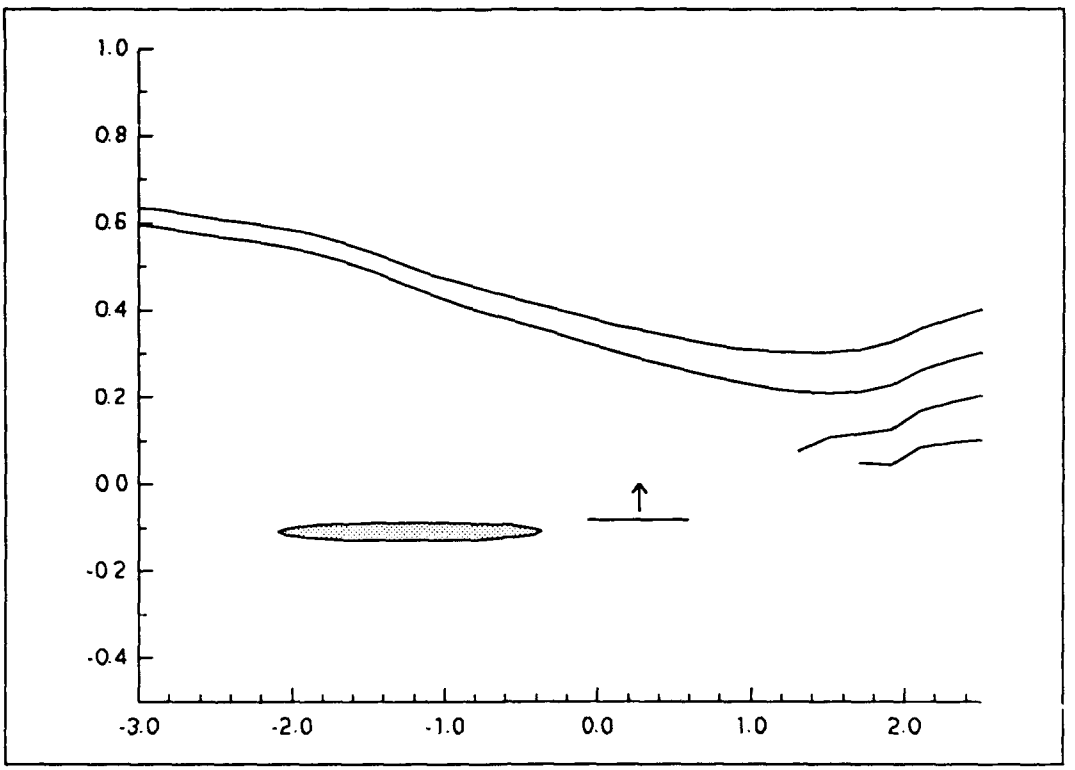

Figure 5.13. Paths of cracks interacting with inclusion with ellipticity ratio 0.9, and starting at varying initial y-coordinates (load normal to crack, R=1., original L/R=1., κ=1.67).

In Figure 5.14, the ellipticity ratio of the inclusion is 0.4. For this inclusion, the crack must have an initial y-coordinate of 0.6 before escaping the inclusion. This location is, however, parallel to the upper edge of the inclusion. For the previous case, cracks were attracted toward the inclusion from a y-coordinate considerably above the upper extent of the inclusion. Long, flat inclusions therefore have a greater tendency to attract cracks than do shorter rounder inclusions. It is also interesting to look at the tip of each crack in Figure 5.14 as it approaches the inclusion. Cracks approaching the inclusion near its major axis are merely attracted

into the inclusion. Cracks coming in at some distance from this axis in the vertical direction seem to be attracted toward the inclusion initially, and then as they get very close to the inclusion, tend to be deflected from it.

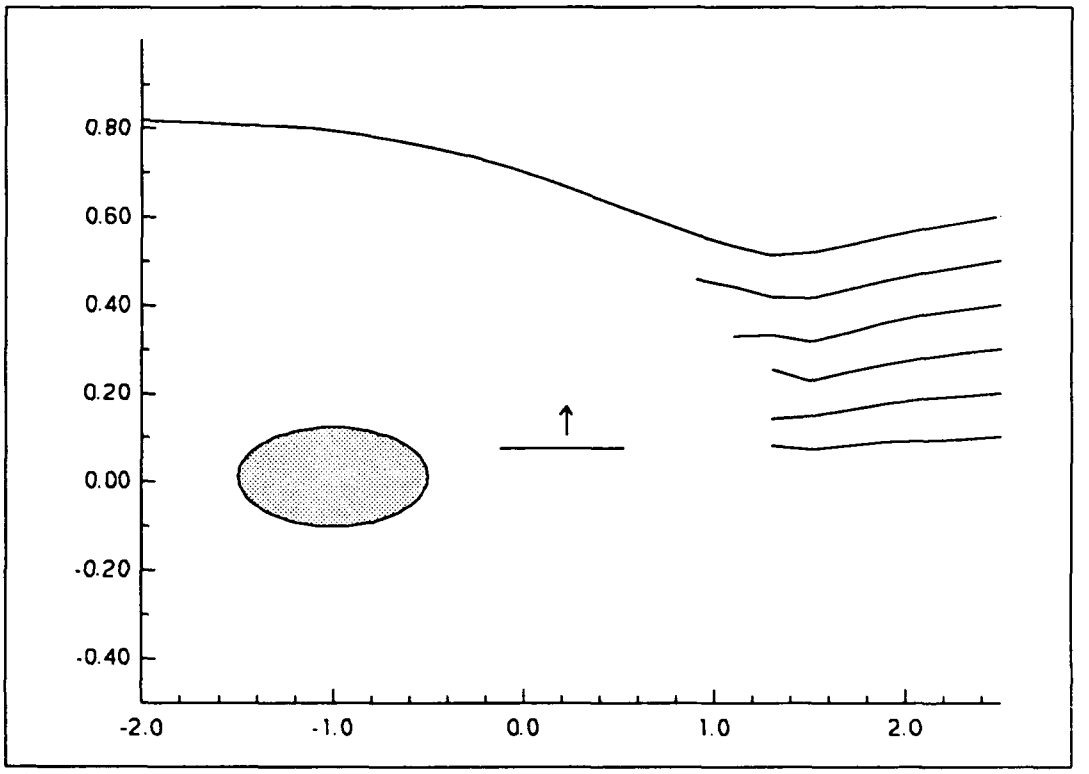

Figure 5.14. Paths of cracks interacting with an inclusion with ellipticity ratio 0.4, and varying y-coordinates (load normal to crack, R=1., original L/R=1., κ=1.67).

There are many more of these types of studies which can be done to learn interesting and useful things about the paths of cracks near inclusions and holes. These results are presented therefore both to provide the reader a sense of the flexibility and general nature of the solution as well as providing some general insight into the quasi-static behavior of cracks near inclusions and holes.

5.3 Energy Absorption Due to Crack Deflection

There are two components to the additional energy absorption associated with a non-straight crack path near an inclusion. The first component is the effect of the local shielding of the crack due to the inclusion. The ratio of the local stress intensity factors to the applied values, or in the present case, the normalized stress intensity factors, quantifies the amount of local shielding due to the presence of the inclusion. In the case of an open hole, this ratio is greater than one, and therefore describes the amount of anti-shielding due to the presence of the hole. This effect is what is calculated and has been presented in this work. The energy absorbed or energy shielding ratio can be calculated by determining the strain energy release rate, as follows:

$$\frac{G}{G_{\infty}} = \frac{K_I^2 + K_{II}^2}{(\sigma_{\infty}\sqrt{\pi a})^2} \tag{5.1}$$

where K_I and K_{II} and G are the local values, and they are normalized by the values that would exist when there is no inclusion. For the case where there is no inclusion, therefore, this equation gives a value of 1. In the presence of an inclusion, if the crack is shielded by the inclusion, the local K_I will be less than 1, and therefore, the normalized G will also be less than 1. This decrement is energy can be thought of as the interaction toughness ratio, or the ratio of energy release rate for an inclusion present to that with no inclusion. In the present work, this ratio can be calculated at each increment of crack growth, and the total can be averaged by the number of

increments of crack growth that have occurred.

The second component of the energy absorption is that due to the path itself. The interaction toughness ratio described above inherently assumes a rectilinear crack path. However, if the crack is deflected from a rectilinear path, as it will be near an inclusion, then the path itself also represents a toughening mechanism. This crack deflection toughness ratio can also be assessed using the technique described in this work, because the final location of the advancing crack tip is known, and the distance that the crack would have travelled in its original rectilinear direction is also known.

Therefore, to assess the overall energy absorption due to the crack interacting with an inclusion, and being deflected by the inclusion during its quasi-static crack growth, both of these ratios should be used. The total energy absorbed, or total toughness ratio would then be the product of these two ratios. An implementation of that idea would be as follows for an initially horizontal crack: note the final x-location of the growing tip of the initially horizontal crack, keeping track of how many increments of crack growth have taken place; then divide the total x-distance that the crack has travelled by the distance that it could have travelled if it had not curved (increment length times number of increments). This number will be less than one, and will also represent an energy decrement, or an amount of energy absorbed by path deflection only. This path deflection ratio can then be multiplied by the interaction toughness ratio calculated as an average over all of the increments of

crack growth, to determine the overall energy absorption or toughness ratio for the crack.

Energy absorption for several different cracks has been calculated using this procedure, for a both a rigid inclusion and an open hole, and is presented in Tables 5.1 and 5.2. The crack parameters are the same as those for the paths calculated for Figures 5.10 and 5.11, where the initial tip of the crack is at an x-coordinate of 2.5/R, and the y-coordinate is at the uppermost extent of the edge of the inclusion. Ellipticity ratios varying from .9 to 0. are displayed in the table. The numbers in the table represent the various toughness ratios described, where the second column is the overall toughness ratio, and the third and fourth columns are the path deflection or shortening ratio, and the shielding or interaction ratio respectively.

It is interesting to note from a first glance at Table 5.1 that the greatest energy absorption occurs when the crack is attracted into the side of the inclusion. However, upon closer inspection of the values in the table, one can see that it is important to compare similar cracks. The energies reported in the table for ellipticity ratios greater than 0.4 are for cracks which are considerably shorter than those for ellipticity ratios 0.4 and less, since they are attracted into the side of these inclusions.

For those cracks which pass the inclusion, the shortening ratio is relatively constant. This is a reasonable result, referring to Figure 5.10. In this figure, it appears that the paths of the cracks which escape the ellipse are nearly parallel to each other for the set of conditions described. It is expected, therefore, that their crack length

Table 5.1. Toughness ratios for cracks initially parallel to the top of the inclusion, for differing inclusion ellipticity ratios.

Ellipticity Ratio	Toughness Ratio	Crack Length Shortening	Shielding Ratio
.9	.713	.795	.897
.8	.665	.829	.801
.7	.659	.853	.773
.6	.662	.886	.748
.5	.672	.896	.750
.4	.937	.962	.975
.3	.944	.961	.982
.2	.952	.962	.989
.1	.958	.962	.997
0.	.962	.962	1.00

shortening ratios would all be similar. For those cracks which are attracted into the side of the ellipse, all of the shortening ratios will be different, as the cracks are all of different lengths. If the toughness ratios of the cracks interacting with inclusions with ellipticities of 0.5 and greater are compared, it would seem that more energy is absorbed by shorter, fatter inclusions. In these cases, the shielding ratio dominates the energy absorption. For inclusions with ellipticities less than 0.5, however, exactly the opposite is true. If this result is, in fact, the true case in real materials, it could have

Table 5.2 Toughness ratios for cracks initially parallel to the top of the hole, for different hole ellipticity ratios

Ellipticity Ratio	Toughness Ratio	Crack Length Ratio	Anti-Shielding Ratio
.9	3.45	.819	4.21
.8	3.21	.809	3.97
.7	2.48	.838	2.96
.6	2.36	.880	2.68
.5	2.15	.865	2.48
.4	1.89	.879	2.25
.3	1.69	.892	1.89
.2	1.72	.894	1.92
.1	1.73	.905	1.91
0.	1.55	.905	1.71

a strong impact on the design of the shapes of reinforcements.

Table 5.2 shows a somewhat different result, in that the overall toughness ratios are greater than one, as these are results for cracks growing toward an open hole. Since all of these cracks are eventually stopped by the open hole, a comparison of all of the results together in this table is reasonable. Note that the crack length shortening ratio or crack deflection toughness ratio remains relatively constant, whereas the anti-shielding ratio, or crack inclusion interaction ratio varies significantly, and provides a majority of the propensity for crack growth. Also, long, thin holes have a

considerably stronger attractive effect on the crack than do rounder, more circular holes. This result could also have a strong effect on toughening mechanisms and reinforcing mechanisms in materials, as it seems to suggest that if the reinforcement becomes debonded from the surrounding material, the resulting open hole will attract a crack, and cause it to propagate.

Chapter 6

CONCLUSIONS

6.1 Summary of Findings

In this work, a new technique has been presented which will predict the path of a naturally growing crack near a rigid elliptical inclusion, where the stress field can be modelled as two dimensional. The technique uses a boundary integral approach to the solution of the stress field at the tips of the crack which is in general not straight, and is interacting with a rigid elliptical inclusion. The crack path is parameterized as a cubic spline, and the results of both a Green's Function solution to the interaction of a dislocation with an elliptical inclusion, and a first order perturbation solution to account for the generally curvilinear nature of the crack have been employed. The singular nature of the stresses is accounted for using a numerical technique which describes the distribution of dislocations along the crack as a piecewise quadratic polynomial to transform the problem's resulting integral equations into algebraic equations well suited to a matrix-type solution. Results of each step of the analysis have been verified with previously published results that are commonly

accepted as correct, and with experimental results of a crack propagating near an open circular hole. New and significant results are also presented as paths of cracks interacting with inclusions of differing ellipticity ratios, and at different orientations with respect to the initial crack. The technique is much less computationally intensive than current combination analytical and finite element approaches to crack path prediction. All of the predictions presented in this work were generated on an engineering workstation type computer. There was no need to go to a larger computer for the predictions. This indicates that sensitivity studies using the technique are quite easily accomplished, and provide some new insight into the mechanisms of fracture near inclusions and/or reinforcements in materials. The angle that the crack has with the x-axis is not limited, nor is the angle that the applied load makes with respect to the initial crack, except for the case in which the crack faces would overlap. Original results reported in this work were for an applied load which was oriented normal to the original crack, mainly for simplicity in their presentation. That is not a limitation of the method, except that the crack path direction predictor is still controversial.

There are several interesting results that come from the parametric studies shown in figures in the previous section. First, it seems that, given the limited number of cases examined in the figures, longer, flatter inclusions may tend to attract cracks, whereas shorter, rounder inclusions may tend to repel cracks. This result may be significant in the design of reinforcements in materials if the energy absorption due to crack blunting and crack path deflection are intended to be toughening mechanisms.

Real materials, however, have more than one inclusion, and a naturally growing crack will interact with all of the inclusions present. The method presented in this work, however, can be extended to deal with multiple inclusions and/or multiple cracks. The method is not intended to provide stochastic information about cracks in reinforced materials. Rather, it is a fundamental building block of what could become a competent micromechanics model for dealing with cracks near inclusions in reinforced materials, or precipitation hardened metals.

6.2 Limitations of Method

The inclusion is at present rigid and rigidly bonded to the surrounding medium. In the predictions given, the computation was forced to stop if the crack attempted to enter the inclusion. Also, no attention was paid to the bond strength of the inclusion to the surrounding medium. In real materials, when a crack propagates to an interface with a reinforcing particle, one of three things can happen. Either the particle can debond with the material, or the crack will be arrested at the particle, or the particle itself will fracture. Real composite materials and strengthened metals exhibit all three of these phenomena during fracture processes. The methodology proposed in this work does not take these effects into account, and must be extended to include those effects if that is deemed to be critical for a certain application. The results shown for energy absorption for cracks near open holes compared to cracks near inclusions is evidence of this limitation. It has been known for some time that

drilling a hole slightly ahead of an advancing crack tip will often arrest the progression of the crack. In that case it would appear that the hole had absorbed energy when in fact what has been done is to blunt the sharp tip of the crack, or in the terms of the work presented here, to remove the singularity at the advancing crack tip.

There is also at present only one inclusion included in the analysis. Most real materials of interest have a multitude of inclusions or reinforcing particles and/or fibers in a multitude of orientations. The method can be extended to include the effect of more than one inclusion, but a large number of inclusions would be difficult to treat with this method. One would then have to resort to stochastic models of inclusion or reinforcement orientation and density to determine the energy absorbed by crack path deflection. These models are inherently much more approximate in nature, and have yet to yield real insight into the process of fracture in very complicated stress fields.

The method is also limited to regions whose stresses are two dimensional in nature or that can be modelled as two dimensional, and to cases in which the two crack faces do not touch or try to overlap. Potential methods are usually limited to two dimensions as the potentials are significantly easier to calculate. Three dimensional potential methods, while they exist, are not commonly used because of their complexity. If the stress field is truly three dimensional, the techniques described in this work should not be used. Also, if the crack is under compression in that its faces would touch, an extension of this work would be required.

6.3 Future Areas of Investigation

The two most likely areas that should be investigated following this work are those identified as limitations to the method. First, for those inclusions which are relatively flat, with cracks that are attracted to them, modelling the crack propagation will require following the path of the crack either through the inclusion or along the boundary between the inclusion and the surrounding material. Each of these cases would have to be treated separately, and new solutions would have to be found for the stress analysis of the crack, using Green's Functions, or some other appropriate method to calculate interaction stresses. Once these solutions were found, they could be relatively easily implemented within the structure of the prediction model proposed in this work.

The second area of future investigation that seems to come directly from this analysis is that real materials that are reinforced do not have just one inclusion. The potential for adding multiple inclusions in the analysis exists within the framework of the analysis presented here. Each inclusion would merely add its own set of non-singular terms to the kernel of the analysis, and each would also add stresses on the right hand sides of the integral equations. Two or three inclusions would be a fairly simple task to handle within the scope of the technique as it exists now. A hundred or more inclusions would require the use of stochastic techniques which are outside the scope of what has been presented. These stochastic techniques could, however, be built from knowledge gained from parametric studies of a crack interacting with many

fewer inclusions. In any case, these stochastic models would have to be much more approximate in nature, and are outside the present scope. Another area which should be investigated is some type of self consistent micromechanics model of multiple inclusions and multiple cracks in an elastic material. Some of these techniques are very powerful, and should be explored in relation to the solution presented here.

REFERENCES

[1] Griffith, A. A. The Phenomenon of Rupture and Flow in Solids. *Philosophical Transactions of the Royal Society of London,* series A, 221:163-198, 1920.

[2] Irwin, G. R. Analysis of Stresses and Strains Near the End of a Crack Traversing a Plate *Journal of Applied Mechanics* 24:361-364, 1957.

[3] Muskhelishvili, N. I. *Some Basic Problems of the Mathematical Theory of Elasticity* P. Noordhoff Ltd. Leyden, The Netherlands 1953.

[4] Paris, P. C. and Erdogan, F. A Critical Analysis of Crack Propagation Laws *Journal of Basic Engineering* 85:528-534, 1963.

[5] Erdogan, F. Stress Intensity Factors *Journal of Applied Mechanics* 50:992-1002, 1983.

[6] Atkinson, C. The Interaction Between a Crack and a Circular Inclusion *International Journal of Engineering Science* 10:127-136, 1972.

[7] Erdogan, F., Gupta, G. D., and Ratwani, M. Interaction Between a Circular Inclusion and an Arbitrarily Oriented Crack *Journal of Applied Mechanics* 41:1007-1013, December, 1974.

[8] Erdogan, F. and Gupta, G. D. The Inclusion Problem With the Crack Crossing the Boundary *International Journal of Fracture* 11:13-27, 1975.

[9] Dundurs, J. and Mura, T. Interaction Between an Edge Dislocation and a Circular Inclusion *Journal of the Mechanics and Physics of Solids* 12:177-189, 1964.

[10] Dundurs, J. and Sendeckyj, G. P. Edge Dislocation Inside a Circular Inclusion *Journal of the Mechanics and Physics of Solids* 13:141-147, 1965.

[11] Grief, R. and Sanders, J. L. The Effect of a Stringer on the Stress in a Cracked Sheet *Journal of Applied Mechanics* 32:59-66, March 1965.

[12] Santare, M. H. and Keer, L. M. Interaction Between an Edge Dislocation and a Rigid Elliptical Inclusion *Journal of Applied Mechanics* 53:382-385, 1986.

[13] Stagni, L. and Lizzio, R. Shape Effects in the Interaction Between an Edge Dislocation and an Elliptical Inhomogeneity *Applied Physics* 30:217-221, 1983.

[14] Santare, M. H., Keer, L. M., and Lewis, J. L. Cracks Emanating From a Fluid Filled Void Loaded in Compression: Application to the Bone-Implant Interface *Journal of Biomechanical Engineering* 109:55-59, 1987.

[15] Cerasoulis, A. The Use of Piecewise Quadratic Polynomials for the Solution of Singular Integral Equations of Cauchy Type *Computers and Mathematics with Applications* 8:1:15-22, 1982.

[16] Patton, E. M. and Santare, M. H. The Effect of a Rigid Elliptical Inclusion on a Straight Crack *International Journal of Fracture* 46:71-79, 1990.

[17] Palaniswamy, K. and Knauss, W. G. On the Problem of Crack Extension in Brittle Solids Under General Loading *Mechanics Today* 4:87-148, 1978.

[18] Bilby, B. A. and Cardew, G. E. The Crack With a Kinked Tip *International Journal of Fracture* 11:708-712, 1975.

[19] Dudukalenko, V. V. and Romalis, N. B. Direction of Crack Growth Under Plane-Stress-State Conditions *Izvestia, AN SSSR, Mekhanika Tverdogo Tela.* 8:129-136, 1973 (in Russian).

[20] Hussain, M. A., Pu, S. L., and Underwood, J. Strain Energy Release Rate for a Crack Under Combined Mode I and Mode II *Fracture Analysis, ASTM STP 560* American Society for Testing and Materials, 1974, pp. 2-28.

[21] Chatterjee, S. N. The Stress Field in the Neighborhood of a Branched Crack in an Infinite Sheet *International Journal of Solids and Structures* 2:521-538, 1975.

[22] Gupta, G. D. Strain Energy Release Rate for Mixed Mode Crack Problem *ASME Paper No. 76-WA/PVP-7.*

[23] Kitigawa, H., Yuuki, R., and Ohira, T. Crack Morphological Aspects in Fracture Mechanics *Engineering Fracture Mechanics* 7:515-529, 1975.

[24] Lo, K. K. Analysis of Branched Cracks *Journal of Applied Mechanics* 45:797-802, 1978.

[25] Banichuk, N. V. Determination of the Form of a Curvilinear Crack by Small Parameter Technique *Izvestia AN SSSR Mekhanika Tverdogo Tela* 7:130-137, 1970 (in Russian).

[26] Goldstein, R. V. and Salganik, R. L. Plane Problem of Curvilinear Cracks in an Elastic Solid *Izvestia AN SSSR Mekhanika Tverdogo Tela* 7:69-82, 1970 (in Russian).

[27] Goldstein, R. V. and Salganik, R. L. Brittle Fracture of Solids with Arbitrary Cracks *International Journal of Fracture* 10:507-523, 1974.

[28] Cottrell, B. and Rice J. R. Slightly Curved or Kinked Cracks *International Journal of Fracture* 16:155-169, 1980.

[29] Karihaloo, B. L., Keer, L. M., Nemat-Nasser, S., and Oranratnachai, A. Approximate Description of Crack Kinking and Curving *Journal of Applied Mechanics* 48:515-519, 1981.

[30] Sumi, Y., Nemat-Nasser, S., and Keer, L. M. In Crack Branching and Kinking in a Finite Body *International Journal of Fracture* 21:67-79, 1983.

[31] Sumi, Y., Nemat-Nasser, S., and Keer, L. M. A New Combined Analytical and Finite Element Solution Method for Stability Analysis of the Growth of Interacting Tension Cracks in Brittle Solids *International Journal of Engineering Science* 18:211-224, 1980.

[32] Sumi, Y. Computational Crack Path Prediction for Brittle Fracture in Welding Residual Stress Fields *International Journal of Fracture* in press.

[33] Sumi, Y. On Crack Arrestability by a Circular Hole Based on Computational Crack Path Prediction *Naval Architecture and Ocena Engineering* 25:173-180, 1989.

[34] Sur, U. and Altiero, N. J. An Alternative Integral Equation Approach for Curved and Kinked Cracks *International Journal of Fracture* 38:25-41, 1988.

[35] Ioakimidis, N. I. A New Singular Integral Equation for the Classical Crack Problem in Plane and Anti-Plane Elasticity *International Journal of Fracture* 21:115-122, 1983.

[36] Erdogan, F. and Sih, G. C. On the Crack Extension in Plates Under Plane Loading and Transverse Shear *Journal of Basic Engineering* 85:519-527, 1963.

[37] McClintock, F. A. Discussion of [36] included at end of [36].

[38] Cottrell, B. The Paradox Between the Theories for Tensile and Compressive Fracture *International Journal of Fracture Mechanics* 5:251-252, 1969.

[39] Williams, J. G. and Ewing, P. D. Fracture Under Complex Stress - The Angled Crack Problem *International Journal of Fracture Mechanics* 8:441-446, 1972.

[40] Finnie, I. and Saith, A. A Note on the Angled Crack Problem and the Directional Stability of Cracks *International Journal of Fracture Mechanics* 9:484-486, 1973.

[41] Ewing, P. D. and Williams, J. G. Further Observations on the Angled Crack Problem *International Journal of Fracture Mechanics* 10:135, 1973.

[42] Sih, G. C. Some Basic Problems in Fracture Mechanics and New Concepts *Engineering Fracture Mechanics* 5:356-377, 1973.

[43] Wu, C. H. Maximum-Energy-Release-Rate Criterion Applied to a Tension-Compression Specimen With a Crack *Journal of Elasticity* 8:235-257, 1978.

[44] Press, W. H., Flannery, B. P., Teukolsky, S. A.. and Vetterling, W. T. *Numerical Recipes in Fortran* Cambridge University Press, Cambridge, England, 1986.

[45] Rubinstein, A. A. Crack-Path Effect on Material Toughness *Journal of Applied Mechanics* 57:97-103, 1990.

APPENDIX A

CRACK PATH PREDICTION PROGRAM

The following pages contain the computer program used to perform the crack path predictions presented in this work. The program is written in FORTRAN, and can be compiled as is to function on most computers.

```
      PROGRAM CRACKY
C     ****************************************************************
C     THIS PROGRAM PREDICTS THE PATH OF A NATURALLY GROWING CRACK
C     WHICH IS INTERACTING WITH AN ELLIPTIC INCLUSION.  THE
C     INCLUSION IS RIGID AND RIGIDLY BONDED.
C     ****************************************************************
C
C
C     ****************************************************************
C
C     WRITTEN BY EDWARD M. PATTON, 1987-1991
C     IN PARTIAL FULFILLMENT OF THE REQUIREMENTS FOR
C     THE DOCTOR OF PHILOSOPHY DEGREE IN MECHANICAL
C     ENGINEERING AT THE UNIVERSITY OF DELAWARE
C
C     HOPEFULLY THE VARIABLE NAMES THAT I HAVE CHOSEN WILL
C     BE APPARENT TO THE READER OF THE CODE.  IF NOT, THEN
C     CAREFUL READING OF MY THESIS SHOULD ELUCIDATE.
C
C     ****************************************************************
C
      REAL*4 M,KAP
      COMPLEX RKHAT(70),SIHAT(70),Z1,Z2,FAC1,FAC2,zstr
      COMPLEX XSHEAR(70,70),YSHEAR(70,70)
      COMMON /SPLIN/ X(70),Y(70),Y1(70),Y2(70)
      COMMON /GEOM/ R,M,KAP,ALPHA,Z1,Z2,STRESS,PHIIN
      COMMON /GEOM2/ ITIP,THETA,DZ,PHI(70)
      COMMON /RUSS/ YSTAR(70,70),YPSTAR(70,70),CAPY(70,70)
      COMMON /MATBLK/ ALHS(140,140),RHS(140),RSS(140),ALSS(140,140)
      COMMON /BLOK3/ SI(70),RK(70),N2,H,H2,N2P2,FAC1,FAC2,ABSFAC
      COMMON /BLOK4/ PSI(70),TAU(70)
      COMMON /BLOK5/ VI(70),RKHAT,WIK(70,70),SIHAT
      COMMON /BLOK6/ EJ,FJ,GJ
      COMMON /KERNEL/ XNORM(70,70),YNORM(70,70),XSHEAR,YSHEAR
C
C     OPEN NECESSARY FILES FOR OUTPUT
C
      OPEN (UNIT=1,FILE='crackout',FORM='FORMATTED')
      OPEN (UNIT=2,file='crackpath',FORM='FORMATTED')
      REWIND 1
      REWIND 2
C
C     WRITE HEADER FOR TECPLOT - YOU CAN USE ANY PLOTTING PROGRAM
C     THAT YOU LIKE FOR OFF-LINE PLOTTING OF THE CRACK PATH.
C
      WRITE (2,*) 'TITLE = ""'
      WRITE (2,*) 'VARIABLES = X Y '
      WRITE (2,*) 'ZONE'
C
C     SET CONSTANTS
```

```
C
      R = 1.
      PI = 3.1415926536
      ITIP = 0
      ITRAP = 0
      THETA = 0.
C
C     BEGIN THE PROGRAM.
C
C     THE FOLLOWING SEQUENCE OF SUBROUTINE CALLS
C     SETS UP AND SOLVES THE BOUNDARY VALUE PROBLEM OF A CRACK
C     INTERACTING WITH A RIGID ELLIPTICAL INCLUSION.
C
C     FIRST WE GET THE REQUIRED INPUT, LIKE WHERE THE CRACK IS, AND
C     WHAT SHAPE THE ELLIPSE IS
C
      CALL INPUT(N)
C
C     NOW THE MAIN LOOP OF THE PROGRAM
C     FIRST WE NEED TO PARAMETERIZE THE CRACK ITSELF
C
  100 CALL EXTEND(N,ITRAP)
C
C     NOW TO SET UP THE CONSTANTS FOR GERASOULIS' METHOD
C
      CALL POINTS
C
C     BUILD THE MATRIX AND CALL THE MATRIX INVERTER
C
      CALL BUILD(NB,IER)
C
C     IF BUILD OR THE MATRIX INVERTER SEES AN ERROR, WE STOP
C
        IF (IER.EQ.1) GO TO 9999
C
C     NOW TO CALCULATE THE K1 (P1 AND P2) AND K2 (BT AND BT2)
C     FOR THE CRACK.  THE 1 END IS THE LEFT END, AND THE
C     2 END IS THE RIGHT END.  THE CRACK IS ONLY ALLOWED TO
C     GROW FROM THE LEFT END.  IF YOPU WANT TO GROW FROM THE
C     RIGHT END, YOU MUST EDIT SUBROUTINE EXTEND
C
      P1 =-COS(PHI(2))*RSS(1)*2.*PI/ABSFAC
     !               +SIN(PHI(2))*RSS(N2P2)*2.*PI/ABSFAC
      BT = (COS(PHI(2))*RSS(N2P2)+SIN(PHI(2))*RSS(1))
     !    *2.*PI/ABSFAC
      P2 =-COS(PHI(N2P2))*RSS(n2p2-1)*2.*PI/ABSFAC
     !               +SIN(PHI(N2P2))*RSS(2*N2P2-2)*2.*PI/ABSFAC
      BT2 = (COS(PHI(N2P2))*RSS(2*N2P2-2)+SIN(PHI(N2P2))*RSS(N2P2-1))
     !    *2.*PI/ABSFAC
C
```

```
C     NOW CALCULATE THE ENERGY, EVEN THOUGH WE DO NOT USE IT
C
      G = P1**2+BT**2
C
C     WRITE THE RESULTS
C
      WRITE (*,*) Z1,P1,BT,P2,BT2,G,ABSFAC,N2
      WRITE (1,*) Z1,P1,BT,P2,BT2,ABSFAC,N2
C
C     CALL THE OUTPUT ROUTINE
C
      CALL OUT
C
C      WRITE COORDINATES OF NEW CRACK TIP ON FILE 2
C
      XTIP = REAL(SIHAT(2))
      YTIP = AIMAG(SIHAT(2))
      WRITE (2,10) XTIP,YTIP
   10 FORMAT (G15.6,3X,G15.6)
C
C     NOW FOR THE CRACK PATH PREDICTION.  THIS IS AN ITERATIVE
C     PROCESS THAT KEEPS GOING UNTIL N GETS TOO LARGE, OR THE
C     CRACK GROWS PAST THE POINT X = -3
C
C     GROW OFF THE LEFT TIP
C
      ITIP = 1
C
C     TEST TO SEE WHETHER WE HAVE REACHED OUR LIMIT
C
      IF (N2.LE.150.AND.REAL(Z1).GT.-3.) THEN
C
C     SET CONSTANTS AND COUNTERS FOR THE PREDICTION
C
      THOLD = 0.
      BTOLD = .2
      IBACK = 0
      THETA = 0.
      DTHETA = 4.*PI/180.
      NITTER = 0
C
C     CALCULATE THE POSITION OF THE NEW CRACK TIP, AND SEE IF IT
C     IS INSIDE THE ELLIPSE
C
  110 ZSTR = Z1-CMPLX(COS(THETA)*DZ,SIN(THETA)*DZ)
      XTIP = REAL(ZSTR)
      YTIP = AIMAG(ZSTR)
      ZSANG = ATAN(YTIP/XTIP)
      ZSTRMAG = SQRT(XTIP**2+YTIP**2)
      RADIUS = SQRT((1.-M*M)**2/(COS(ZSANG)**2*(1.-M)**2
```

```
!    SIN(ZSANG)**2*(1.+M)**2))
C
C    IF THE CRACK TIP IS IN THE ELLIPSE, STOP
C
     IF (ZSTRMAG-RADIUS.LT.0.) GO TO 9999
C
C    OTHERWISE, GO ON TO THE ITERATIVE SOLUTION.  I HAVE
C    GIVEN THIS THING AN ARBITRARY MAXIMUM OF 50 ITERATIONS
C    TO FIND WHERE IT WANTS TO GO.  IF THE PROBLEM IS POSED
C    CORRECTLY, YOU SHOULD NEED NO MORE THAN 15 ITERATIONS,
C    WITH AN AVERAGE OF ABOUT 10 PER INCREMENT OF GROWTH
C
     DO 200 ITRAP = 1,50
C
C    SAME SET OF SUBROUTINES.  WHAT THIS DOES IS TO TRY
C    SEVERAL DIFFERENT DIRECTIONS UNTIL IT FINDS THE
C    DIRECTION OF MINIMUM SHEAR STRESS.  THEN IT GOES
C    BACK TO STATEMENT 100 AND STARTS FRESH WITH A NEW
C    CRACK GROWTH INCREMENT
C
        CALL EXTEND(N,ITRAP)
C
        CALL POINTS
C
        CALL BUILD(NB,IER)
C
        IF (IER.EQ.1) GO TO 9999
C
        P1 =-COS(PHI(2))*RSS(1)*2.*PI/ABSFAC
     !           +SIN(PHI(2))*RSS(N2P2)*2.*PI/ABSFAC
        bt = (COS(PHI(2))*RSS(N2P2)+SIN(PHI(2))*RSS(1))
     !  *2.*PI/ABSFAC
        G = P1**2+BT**2
C
C    LET THE USER KNOW THAT YOU HAVE COMPLETED AN INTERATION,
C    AND SHOW HIM THE PERTINENT RESULTS
C
         WRITE (*,*) P1,BT,G,THETA*180./PI
C
C    NOW, IF THE NEW K2 IS LESS THAN THE OLD K2, DIVIDE DTHETA
C    IN HALF AND GO BACKWARDS.  IF YOU HAVEN'T BEEN BACKWARDS
C    TWICE YET, YOU HAVEN'T FOUND THETA
C
        IF (ABS(BT).GT.BTOLD.AND.IBACK.LT.2) THEN
            DTHETA = -DTHETA/2.
            THOLD = THETA
205             THETA = THETA+DTHETA
C
C    PUT SOME REASONABLE LIMITS ON THETA
C
```

```
            IF (THETA*180./PI.GT.90.) THEN
                THETA = 90.*PI/180.
                GO TO 201
            ELSEIF(THETA*180./PI.LT.-90.) THEN
                THETA = -90.*PI/180.
                GO TO 201
            ENDIF
C
C     CHECK TO SEE IF YOU ARE INSIDE THE ELLIPSE
C
            ZSTR = SIHAT(4)-CMPLX(COS(THETA)*DZ,SIN(THETA)*DZ)
            XTIP = REAL(ZSTR)
            YTIP = AIMAG(ZSTR)
            ZSANG = ATAN(YTIP/XTIP)
            ZSTRMAG = SQRT(XTIP**2+YTIP**2)
            RADIUS = SQRT((1.-M*M)**2/(COS(ZSANG)**2*(1.-M)**2
     !                +SIN(ZSANG)**2*(1.+M)**2))
            IF (ZSTRMAG-RADIUS.LT.0.) GO TO 9999
C
C     YOU JUST WENT BACKWARDS, SO INCREMENT IBACK
C
            IBACK = IBACK+1
C
C     RESET THE VALUE OF OLD K2
C
            BTOLD = ABS(BT)
C
C     AND COUNT THE ITERATION
C
            NITTER = NITTER+1
C
C     TRY AGAIN
C
            GO TO 200
C
C     OR IF YOU ARE STILL GOING DOWN IN MAGNITUDE, GO THE SAME
C     DIRECTION AND RESET OLD K2
C
            ELSEIF (ABS(BT).LE.BTOLD) THEN
            BTOLD = ABS(BT)
            THOLD = THETA
 206            THETA = THETA+DTHETA
C
C     SET LIMITS ON THETA
C
            IF (THETA*180./PI.GT.90.) THEN
                THETA = 90.*PI/180.
                GO TO 201
            ELSEIF(THETA*180./PI.LT.-90.) THEN
                THETA = -90.*PI/180.
```

```
                GO TO 201
            ENDIF
C
C     CHECK TO SEE IF YOU HAVE GONE IN THE ELLIPSE
C
            ZSTR = SIHAT(4)-CMPLX(COS(THETA)*DZ,SIN(THETA)*DZ)
            XTIP = REAL(ZSTR)
            YTIP = AIMAG(ZSTR)
            ZSANG = ATAN(YTIP/XTIP)
            ZSTRMAG = SQRT(XTIP**2+YTIP**2)
            RADIUS = SQRT((1.-M*M)**2/(COS(ZSANG)**2*(1.-M)**2
     !                 +SIN(ZSANG)**2*(1.+M)**2))
            IF (ABS(RADIUS-ZSTRMAG).LT..00001) GO TO 9999
C
C     COUNT THE ITERATION AND GO AGAIN
C
            NITTER = NITTER+1
            GO TO 200
C
C     OR, IF THE NEW K2 IS BIGGER, AND YOU HAVE BEEN BACKWARDS
C     TWICE, YOU HAVE FOUND THETA.  INCREMENT THE CRACK AND
C     GO OUT OF THE INNER LOOP
C
         ELSEIF (ABS(BT).GT.BTOLD.AND.IBACK.EQ.2) THEN
            THETA = THOLD
            GO TO 201
         ENDIF
C
      CALL OUT
C
  200 CONTINUE
C
  201 CONTINUE
C
C     TELL THE USER
C
      WRITE (*,*) 'AT N*2 = ',N2,' THETA = ',THETA*180./PI,
     !  ' ITERATIONS ',NITTER
C
C     AND GO BACK TO THE BEGINNING
C
      GO TO 100
C
C     HERE IS WHERE YOU GO IF N IS TOO BIG OR IF THE CRACK
C     IS FAR ENOUGH TO THE LEFT
C
      ENDIF
C
C     ALL DONE
C
```

```
9999 CONTINUE
     CLOSE (UNIT=1)
     CLOSE (UNIT=2)
     STOP
     END
C
C
     SUBROUTINE INPUT(N)
C
C    ****************************************************************
C    THIS ROUTINE PROVIDES ALL OF THE REQUIRED INPUT TO CRACKY
C    ****************************************************************
C
     REAL*4 M,KAP
     COMPLEX RKHAT(70),SIHAT(70),Z1,Z2,FAC1,FAC2
     COMPLEX XSHEAR(70,70),YSHEAR(70,70)
     COMMON /GEOM/ R,M,KAP,ALPHA,Z1,Z2,STRESS,PHIIN
     COMMON /GEOM2/ ITIP,THETA,DZ,PHI(70)
     COMMON /MATBLK/ ALHS(140,140),RHS(140),RSS(140),ALSS(140,140)
     COMMON /BLOK3/ SI(70),RK(70),N2,H,H2,N2P2,FAC1,FAC2,ABSFAC
     COMMON /BLOK4/ PSI(70),TAU(70)
     COMMON /BLOK5/ VI(70),RKHAT,WIK(70,70),SIHAT
     COMMON /BLOK6/ EJ,FJ,GJ
     COMMON /KERNEL/ XNORM(70,70),YNORM(70,70),XSHEAR,YSHEAR
C
     CONVER = 3.1415926536/180.
  200 FORMAT (2G10.4)
C
C    CRACK HAS A LENGTH OF 1 UNIT, WITH LEFT TIP AT Z1 AND
C    RIGHT TIP AT Z2
C
     CLEN = 1.
     WRITE (*,*) ' WHERE IS THE CLOSE TIP OF THE CRACK '
     READ (*,200) Z1
     WRITE (*,*) ' NOW WHAT IS THE ELLIPTICITY RATIO OF THE ELIPSE (0 TO 1)'
     READ (*,200) M
     WRITE (*,*) ' WHAT IS THE ANGLE OF THE CRACK '
     READ (*,200) PHIIN
     PHIIN = PHIIN*CONVER
     SINPHI = SIN(PHIIN)
     COSPHI = COS(PHIIN)
C
C    SET UP THE CRACK
C
     Z2 = CMPLX(REAL(Z1)+CLEN*COSPHI,AIMAG(Z1)+CLEN*SINPHI)
     WRITE (*,100) Z1,Z2,PHIIN/CONVER
  100 FORMAT (' Z1 = ',2G10.4,' Z2 = ',2G10.4,' PHI = ',G10.4)
C
C    UNCOMMENT THE COMMENTED LINES AND COMMENT OUT THE ASSIGNMENTS
C    IF YOU WANT TO HAVE MORE CONTROL OVER THE INPUT
```

```
C
C     WRITE (*,*) ' WHAT IS THE ANGLE BETWEEN THE CRACK AND THE LOAD'
C     READ (*,200) ALPHA
C     ALPHA = ALPHA*CONVER+PHIIN
      ALPHA = 90.*CONVER+PHIIN
      N = 5
C     WRITE (*,*) ' WHAT WOULD YOU LIKE FOR THE VALUE OF N'
C     READ (*,*) N
      WRITE (*,*) ' WHAT WOULD YOU LIKE FOR KAPPA'
      READ (*,200) KAP
C     KAP = 1.67
C
C     NOW SET UP THE CRACK PARAMETERS THAT WE NEED FOR THE SOLUTION
C
      FAC1 = (Z2+Z1)/2.
      FAC2 = (Z2-Z1)/2.
      ABSFAC = SQRT(REAL(FAC2)**2+AIMAG(FAC2)**2)
      DZ = ABSFAC/FLOAT(N)
C
C     DONE
C
      RETURN
      END
C
      SUBROUTINE OUT
C
C
      REAL*4 M,KAP
      COMPLEX RKHAT(70),SIHAT(70),Z1,Z2,FAC1,FAC2
      COMPLEX XSHEAR(70,70),YSHEAR(70,70)
      COMMON /GEOM/ R,M,KAP,ALPHA,Z1,Z2,STRESS,PHIIN
      COMMON /GEOM2/ ITIP,THETA,DZ,PHI(70)
      COMMON /MATBLK/ ALHS(140,140),RHS(140),RSS(140),ALSS(140,140)
      COMMON /BLOK3/ SI(70),RK(70),N2,H,H2,N2P2,FAC1,FAC2,ABSFAC
      COMMON /BLOK4/ PSI(70),TAU(70)
      COMMON /BLOK5/ VI(70),RKHAT,WIK(70,70),SIHAT
      COMMON /BLOK6/ EJ,FJ,GJ
      COMMON /KERNEL/ XNORM(70,70),YNORM(70,70),XSHEAR,YSHEAR
C
C     ****************************************************************
C     THIS ROUTINE PERFORMS ALL OF THE OUTPUT NECESSARY FOR CRACKY
C     ****************************************************************
C
C
      WRITE (1,*) ' Output from Crack Program'
C
      WRITE (1,*)
C
      WRITE (1,200) (RSS(I)*2.*3.1415926536/ABSFAC,I=1,2*N2P2-2)
      WRITE (1,*)
```

```
      WRITE (1,200) (RHS(I),I=1,2*N2P2-2)
  200 FORMAT (G15.5)
C
      WRITE (1,*)
C
C     DONE
C
      RETURN
      END
C
C
      SUBROUTINE EXTEND(N,ITRAP)
C
C
C     ********************************************************
C     THIS ROUTINE PROVIDES THE PROPER VALUES OF THE COORDINATES
C     OF THE EXTENDED CRACK IN TABULAR FORM, AND ALSO INCREASES
C     N BY THE APPROPRIATE AMOUNT (1), AT AN ANGLE CALCULATED
C     IN FUNCTION CRACK
C     ********************************************************
C
      REAL*4 M,KAP
      COMPLEX RKHAT(70),SIHAT(70),Z1,Z2,FAC1,FAC2
      COMPLEX XSHEAR(70,70),YSHEAR(70,70)
      COMMON /GEOM/ R,M,KAP,ALPHA,Z1,Z2,STRESS,PHIIN
      COMMON /GEOM2/ ITIP,THETA,DZ,PHI(70)
      COMMON /SPLIN/ X(70),Y(70),Y1(70),Y2(70)
      COMMON /MATBLK/ ALHS(140,140),RHS(140),RSS(140),ALSS(140,140)
      COMMON /BLOK3/ SI(70),RK(70),N2,H,H2,N2P2,FAC1,FAC2,ABSFAC
      COMMON /BLOK4/ PSI(70),TAU(70)
      COMMON /BLOK5/ VI(70),RKHAT,WIK(70,70),SIHAT
      COMMON /BLOK6/ EJ,FJ,GJ
      COMMON /KERNEL/ XNORM(70,70),YNORM(70,70),XSHEAR,YSHEAR
C
C     ONLY INCREMENT N IF WE HAVE BEEN THROUGH THE FIRST SOLUTION
C     AND AT THE FIRST ITERATION LOOKING FOR THETA (ITRAP = 1)
C
      IF (ITIP.EQ.1.AND.ITRAP.EQ.1) N=N+1
C
      N2 = N*2
      N2P2 = N2+2
      N2P2M1 = N2P2-1
      H = 1./FLOAT(N)
C
C     FOR ITERATIONS AFTER THE FIRST, BACK OFF TO WHERE THE CRACK
C     TIP WAS AT THE START OF THIS INCREMENT
C
      IF(ITRAP.GT.1) Z1 = SIHAT(4)
C
C     FIRST TIME THROUGH FOR THE WHOLE PROGRAM, SET UP THE CRACK
```

```
C
      IF (ITIP.EQ.0) THEN
C
      DO 1 I = 2,N2P2
         SIHAT(I) = ((FLOAT(I)-2.)*H-1.)*FAC2+FAC1
         IF (I.EQ.2) SIHAT(I) = Z1
         IF (I.EQ.N2P2) SIHAT(I) = Z2
         PHI(I) = PHIIN
         X(I-1) = REAL(SIHAT(I))
         Y(I-1) = AIMAG(SIHAT(I))
         Y1(I-1) = TAN(PHI(I))
    1 CONTINUE
C
C     CALL THE SPLINE ROUTINE
C
      CALL SPLINE (N2P2M1,X,Y,Y1,Y2)
      DO 2 K = 2,N2P2
         RKHAT(K) = (((FLOAT(K)-2.)*H-1.)+H/2.)*FAC2+FAC1
    2 CONTINUE
C
C     FOR SUBSEQUENT TRIPS THROUGH THE PROGRAM, WE NEED TO
C     ADD AN INCREMENT IN THE SPECIFIED DIRECTION, AND THEN
C     GET THE FIRST AND SECOND SPATIAL DERIVATIVES OF THE
C     CRACK BY CALLING SPLINE
C
      ELSEIF (ITIP.EQ.1) THEN
C
C     FIRST ITERATION AGAIN, SHOVE ALL OF THE CRACK GEOMETRY
C     TWO SPACES HIGHER IN EACH OF THE ARRAYS THAT HOLD CRACK
C     GEOMETRY
C
      IF (ITRAP.EQ.1) THEN
      DO 5 J=2,N2
         I = N2P2+2-J
         RKHAT(I) = RKHAT(I-2)
         SIHAT(I) = SIHAT(I-2)
         PHI(I) = PHI(I-2)
         X(I-1) = X(I-3)
        Y(I-1) = Y(I-3)
        Y1(I-1) = Y1(I-3)
    5 CONTINUE
      ABSFAC = ABSFAC+DZ
      ENDIF
C
C     THIS PART ACTUALLY PERFORMS THE INCREMENT
C
      PHI(3) = -THETA
      PHI(2) = -THETA
      SIHAT(2) = Z1-CMPLX(COS(PHI(2))*2.*DZ,SIN(PHI(2))*2.*DZ)
      SIHAT(3) = Z1-CMPLX(COS(PHI(3))*DZ,SIN(PHI(3))*DZ)
```

```
      RKHAT(2) = Z1-CMPLX(COS(PHI(2))*3.*DZ/2.,SIN(PHI(2))*3.*DZ/2.)
      RKHAT(3) = Z1-CMPLX(COS(PHI(3))*DZ/2.,SIN(PHI(3))*DZ/2.)
      X(1) = REAL(SIHAT(2))
      X(2) = REAL(SIHAT(3))
      Y(1) = AIMAG(SIHAT(2))
      Y(2) = AIMAG(SIHAT(3))
      Y1(1) = TAN(PHI(2))
      Y1(2) = TAN(PHI(3))
      Z1 = SIHAT(2)
C
C     GET OUR SPATIAL DERIVATIVES
C
      CALL SPLINE (N2P2M1,X,Y,Y1,Y2)
C
      ENDIF
C
      RETURN
      END
C
      SUBROUTINE SPLINE (N,X,Y,Y1,Y2)
C
C     ************************************************************
C     THIS ROUTINE, EXERPTED FROM "NUMERICAL RECIPES IN FORTRAN",
C     CALCULATES THE LOCAL FIRST AND SECOND DERIVATIVES FOR USE
C     IN SUBROUTINE RUSSIAN
C     ************************************************************
C
      DIMENSION U(70),X(70),Y(70),Y1(70),Y2(70)
C
      YP1 = 1.e35
      YPN = 1.e35
      DO 10 IN = 1,N
         Y2(IN) = 0.
   10 CONTINUE
      IF (YP1.GT..99E30) THEN
         Y2(1) = 0.
         U(1) = 0.
      ELSE
         Y2(1) = -.5
         U(1) = (3./(X(2)-X(1)))*((Y(2)-Y(1))/(X(2)-X(1))-YP1)
      ENDIF
      DO 11 I=2,N-1
         SIG = (X(I)-X(I-1))/(X(I+1)-X(I-1))
         P = SIG*Y2(I-1)+2.
         Y2(I) = (SIG-1.)/P
         U(I) = (6.*((Y(I+1)-Y(I))/(X(I+1)-X(I))-(Y(I)-Y(I-1))
     !        /(X(I)-X(I-1)))/(X(I+1)-X(I-1))-SIG*U(I-1))/P
   11 CONTINUE
      IF(YPN.GT..99E30) THEN
         QN = 0.
```

```
      UN = 0.
    ELSE
      QN = .5
      UN = (3./(X(N)-X(N-1)))*(YPN-(Y(N)-Y(N-1))/(X(N)-X(N-1)))
    ENDIF
    Y2(N) = (UN-QN*U(N-1))/(QN*Y2(N-1)+1.)
    DO 12 K = N-1,1,-1
      Y2(K) = Y2(K)*Y2(K+1)+U(K)
 12 CONTINUE
    RETURN
    END
C
C
    SUBROUTINE POINTS
C
C    ****************************************************************
C    CALCULATES THE SI AND RK QUANTITIES FOR GERASOULIS'
C    TECHNIQUE.  ALSO SETS UP THE WEIGHT FUNCTIONS BY CALLING
C    SUBROUTINE VWGT AND WTFUNS
C    ****************************************************************
C
    REAL*4 M,KAP
    COMPLEX RKHAT(70),SIHAT(70),Z1,Z2,FAC1,FAC2
    COMPLEX XSHEAR(70,70),YSHEAR(70,70)
    COMMON /GEOM/ R,M,KAP,ALPHA,Z1,Z2,STRESS,PHIIN
    COMMON /GEOM2/ ITIP,THETA,DZ,PHI(70)
    COMMON /MATBLK/ ALHS(140,140),RHS(140),RSS(140),ALSS(140,140)
    COMMON /BLOK3/ SI(70),RK(70),N2,H,H2,N2P2,FAC1,FAC2,ABSFAC
    COMMON /BLOK4/ PSI(70),TAU(70)
    COMMON /BLOK5/ VI(70),RKHAT,WIK(70,70),SIHAT
    COMMON /BLOK6/ EJ,FJ,GJ
    COMMON /KERNEL/ XNORM(70,70),YNORM(70,70),XSHEAR,YSHEAR
C
    N2P2M1 = N2P2-1
C
C     CALCULATE SI ARRAY
C
    DO 1 I = 2,N2P2
      SI(I) = (FLOAT(I)-2.)*H-1.
      SI(2) = -1.
      SI(N2P2) = 1.
 1  CONTINUE
C
C     CALCULATE RK ARRAY
C
    DO 2 K = 2,N2P2
      RK(K) = SI(K)+H/2
 2  CONTINUE
C
C    SET CONSTANT WEIGHTS
```

```
C
      CALL VWGT
C
      DO 3 K = 2,N2P2M1
         DO 4 I = 2,N2P2
            CALL WTFUNS(RK(K),I)
            WIK(K,I) = EJ+FJ+GJ
    4    CONTINUE
    3 CONTINUE
C
      RETURN
      END
C
C
      SUBROUTINE WTFUNS(S,K)
C
C     ***************************************************************
C     THIS SUBROUTINE COMPUTES THE APPROPRIATE WEIGHT FUNCTIONS FOR
C     THE PIECE-WISE SMOOTH POLYNOMIAL APPROXIMATION
C     ***************************************************************
C
      REAL*4 M,KAP
      COMPLEX RKHAT(70),SIHAT(70),Z1,Z2,FAC1,FAC2
      COMPLEX XSHEAR(70,70),YSHEAR(70,70)
      COMMON /GEOM/ R,M,KAP,ALPHA,Z1,Z2,STRESS,PHIIN
      COMMON /GEOM2/ ITIP,THETA,DZ,PHI(70)
      COMMON /MATBLK/ ALHS(140,140),RHS(140),RSS(140),ALSS(140,140)
      COMMON /BLOK3/ SI(70),RK(70),N2,H,H2,N2P2,FAC1,FAC2,ABSFAC
      COMMON /BLOK4/ PSI(70),TAU(70)
      COMMON /BLOK5/ VI(70),RKHAT,WIK(70,70),SIHAT
      COMMON /BLOK6/ EJ,FJ,GJ
      COMMON /KERNEL/ XNORM(70,70),YNORM(70,70),XSHEAR,YSHEAR
C
C
C     CHECK TO SEE IF K IS ODD OR EVEN
C
      KCHEK1 = K/2
      KCHEK2 = 2*KCHEK1
      IF (KCHEK2.NE.K) THEN
C
C     K IS ODD
C
         EJ = 0.
         GJ = 0.
         J = (K+1)/2
         FJ = -RM(S,SI(2*J),SI(2*J-2),J)/H2
         RETURN
C
      ELSEIF (K.EQ.2) THEN
C
```

```
C     K = 2
C
          FJ = 0.
          GJ = 0.
          J = (K+2)/2
          EJ = RM(S,SI(2*J),SI(2*J-1),J)/(2.*H2)
          RETURN
C
      ELSEIF (K.EQ.N2P2) THEN
C
C     K = N2P2
C
          FJ = 0.
          EJ = 0.
          J = K/2
          GJ = RM(S,SI(J*2-1),SI(J*2-2),J)/(2.*H2)
          RETURN
C
      ELSE
C
C     K IS EVEN
C
          J = (K+2)/2
          EJ = RM(S,SI(J*2),SI(J*2-1),J)/(2.*H2)
          J = K/2
          GJ = RM(S,SI(J*2-1),SI(J*2-2),J)/(2.*H2)
          FJ = 0.
          RETURN
C
      ENDIF
      END
C
C
      SUBROUTINE VWGT
C
C     ************************************************************
C     THIS ROUTINE COMPUTES THE CONSTANTS FOR THE POLYNOMIAL
C     APPROXIMATION - SEE GERASOULIS' PAPER
C     ************************************************************
C
      REAL*4 M,KAP
      COMPLEX RKHAT(70),SIHAT(70),Z1,Z2,FAC1,FAC2
      COMPLEX XSHEAR(70,70),YSHEAR(70,70)
      COMMON /GEOM/ R,M,KAP,ALPHA,Z1,Z2,STRESS,PHIIN
      COMMON /GEOM2/ ITIP,THETA,DZ,PHI(70)
      COMMON /MATBLK/ ALHS(140,140),RHS(140),RSS(140),ALSS(140,140)
      COMMON /BLOK3/ SI(70),RK(70),N2,H,H2,N2P2,FAC1,FAC2,ABSFAC
      COMMON /BLOK4/ PSI(70),TAU(70)
      COMMON /BLOK5/ VI(70),RKHAT,WIK(70,70),SIHAT
      COMMON /BLOK6/ EJ,FJ,GJ
```

```
      COMMON /KERNEL/ XNORM(70,70),YNORM(70,70),XSHEAR,YSHEAR
C
C
      H2 = H**2
      NP1 = N2P2/2
C
      DO 1 J1 = 2,N2P2
         PSI(J1) = ASIN(SI(J1))
    1 CONTINUE
C
      DO 2 J2 = 1,NP1
         TAU(J2) = TAN(PSI(J2*2)/2.)
    2 CONTINUE
C
      DO 3 J3 = 2,N2P2
         J3CHK1 = J3/2
         J3CHK2 = J3CHK1*2
C
C        J3 IS ODD
C
         IF (J3.NE.J3CHK2) THEN
C
            AJ = 0.
            CJ = 0.
            J3P = (J3+1)/2
            BJ = -HCON(J3P,SI(J3P*2),SI(J3P*2-2))/H2
            GO TO 4
C
C        J3 = 2
C
         ELSEIF (J3.EQ.2) THEN
C
            J3P = 2
            AJ = HCON(J3P,SI(J3P*2),SI(J3P*2-1))/(2.*H2)
            BJ = 0.
            CJ = 0.
            GO TO 4
C
C        J3 = N2P2
C
         ELSEIF (J3.EQ.N2P2) THEN
C
            J3P = NP1
            CJ = HCON(J3P,SI(J3P*2-1),SI(J3P*2-2))/(2.*H2)
            AJ = 0.
            BJ = 0.
            GO TO 4
C
C        J3 IS EVEN
C
```

```
      ELSE
C
          BJ = 0.
          J3P = (J3+2)/2
          AJ = HCON(J3P,SI(J3P*2),SI(J3P*2-1))/(2.*H2)
          J3P = J3/2
          CJ = HCON(J3P,SI(J3P*2-1),SI(J3P*2-2))/(2.*H2)
C
      ENDIF
C
  4   VI(J3) = AJ+BJ+CJ
C
  3 CONTINUE
    RETURN
    END
C
C
    FUNCTION HCON(J,X,Y)
C
C   ************************************************************
C   THIS FUNCTION IS USED TO DETERMINE THE WEIGHTS
C   FOR THE PIECEWISE SMOOTH POLYNOMIAL APPROXIMATION
C   ************************************************************
C
    REAL*4 M,KAP
    COMPLEX RKHAT(70),SIHAT(70),Z1,Z2,FAC1,FAC2
    COMPLEX XSHEAR(70,70),YSHEAR(70,70)
    COMMON /GEOM/ R,M,KAP,ALPHA,Z1,Z2,STRESS,PHIIN
    COMMON /GEOM2/ ITIP,THETA,DZ,PHI(70)
    COMMON /MATBLK/ ALHS(140,140),RHS(140),RSS(140),ALSS(140,140)
    COMMON /BLOK3/ SI(70),RK(70),N2,H,H2,N2P2,FAC1,FAC2,ABSFAC
    COMMON /BLOK4/ PSI(70),TAU(70)
    COMMON /BLOK5/ VI(70),RKHAT,WIK(70,70),SIHAT
    COMMON /BLOK6/ EJ,FJ,GJ
    COMMON /KERNEL/ XNORM(70,70),YNORM(70,70),XSHEAR,YSHEAR
C
C
    J2 = J*2
    TERM1 = (X*Y+.5)*(PSI(J2)-PSI(J2-2))
    TERM2 = (X+Y)*(COS(PSI(J2))-COS(PSI(J2-2)))
    TERM3 = (SIN(2.*PSI(J2))-SIN(2.*PSI(J2-2)))/4.
    HCON = TERM1+TERM2-TERM3
    RETURN
    END
C
C
    FUNCTION RM(S,X,Y,J)
C
C   ************************************************************
C   THIS FUNCTION IS CALLED BY POINTS AND IS USED
```

```
C     IN DETERMINING WEIGHTS FOR THE POLYNOMIAL
C     APPROXIMATION
C     ************************************************************
C
      REAL*4 M,KAP
      COMPLEX RKHAT(70),SIHAT(70),Z1,Z2,FAC1,FAC2
      COMPLEX XSHEAR(70,70),YSHEAR(70,70)
      COMMON /GEOM/ R,M,KAP,ALPHA,Z1,Z2,STRESS,PHIIN
      COMMON /GEOM2/ ITIP,THETA,DZ,PHI(70)
      COMMON /MATBLK/ ALHS(140,140),RHS(140),RSS(140),ALSS(140,140)
      COMMON /BLOK3/ SI(70),RK(70),N2,H,H2,N2P2,FAC1,FAC2,ABSFAC
      COMMON /BLOK4/ PSI(70),TAU(70)
      COMMON /BLOK5/ VI(70),RKHAT,WIK(70,70),SIHAT
      COMMON /BLOK6/ EJ,FJ,GJ
      COMMON /KERNEL/ XNORM(70,70),YNORM(70,70),XSHEAR,YSHEAR
C
C
      JM1 = J-1
      J2 = J*2
      J2M2 = J2-2
C
      AINT1 = SQRT(1.-S**2)
      AINT2 = (-1.+AINT1+S*TAU(J))*TAU(JM1)+S-(1.+AINT1)*TAU(J)
      AINT3 = (-1.-AINT1+S*TAU(J))*TAU(JM1)+S-(1.-AINT1)*TAU(J)
      AINT4 = ABS(AINT2/AINT3)
      AJOFS =ALOG(AINT4)/AINT1
C
      TERM1 = SQRT(1.-SI(J2)**2)
      TERM2 = SQRT(1.-SI(J2M2)**2)
      TERM3 = (S**2+X*Y-S*(X+Y))*AJOFS
      TERM4 = (S-X-Y)*(PSI(J2)-PSI(J2M2))
C
      RM = -TERM1+TERM2+TERM3+TERM4
      RETURN
      END
C
C
      SUBROUTINE BUILD (NB,IER)
C
C     ************************************************************
C     THIS ROUTINE BUILDS THE MATRIX AND PERFORMS THE
C     INVERSION OF THE MATRIX TO SOLVE THE PROBLEM
C     ************************************************************
C
      REAL*4 M,KAP
      COMPLEX RKHAT(70),SIHAT(70),Z1,Z2,FAC1,FAC2
      COMPLEX XSHEAR(70,70),YSHEAR(70,70)
      COMMON /GEOM/ R,M,KAP,ALPHA,Z1,Z2,STRESS,PHIIN
      COMMON /GEOM2/ ITIP,THETA,DZ,PHI(70)
      COMMON /SPLIN/ X(70),Y(70),Y1(70),Y2(70)
```

```
      COMMON /RUSS/ YSTAR(70,70),YPSTAR(70,70),CAPY(70,70)
      COMMON /MATBLK/ ALHS(140,140),RHS(140),RSS(140),ALSS(140,140)
      COMMON /BLOK3/ SI(70),RK(70),N2,H,H2,N2P2,FAC1,FAC2,ABSFAC
      COMMON /BLOK4/ PSI(70),TAU(70)
      COMMON /BLOK5/ VI(70),RKHAT,WIK(70,70),SIHAT
      COMMON /BLOK6/ EJ,FJ,GJ
      COMMON /KERNEL/ XNORM(70,70),YNORM(70,70),XSHEAR,YSHEAR
      COMPLEX SFORCE,PFORCE
C
C     ZERO OUT THE MATRICES AND RIGHT HAND SIDES, INCLUDING
C     THE RUSSIAN STUFF
C
      DO 30 IA = 1,N2P2
          RHS(IA) = 0.
          RSS(IA) = 0.
      DO 30 JA = 1,N2P2
          ALHS(IA,JA) = 0.
          ALSS(IA,JA) = 0.
          YSTAR(IA,JA) = 0.
          YPSTAR(IA,JA) = 0.
          CAPY(IA,JA) = 0.
 30       CONTINUE
      N2P2M1 = N2P2-1
      NB = 2*N2P2M1
C
C     NOW SET UP THE INTERACTION TERMS FROM THE KERNEL
C
      DO 50 I = 2,N2P2
      DO 60 J = 2,N2P2M1
      CALL KERNEL(SIHAT(I),RKHAT(J),I,J)
 60   CONTINUE
 50   CONTINUE
C
C
C     AND NOW THE STUFF FROM THE RUSSIAN PAPER
C
      CALL RUSSIAN (N2P2)
C
C
C     NOW LOOP THROUGH AND SET UP THE LEFT AND RIGHT SIDES
C     OF THE EQUATION (A)X(SOLUTION) = (B)
C
      DO 1 JN = 1,N2P2M1
       J = JN+1
       IT = JN
C
C     GET THE LOCAL ANGLES RIGHT, AND THEIR SINES AND COSINES
C
       SINPHI = SIN(PHI(J))
       COSPHI = COS(PHI(J))
```

```
      COS3PHI = COS(3.*PHI(J))
      SIN3PHI = SIN(3.*PHI(J))
      JT = JN+N2P2M1
C
C     DO THE RIGHT HAND SIDE FIRST
C
      IF(J.EQ.N2P2) THEN
        RHS(JN) = 0.
        RHS(JT) = 0.
      ELSE
        RHS(JN) = COSPHI**2*REAL(PFORCE(RKHAT(J))
     !    +SFORCE(RKHAT(J)))+SINPHI**2*REAL(PFORCE(RKHAT(J))
     !    -SFORCE(RKHAT(J)))-2.*SINPHI*COSPHI
     !    *AIMAG(SFORCE(RKHAT(J)))
        RHS(JT) = -2.*SINPHI*COSPHI*(REAL(SFORCE(RKHAT(J))))
     !    +(SINPHI**2-COSPHI**2)*AIMAG(SFORCE(RKHAT(J)))
      ENDIF
C
C     NOW THE REST OF THE MATRIX
C
      DO 1 IY = 1,N2P2M1
        I = IY+1
        ITAU = IY
        IX = IY+N2P2M1
C
C     FIRST THE KERNEL STRESSES
C
        XSIGX = XNORM(I,J)-REAL(XSHEAR(I,J))
        XSIGY = XNORM(I,J)+REAL(XSHEAR(I,J))
        XSIGXY = AIMAG(XSHEAR(I,J))
        YSIGX = YNORM(I,J)-REAL(YSHEAR(I,J))
        YSIGY = YNORM(I,J)+REAL(YSHEAR(I,J))
        YSIGXY = AIMAG(YSHEAR(I,J))
C
C     NOW THE ANGULAR COEFFICIENTS FOR AN ARBITRARILY ORIENTED
C    STRAIGHT CRACK
C
        BYX= COSPHI+COS3PHI
        BYY = 3.*COSPHI-COS3PHI
        BYXY = SIN3PHI-SINPHI
        BXX = -(3.*SINPHI+SIN3PHI)
        BXY = SIN3PHI-SINPHI
        BXXY = COS3PHI+COSPHI
        SNY = SINPHI**2*BYX+COSPHI**2*BYY
     !       -2.*SINPHI*COSPHI*BYXY
        SNX = SINPHI**2*BXX+COSPHI**2*BXY
     !       -2.*SINPHI*COSPHI*BXXY
        STY = SINPHI*COSPHI*(BYX-BYY)
     !       +BYXY*(SINPHI**2-COSPHI**2)
        STX = SINPHI*COSPHI*(BXX-BXY)
```

```
     !          +BXXY*(SINPHI**2-COSPHI**2)
C
C     NOW THE RUSSIAN STUFF FOR A NON-STRAIGHT CRACK
C
          BOTTOM = (1.+YSTAR(IT,ITAU)**2)**2
          RNX = CAPY(IT,ITAU)*(YSTAR(IT,ITAU)**2-1.-Y1(IT)*
     !       YSTAR(IT,ITAU)*(3.+YSTAR(IT,ITAU)**2))/BOTTOM-
     !       YPSTAR(IT,ITAU)
          RNY = (YPSTAR(IT,ITAU)-CAPY(IT,ITAU))*(YSTAR(IT,ITAU)**2-1.)
     !       *(YSTAR(IT,ITAU)-Y1(IT))/BOTTOM
          RTX = (YPSTAR(IT,ITAU)-CAPY(IT,ITAU))*(YSTAR(IT,ITAU)
     !       *(3.+YSTAR(IT,ITAU)**2)+Y1(IT)*(YSTAR(IT,ITAU)**2-1.))
     !       /BOTTOM
          RTY = (YPSTAR(IT,ITAU)-CAPY(IT,ITAU))*(YSTAR(IT,ITAU)**2-1.)
     !       *(1.+Y1(IT)*YSTAR(IT,ITAU))/BOTTOM+YPSTAR(IT,ITAU)
C
C     NOW BUILD THE MATRIX ALHS THAT IS TO BE SENT OFF TO THE
C     GAUSS-JORDAN MARTIX INVERSION ROUTINE
C
          IF (J.EQ.N2P2) THEN
           ALHS(JN,IY) = VI(I)*COSPHI
           ALHS(JN,IX) = -VI(I)*SINPHI
           ALHS(JT,IY) = VI(I)*SINPHI
           ALHS(JT,IX) = VI(I)*COSPHI
          ELSE
           ALHS(JN,IY) = SNY*WIK(J,I)/ABSFAC-VI(I)*(YSIGX*SINPHI**2+
     !                YSIGY*COSPHI**2-2.*YSIGXY*SINPHI*COSPHI)
     !                -VI(I)*RNY
           ALHS(JT,IY) = STY*WIK(J,I)/ABSFAC-VI(I)*(SINPHI*COSPHI*
     !                (YSIGX-YSIGY)+YSIGXY*(SINPHI**2-COSPHI**2))
     !                -VI(I)*RTY
           ALHS(JN,IX) = SNX*WIK(J,I)/ABSFAC-VI(I)
     !                *(XSIGX*SINPHI**2+XSIGY*COSPHI**2
     !                -2.*XSIGXY*SINPHI*COSPHI)
     !                -VI(I)*RNX
           ALHS(JT,IX) = STX*WIK(J,I)/ABSFAC-VI(I)
     !                *(SINPHI*COSPHI*(XSIGX-XSIGY)
     !                +XSIGXY*(SINPHI**2-COSPHI**2))
     !                -VI(I)*RTX
          ENDIF
    1  CONTINUE
C
C     NOW SAVE THE LEFT HAND SIDE OF THE EQUATION, AND
C     SAVE THE FORCING FUNCTIONS FROM THE RIGHT HAND SIDE
C
       DO 110 I=1,NB
       RSS(I) = RHS(I)
       DO 110 K=1,NB
       ALSS(I,K) = ALHS(I,K)
  110  CONTINUE
```

```
C
C    NOW CALL THE MATRIX INVERSION ROUTINE - ALSS GETS
C    REPLACED WITH ITS INVERSE, AND RSS GETS REPLACED
C    WITH THE SOLUTION VECTOR
C
     CALL GAUSSJ (ALSS,NB,140,RSS,IER)
C
C    IF ERROR - BOMB THE TURKEY
C
     IF (IER.EQ.-1) GO TO 9999
C
     RETURN
C
 9999 WRITE (*,*) ' MATRIX IS SINGULAR - CHECK YOUR INPUT'
     RETURN
     END
C
     SUBROUTINE KERNEL (Z0,Z,IZ0,IZ)
C
C    ************************************************************
C    THIS SUBROUTINE CONTAINS THE NON-CAUCHY SINGULAR
C    PORTION OF THE GREEN'S FUNCTION THAT IS USED TO
C    SOLVE THE PROBLEM
C    ************************************************************
C
     REAL*4 M,KAP
     COMPLEX RKHAT(70),SIHAT(70),Z1,Z2,FAC1,FAC2
     COMPLEX XSHEAR(70,70),YSHEAR(70,70)
     COMMON /GEOM/ R,M,KAP,ALPHA,Z1,Z2,STRESS,PHIIN
     COMMON /GEOM2/ ITIP,THETA,DZ,PHI(70)
     COMMON /MATBLK/ ALHS(140,140),RHS(140),RSS(140),ALSS(140,140)
     COMMON /BLOK3/ SI(70),RK(70),N2,H,H2,N2P2,FAC1,FAC2,ABSFAC
     COMMON /BLOK4/ PSI(70),TAU(70)
     COMMON /BLOK5/ VI(70),RKHAT,WIK(70,70),SIHAT
     COMMON /BLOK6/ EJ,FJ,GJ
     COMMON /KERNEL/ XNORM(70,70),YNORM(70,70),XSHEAR,YSHEAR
     COMPLEX ZETA,ZETA0,ZETAB,ZETA0B,EYE,A,C,EMOZ0,Z0BINV,Z,Z0
     COMPLEX Z0BOM,YEP0,XEP0,T1,T1A,T1B,T1C,T1D,T1TIME
     COMPLEX T2,T3,T4,T5,T6,T6A,T6B,T6C,T6D,T6TIME
     COMPLEX T7,T7A,T7B,T7C,T7D,T7TIME,PHI1,PHI2,PHI3,PHI4
     COMPLEX TRY
C
C    CALCULATE CONSTANTS TO BE USED IN THE CALCULATIONS
C    STARTING BY TRANSFORMING Z AND Z0 INTO ZETA AND ZETA0
C
     TRY = CSQRT(Z**2-4.*R*R*M)
C
C     MAKE SURE YOU PICK THE RIGHT ROOT
C
     IF (REAL(Z).LE.0..AND.REAL(TRY).GT.0.)      TRY = -1.*TRY
```

```
      ZETA = (Z+TRY)/(2.*R)
      TRY = CSQRT(Z0**2-cmplx(4.*R*R*M,0.))
      IF (REAL(Z0).LE.0..AND.REAL(TRY).GT.0.) TRY = -1.*TRY
      ZETA0 = (Z0+TRY)/(2.*R)
C
C     NOW THE REST OF THE CONSTANTS
C
      ZETAB = CONJG(ZETA)
      ZETA0B = CONJG(ZETA0)
      Z0BINV = 1./ZETA0B
      EMOZ0 = M/ZETA0
      Z0BOM = ZETA0B/M
      EYE = (0.,1.)
      A = (Z0BINV-EMOZ0)*(Z0BINV-ZETA0)/(Z0BINV-Z0BOM)
      C = (EMOZ0-Z0BINV)*(EMOZ0-Z0BOM)/(EMOZ0-ZETA0)
      YEP0 = EMOZ0-KAP/ZETA0B+M*M/ZETA0-M/(KAP*ZETA0B)-M*C+A/KAP
      XEP0 =EYE*EMOZ0-EYE*KAP/ZETA0B-EYE*M*M/ZETA0+
     !     EYE*M/(KAP*ZETA0B)+EYE*M*C+EYE*A/KAP
      RYEP0 = REAL(EYE*YEP0)
      RXEP0 = REAL(EYE*XEP0)
C
C     CALCULATE THE TERMS IN THE KERNEL
C     I REALIZE THAT THIS IS A MESS, BUT YOU SHOULD SEE THE
C     PAGES OF ALGEBRA THAT MAKE THIS THING UP.  MIKE SANTARE
C     CAN HELP YOU WITH THIS IF YOU NEED IT
C
      T1A = (-2.*ZETA**3+ZETA**2/ZETA0B+M/ZETA0B)
     !      /(KAP*R*ZETA0B*(ZETA-Z0BINV)**2)
      T1B = -(-2.*M*ZETA**3+M*M*ZETA**2/ZETA0+M**3/ZETA0)
     !      /((ZETA-EMOZ0)**2*R*ZETA0)
      T1C = -2.*A*(-ZETA**4+M*ZETA/ZETA0B)
     !      /(R*M*KAP*(ZETA-Z0BINV)**3)
      T1D = 2.*EYE*M*ZETA/(KAP*R*(1.+M*M/KAP))
      T1TIME = (ZETA**2*(ZETAB**2+M))/(ZETAB*(ZETA**2-M)**3)
C
      T2 = KAP*ZETA/(R*ZETA0B*(ZETA-Z0BINV)*(ZETA**2-M))
      T3 = -M*ZETA/(R*ZETA0*(ZETA-EMOZ0)*(ZETA**2-M))
      T4 = M*C*ZETA**2/(R*(ZETA-EMOZ0)**2*(ZETA**2-M))
      T5 = -EYE/(R*(ZETA**2-M)*(1.+M*M/KAP))
C
      T6A = 1./(KAP*R*ZETA0B*(ZETA-Z0BINV)*ZETA)
      T6B = -M/(R*ZETA0*(ZETA-EMOZ0)*ZETA)
      T6C = -A/(R*M*KAP*(ZETA-Z0BINV)**2)
      T6D = -EYE*M/(R*KAP*(1.+M*M/KAP)*ZETA**2)
      T6TIME = -(M*ZETA**6-ZETA**4*(3.*M*M+1.)-M*ZETA**2)
     !       /((ZETA**2-M)**3)
C
      T7A = -(2.*ZETA-Z0BINV)/(KAP*ZETA0B*ZETA**2*(ZETA-Z0BINV)**2)
      T7B = M*(2.*ZETA-EMOZ0)/(ZETA0*ZETA**2*(ZETA-EMOZ0)**2)
      T7C = 2.*A/(M*KAP*(ZETA-Z0BINV)**3)
```

```
      T7D = 2.*EYE*M/(KAP*ZETA**3*(1.+M**2/KAP))
      T7TIME = -ZETA**3*(1.+M*ZETA**2)/(R*(ZETA**2-M)**2)
C
      PHI1 = T2/KAP**2
      PHI2 = T3
      PHI3 = -A*ZETA**2/(R*M*KAP*(ZETA-Z0BINV)**2*(ZETA**2-M))
      PHI4 = T5*M/KAP
C
C     NOW TO CALCULATE THE NORMAL AND SHEAR COMPONENTS OF
C     THE KERNELS.  THE NORMAL COMPONENT IS THE REAL PART
C     OF PHI_PRIME.  THE "SHEAR" COMPONENT IS THE OTHER
C     PART OF MUSHKELISHVILI'S POTENTIAL EQUATION
C
      T1 = (T1A+T1B+T1C+T1D*RYEP0)*T1TIME
      T6 = (T6A+T6B+T6C+T6D*RYEP0)*T6TIME
      T7 = (T7A+T7B+T7C+T7D*RYEP0)*T7TIME
      YSHEAR(IZ0,IZ) = T1+T2+T3+T4+T5*RYEP0+T6+T7
C
      T1 = (-EYE*T1A-EYE*T1B+EYE*T1C+T1D*RXEP0)*T1TIME
      T6 = (-EYE*T6A-EYE*T6B+EYE*T6C+T6D*RXEP0)*T6TIME
      T7 = (-EYE*T7A-EYE*T7B+EYE*T7C+T7D*RXEP0)*T7TIME
      XSHEAR(IZ0,IZ) = T1+EYE*T2+EYE*T3-EYE*T4+T5*RXEP0+T6+T7
C
      YNORM(IZ0,IZ) = 2.*REAL(PHI1+PHI2+PHI3+PHI4*RYEP0)
      XNORM(IZ0,IZ) = 2.*REAL(-EYE*PHI1-EYE*PHI2+EYE*PHI3+PHI4*RXEP0)
C
      RETURN
      END
C
C
      COMPLEX FUNCTION PFORCE(Z)
C
C     ************************************************************
C     SUBROUTINE THAT CALCULATES THE PHI POTENTIAL FOR THE FORCE
C     DUE TO THE ELLIPSE, TO BE USED IN BUILD TO GENERATE THE
C     RIGHT HAND SIDE OF THE EWUATION.  SEE PAGE 349 IN
C     MUSHKHELISHVILI'S BOOK
C     ************************************************************
C
      REAL*4 M,KAP
      COMPLEX RKHAT(70),SIHAT(70),Z1,Z2,FAC1,FAC2
      COMPLEX XSHEAR(70,70),YSHEAR(70,70)
      COMMON /GEOM/ R,M,KAP,ALPHA,Z1,Z2,STRESS,PHIIN
      COMMON /GEOM2/ ITIP,THETA,DZ,PHI(70)
      COMMON /MATBLK/ ALHS(140,140),RHS(140),RSS(140),ALSS(140,140)
      COMMON /BLOK3/ SI(70),RK(70),N2,H,H2,N2P2,FAC1,FAC2,ABSFAC
      COMMON /BLOK4/ PSI(70),TAU(70)
      COMMON /BLOK5/ VI(70),RKHAT,WIK(70,70),SIHAT
      COMMON /BLOK6/ EJ,FJ,GJ
      COMMON /KERNEL/ XNORM(70,70),YNORM(70,70),XSHEAR,YSHEAR
```

```
      COMPLEX ZETA,EYE,Z,DPHI
      COMPLEX TRY
C
C     GET ZETA
C
      TRY = CSQRT(Z**2-cmplx(4.*R*R*M,0.))
      IF (REAL(Z).LE.0..AND.REAL(TRY).GT.0.)      TRY = -1.*TRY
      ZETA = (Z+TRY)/(2.*R)
      EYE = CMPLX(0.,1.)
C
C     CALCULATE THE FORCE COMPONENTS FROM THE POTENTIALS
C
      EPS = M*SIN(2.*ALPHA)*(1.+KAP)/(4.*(M*M+KAP))
      DPHI = ZETA**2/(4.*(ZETA**2-M))-(2.*M*EPS*EYE+M/4.-
     !     .5*(COS(2.*ALPHA)+EYE*SIN(2.*ALPHA)))/(KAP*(ZETA**2-M))
      PFORCE = cmplx(2.*real(DPHI),0.)
C
      RETURN
      END
C
      COMPLEX FUNCTION SFORCE(Z)
C
C     ************************************************************
C     CALCULATES THE SI POTENTIAL FROM PAGE 349 IN MUSHKHELISHVILI
C     ************************************************************
C
      REAL*4 M,KAP
      COMPLEX RKHAT(70),SIHAT(70),Z1,Z2,FAC1,FAC2
      COMPLEX XSHEAR(70,70),YSHEAR(70,70)
      COMMON /GEOM/ R,M,KAP,ALPHA,Z1,Z2,STRESS,PHIIN
      COMMON /GEOM2/ ITIP,THETA,DZ,PHI(70)
      COMMON /MATBLK/ ALHS(140,140),RHS(140),RSS(140),ALSS(140,140)
      COMMON /BLOK3/ SI(70),RK(70),N2,H,H2,N2P2,FAC1,FAC2,ABSFAC
      COMMON /BLOK4/ PSI(70),TAU(70)
      COMMON /BLOK5/ VI(70),RKHAT,WIK(70,70),SIHAT
      COMMON /BLOK6/ EJ,FJ,GJ
      COMMON /KERNEL/ XNORM(70,70),YNORM(70,70),XSHEAR,YSHEAR
      COMPLEX ZETA,EYE,ZBPHI,SIPRIM,PHITIM,T1,T2,T3,T4
      COMPLEX T5,T6,T7,Z,ZETAB,ZSMM,A
      COMPLEX TRY
C
C     GET ZETA
C
      TRY = CSQRT(Z**2-4.*R*R*M)
      IF (REAL(Z).LE.0..AND.REAL(TRY).GT.0.)      TRY = -1.*TRY
      ZETA = (Z+TRY)/(2.*R)
      EYE = CMPLX(0.,1.)
      ZETAB = CONJG(ZETA)
C
C     CALCULATE THE FORCE COMPONENTS FROM THE POTENTIALS
```

```
C
      EPS = M*SIN(2.*ALPHA)*(1.+KAP)/(4.*(M*M+KAP))
      SINALP = SIN(2.*ALPHA)
      COSALP = COS(2.*ALPHA)
      ZSMM = ZETA**2-M
      PHITIM = ZETA**3*(ZETAB**2+M)/(ZETAB*ZSMM**2)
      A = 2.*M*EPS*EYE+M/4.-(COSALP+EYE*SINALP)/2.
      ZBPHI = PHITIM*(.5-ZETA**2/(2.*ZSMM)+2.*A/(KAP*ZSMM))
      T1 = -ZETA**2*(COSALP-EYE*SINALP)/(2.*ZSMM)
      T2 = -2.*EPS*EYE/ZSMM
      T3 = -KAP/(4.*ZSMM)
      T4 = -ZETA**2*(1.+M**2)/(4.*ZSMM**2)
      T5 = ZETA**4*(1.+M**2)/(2.*ZSMM**3)
      T6 = 2.*A*M*ZETA**2/(KAP*ZSMM**2)
      T7 = -A*(1.+M*ZETA**2)*(3.*ZETA**2-M)/(KAP*ZSMM**3)
      SIPRIM = T1+T2+T3+T4+T5+T6+T7
      SFORCE = ZBPHI+SIPRIM
C
      RETURN
      END
C
C
      SUBROUTINE GAUSSJ (A,N,NP,B,IER)
C
C     ***********************************************************
C     GAUSS-JORDAN MATRIX INVERSION WITH FULL PIVOTING EXCERPTED
C     FROM "NUMERICAL RECIPES IN FORTRAN"
C     ***********************************************************
C
      DIMENSION A(NP,NP),B(NP),IPIV(140),INDXR(140),INDXC(140)
      DO 11 J=1,N
       IPIV(J) = 0
 11   CONTINUE
      DO 22 I=1,N
       BIG = 0.
       DO 13 J = 1,N
          IF (IPIV(J).NE.1) THEN
             DO 12 K=1,N
                IF (IPIV(K).EQ.0) THEN
                   IF (ABS(A(J,K)).GE.BIG) THEN
                      BIG = ABS(A(J,K))
                      IROW = J
                      ICOL = K
                   ENDIF
                ELSEIF (IPIV(K).GT.1) THEN
                   WRITE (*,*) ' SINGULAR MATRIX'
                   IER = -1
                   GO TO 999
                ENDIF
 12          CONTINUE
```

```
      ENDIF
13   CONTINUE
     IPIV(ICOL) = IPIV(ICOL)+1
     IF (IROW.NE.ICOL) THEN
        DO 14 L=1,N
           DUM = A(IROW,L)
           A(IROW,L) = A(ICOL,L)
           A(ICOL,L) = DUM
14       CONTINUE
        DUM = B(IROW)
        B(IROW) = B(ICOL)
        B(ICOL) = DUM
     ENDIF
     INDXR(I) = IROW
     INDXC(I) = ICOL
     IF (A(ICOL,ICOL).EQ.0.) THEN
        WRITE (*,*) 'SINGULAR MATRIX'
        IER = -1
        GO TO 999
     ENDIF
     PIVINV = 1./A(ICOL,ICOL)
     A(ICOL,ICOL) = 1.
     DO 16 L = 1,N
        A(ICOL,L) = A(ICOL,L)*PIVINV
16    CONTINUE
     B(ICOL) = B(ICOL)*PIVINV
     DO 21 LL=1,N
        IF (LL.NE.ICOL) THEN
           DUM = A(LL,ICOL)
           A(LL,ICOL) = 0.
           DO 18 L=1,N
              A(LL,L) = A(LL,L)-A(ICOL,L)*DUM
18         CONTINUE
           B(LL) = B(LL)-B(ICOL)*DUM
        ENDIF
21    CONTINUE
22  CONTINUE
    DO 24 L = N,1,-1
     IF (INDXR(L).NE.INDXC(L)) THEN
        DO 23 K=1,N
           DUM = A(K,INDXR(L))
           A(K,INDXR(L)) = A(K,INDXC(L))
           A(K,INDXC(L)) = DUM
23       CONTINUE
     ENDIF
24  CONTINUE
999 CONTINUE
    RETURN
    END
C
```

```
      SUBROUTINE RUSSIAN(N2P2)
C
C     ***********************************************************
C     SUBROUTINE THAT CALCULATES THE POTENTIALS FOR A CURVED CRACK
C     FROM A FIRST ORDER PERTURBATION SOLUTION.  GIVEN IN A PAPER
C     BY GOLDSTEIN AND SALAGANIK, IN RUSSIAN, IN THE IZVESTIA MTT,
C     IN 1970.  SEE MY THESIS TO GET THE FULL CITATION
C     ***********************************************************
C
      COMMON /SPLIN/ X(70),Y(70),Y1(70),Y2(70)
      COMMON /RUSS/ YSTAR(70,70),YPSTAR(70,70),CAPY(70,70)
C
      DO 10 IT = 1,N2P2-1
      DO 10 ITAU = 1,N2P2-1
      IF (IT.EQ.ITAU) THEN
         YSTAR(IT,ITAU) = Y1(IT)
         YPSTAR(IT,ITAU) = Y2(IT)
         CAPY(IT,ITAU) = 0.
      ELSE
         YSTAR(IT,ITAU) = (Y(IT)-Y(ITAU))/(X(IT)-X(ITAU))
         YPSTAR(IT,ITAU) = (Y1(IT)-Y1(ITAU))/(X(IT)-X(ITAU))
         CAPY(IT,ITAU) = (Y1(IT)-YSTAR(IT,ITAU))
     !                 /(X(IT)-X(ITAU))
      ENDIF
   10 CONTINUE
      RETURN
      END
```

No. of Copies	Organization
2	Administrator Defense Technical Info Center ATTN: DTIC-DDA Cameron Station Alexandria, VA 22304-6145
1	Commander U.S. Army Materiel Command ATTN: AMCDRA-ST 5001 Eisenhower Avenue Alexandria, VA 22333-0001
1	Commander U.S. Army Laboratory Command ATTN: AMSLC-DL 2800 Powder Mill Road Adelphi, MD 20783-1145
2	Commander U.S. Army Armament Research, Development, and Engineering Center ATTN: SMCAR-IMI-I Picatinny Arsenal, NJ 07806-5000
2	Commander U.S. Army Armament Research, Development, and Engineering Center ATTN: SMCAR-TDC Picatinny Arsenal, NJ 07806-5000
1	Director Benet Weapons Laboratory U.S. Army Armament Research, Development, and Engineering Center ATTN: SMCAR-CCB-TL Watervliet, NY 12189-4050
(Unclass. only)1	Commander U.S. Army Armament, Munitions and Chemical Command ATTN: AMSMC-IMF-L Rock Island, IL 61299-5000
1	Director U.S. Army Aviation Research and Technology Activity ATTN: SAVRT-R (Library) M/S 219-3 Ames Research Center Moffett Field, CA 94035-1000

No. of Copies	Organization
1	Commander U.S. Army Missile Command ATTN: AMSMI-RD-CS-R (DOC) Redstone Arsenal, AL 35898-5010
1	Commander U.S. Army Tank-Automotive Command ATTN: ASQNC-TAC-DIT (Technical Information Center) Warren, MI 48397-5000
1	Director U.S. Army TRADOC Analysis Command ATTN: ATRC-WSR White Sands Missile Range, NM 88002-5502
1	Commandant U.S. Army Field Artillery School ATTN: ATSF-CSI Ft. Sill, OK 73503-5000
(Class. only)1	Commandant U.S. Army Infantry School ATTN: ATSH-CD (Security Mgr.) Fort Benning, GA 31905-5660
(Unclass. only)1	Commandant U.S. Army Infantry School ATTN: ATSH-CD-CSO-OR Fort Benning, GA 31905-5660
1	Air Force Armament Laboratory ATTN: WL/MNOI Eglin AFB, FL 32542-5000
	Aberdeen Proving Ground
2	Dir, USAMSAA ATTN: AMXSY-D AMXSY-MP, H. Cohen
1	Cdr, USATECOM ATTN: AMSTE-TC
3	Cdr, CRDEC, AMCCOM ATTN: SMCCR-RSP-A SMCCR-MU SMCCR-MSI
1	Dir, VLAMO ATTN: AMSLC-VL-D
10	Dir, BRL ATTN: SLCBR-DD-T

No. of
Copies Organization

2 PEO-Armaments
ATTN: SFAE-AR-PM,
D. Adams
T. McWilliams
Picatinny Arsenal, NJ 07806-5000

1 U.S. Army Belvoir RD&E Center
ATTN: STRBE-JBC, C. Kominos
Fort Belvoir, VA 22060-5606

1 Commander
DARPA
ATTN: J. Kelly
1400 Wilson Blvd.
Arlington, VA 22209

2 Materials Technology Laboratory
ATTN: SLCMT-MEC,
B. Halpin
T. Chou
Watertown, MA 02172-0001

1 Commander
U.S. Army Laboratory Command
ATTN: AMSLC-TD, R. Vitali
Adelphi, MD 20783-1145

1 Commander
U.S. Army Missile Command
ATTN: AMSMI-RD, W. McCorkle
Redstone Arsenal, AL 35898-5010

2 Commander
U.S. Army Laboratory Command
Harry Diamond Laboratory
ATTN: SLCHD-TS-NT, A. Frydman
2800 Powder Mill Road
Adelphi, MD 20783-1197

No. of
Copies Organization

9 Director
Benet Weapons Laboratory
U.S. Army Armament Research,
Development, and Engineering Center
ATTN: SMCAR-CCB,
V. Montuori
J. Keane
T. Allen
J. Vasilakis
G. Friar
J. Zweig
L. Johnson
T. Simkins
J. Wrzockalski
Watervliet, NY 12189-5000

7 Commander
U.S. Army Armament Research,
Development, and Engineering Center
ATTN: SMCAR-CCH-T,
S. Musalli
P. Christian
K. Fehsal
SMCAR-CCH-V, E. Fennell
SMCAR-CCH, J. DeLorenzo
SMCAR-CC,
R. Price
J. Hedderich
Picatinny Arsenal, NJ 07806-5000

2 Commander
U.S. Army Armament Research,
Development, and Engineering Center
ATTN: SMCAR-TD,
M. Lindner
T. Davidson
Picatinny Arsenal, NJ 07806-5000

1 Commander
Production Base Mod. Agency
U.S. Army Armament Research,
Development, and Engineering Center
ATTN: AMSMC-PBM-K
Picatinny Arsenal, NJ 07806-5000

No. of Copies Organization

3 PEO-Armaments
Project Manager
Tank Main Armament Systems
ATTN: SFAE-AR-TMA, COL Hartline
SFAE-AR-TMA-MD, C. Kimker
SFAE-AR-TMA-ME, K. Russell
Picatinny Arsenal, NJ 07806-5000

2 Commander
Wright-Patterson Air Force Base
ATTN: AFWAML,
J. Whitney
R. Kim
Dayton, OH 45433

2 Pacific Northwest Laboratory
A Division of Battelle Memorial Institute
ATTN: M. Smith
M. Garnich
P.O. Box 999
Richland, WA 99352

2 David Taylor Research Center
ATTN: R. Rockwell
W. Phyillaier
Bethesda, MD 20054-5000

1 Director
Los Alamos National Laboratory
ATTN: D. Rabern
WX-4 Division, Mail Stop G-787
P.O. Box 1663
Los Alamos, NM 87545

4 Director
Sandia National Laboratories
Applied Mechanics Department, Division-8241
ATTN: C. Robinson
G. Benedetti
K. Perano
W. Kawahara
P.O. Box 969
Livermore, CA 94550-0096

No. oi Copies Organization

3 Director
Lawrence Livermore National Laboratory
ATTN: R. Christensen
W. Feng
S. deTeresa
P.O. Box 808
Livermore, CA 94550

3 University of Delaware
Center for Composite Materials
ATTN: J. Gillespe
B. Pipes
M. Santare
201 Spencer Laboratory
Newark, DE 19716

2 Civil Engineering Department
N.C. State University
P.O. Box 7908
ATTN: W. Rasdorf
L. Spainhour
Raleigh, NC 27696-7908

1 Pennsylvania State University
Department of Engineering Science and Mechanics
ATTN: T. Hahn
227 Hammond Building
University Park, PA 16802

1 University of Utah
Department of Mechical and Industrial Engineering
ATTN: S. Swanson
Salt Lake City, UT 84112

1 Stanford University
Department of Aeronautics and Aeroballistics Durant Bldg.
ATTN: S. Tsai
Stanford, CA 94305

1 Custon Analytical Engineering Systems, Inc.
ATTN: A. Alexander
Star Route Box 4A
Flintstone, MD 21530

No. of
Copies Organization

1 Zak Technologies, Inc.
ATTN: A. Zak
2310 Belmore Drive
Champaign, IL 61820

2 Chamberlain Manufacturing Corp.
Waterloo Facility
ATTN: T. Lynch
550 Ester St.
P.O. Box 2335
Waterloo, IA 50704

2 Olin Corporation
Flinchbaugh Division
ATTN: E. Steiner
B. Stewart
P.O. Box 127
Red Lion, PA 17356

1 Olin Corporation
ATTN: L. Whitmore
10101 9th St. North
St. Petersburg, FL 33702

3 Alliant Techsystems, Inc.
ATTN: C. Candland
J. Bode
K. Ward
5640 Smetana Drive
Minnetonka, MN 55343

USER EVALUATION SHEET/CHANGE OF ADDRESS

This laboratory undertakes a continuing effort to improve the quality of the reports it publishes. Your comments/answers below will aid us in our efforts.

1. Does this report satisfy a need? (Comment on purpose, related project, or other area of interest for which the report will be used.) _____

2. How, specifically, is the report being used? (Information source, design data, procedure, source of ideas, etc.) _____

3. Has the information in this report led to any quantitative savings as far as man-hours or dollars saved, operating costs avoided, or efficiencies achieved, etc? If so, please elaborate. _____

4. General Comments. What do you think should be changed to improve future reports? (Indicate changes to organization, technical content, format, etc.) _____

BRL Report Number BRL-TR-3277 Division Symbol _____

Check here if desire to be removed from distribution list. ____

Check here for address change. ____

Current address: Organization _____
Address _____

DEPARTMENT OF THE ARMY
Director
U.S. Army Ballistic Research Laboratory
ATTN: SLCBR-DD-T
Aberdeen Proving Ground, MD 21005-5066

OFFICIAL BUSINESS

BUSINESS REPLY MAIL
FIRST CLASS PERMIT No 0001, APG, MD

Postage will be paid by addressee

Director
U.S. Army Ballistic Research Laboratory
ATTN: SLCBR-DD-T
Aberdeen Proving Ground, MD 21005-5066

NO POSTAGE
NECESSARY
IF MAILED
IN THE
UNITED STATES